NIST Special Publication 260-201

Certification of Standard Reference Material® 1450e
Fibrous Glass Board

Robert R. Zarr
N. Alan Heckert

This publication is available free of charge from:
https://doi.org/10.6028/NIST.SP.260-201

National Institute of Standards and Technology
U.S. Department of Commerce

NIST Special Publication 260-201

Certification of Standard Reference Material® 1450e
Fibrous Glass Board

Robert R. Zarr
Energy and Environment Division
Engineering Laboratory

N. Alan Heckert
Statistical Engineering Division
Information Technology Laboratory

This publication is available free of charge from:
https://doi.org/10.6028/NIST.SP.260-201

April 2020

U.S. Department of Commerce
Wilbur L. Ross, Jr., Secretary

National Institute of Standards and Technology
Walter Copan, NIST Director and Undersecretary of Commerce for Standards and Technology

National Institute of Standards and Technology Special Publication 260-201
Natl. Inst. Stand. Technol. Spec. Publ. 260-201, 139 pages (April 2020)
CODEN: NSPUE2

This publication is available free of charge from:
https://doi.org/10.6028/NIST.SP.260-201

Foreword

The National Institute of Standards and Technology (NIST), formerly the National Bureau of Standards (NBS), was established by the U.S. Congress in 1901 and charged with the mission of establishing national standards used in scientific investigations, engineering, manufacturing, and commerce. Standard Reference Materials originated in 1905 with a standard sample program – the array of materials maintained by NIST and certified for their chemical composition, or physical or chemical properties. In response to pressing demands, the early program grew and, with time, NIST has issued several thousand different Standard Samples or Standard Reference Materials® (SRMs). Many of these have been renewed several times; others have been replaced or discontinued as technology changed. Today, over 1300 SRMs are available, together with a large number of scientific publications related to the fundamental and applied characteristics of these materials. Each SRM is provided with a Certificate or a Certificate of Analysis that contains the essential data concerning its properties or characteristics. The SRMs currently available cover a wide range of chemical, physical, and mechanical properties, and a corresponding wide range of measurement interests of fundamental and applied science. These SRMs constitute a unique and invaluable means of transferring to the user accurate data obtained at NIST and provide essential tools that can be used to improve accuracy in areas where measurements are performed.

Preface

Standard Reference Materials (SRMs) as defined by the National Institute of Standards and Technology (NIST) are well-characterized materials, produced in quantity, and certified for one or more physical or chemical properties. They are used to assure the accuracy and compatibility of measurements throughout the nation. SRMs are widely used as primary standards in many diverse fields in science, industry, and technology, both within the United States and throughout the world. They are also used extensively in the fields of environmental and clinical analysis. In many applications, traceability of quality control and measurement processes to the national measurement system is carried out through the mechanism and use of SRMs. For many of the Nation's scientists and technologists, it is therefore more than a passing interest to know the details of the measurements made at NIST in arriving at the certified values of the SRMs produced.

The NIST Special Publication 260 Series (SP 260) is reserved for this purpose. The SP 260 Series is dedicated to the dissemination of information on all phases of the preparation, measurement, certification, and use of NIST SRMs. In general, much more detail will be found in these publications than is generally allowed, or desirable, in scientific journal articles. This level of detail enables the user to assess the validity and accuracy of the measurement processes employed, to judge the statistical analysis, and to learn details of techniques and methods utilized for work entailing greatest care and accuracy. The publications also provide additional information so SRMs can be utilized in new applications in diverse fields not foreseen at the time the SRM was originally issued.

Appendix A of this document is a Change Log that contains amendments to this publication relative to the version published in 2020. Inquiries concerning the technical content of this paper should be directed to the author(s). Other questions concerned with the availability, delivery, price, and so forth, will receive prompt attention from:

NIST Office of Reference Materials
100 Bureau Drive, Stop 2300
Gaithersburg, MD 20899-2300

Telephone: (301) 975-2200
FAX: (301) 948-3730
Email: srminfo@nist.gov

Steven J. Choquette, Chief
Office of Reference Materials

Abstract

Thermal conductivity measurements at and near room temperature are presented as the basis for certified values of thermal conductivity for SRM 1450e, Fibrous Glass Board. The measurements have been conducted in accordance with a randomized full factorial experimental design with three variables (bulk density, mean temperature, and ambient pressure) using the NIST 500 mm guarded-hot-plate apparatus. The thermal conductivity of the SRM specimens was measured over a range of bulk densities from 110 $kg \cdot m^{-3}$ to 154 $kg \cdot m^{-3}$, mean temperatures from 280 K to 360 K, and ambient pressure of 60 kPa to 100 kPa. Uncertainties of the measurements, consistent in format with current international guidelines, have been prepared. Statistical analyses of the physical properties from the SRM are presented and include variations between boards, as well as within board.

Each unit of SRM 1450e is individually certified for bulk density, ρ, and batch certified for thermal conductivity with the following equation:

$$\lambda = -1.9731 \times 10^{-3} + 1.9923 \times 10^{-5}\,\rho + 1.0792 \times 10^{-4}\,T_m$$

where λ is the predicted thermal conductivity ($W \cdot m^{-1} \cdot K^{-1}$), ρ is the bulk density ($kg \cdot m^{-3}$), and T_m is the mean temperature (K) valid over the temperature range of 280 K to 360 K. Certified values of λ are valid for barometric pressures from 60 kPa to 101.3 kPa (sea-level pressure). There is no pressure dependence on the thermal conductivity included in the certification equation above because no statistically significant relationship between λ and pressure was determined over the studied range from 60 kPa to 100 kPa. The expanded uncertainty for λ values from the above equation is 1 % with a coverage factor of approximately $k = 2$.

Key words

calibration; bulk density; fibrous glass board; guarded-hot-plate apparatus; heat-flow-meter apparatus; standard reference material; SRM 1450e; thermal conductivity; thermal insulation; uncertainty.

Table of Contents

List of Tables

List of Figures

Glossary

Symbol	Description (Units)
a	regression coefficient in Eq. (4) ($kg \cdot s^{-1}$)
a_i	regression coefficients in Eq. (15)
A	meter area of the guarded-hot-plate apparatus (m^2)
A_h	damaged area in meter plate as expressed in Eq. (E-41) (m^2)
A_{mp}	area of meter plate in Eq. (E-41) (m^2)
A_p	area of the insulation panel in Eq. (5), Eq. (6), and Eq. (10) (m^2)
A_s	area of the guarded-hot-plate test specimen (m^2)
b	half-width of uniform rectangular distribution
c_i	sensitivity coefficient for uncertainty analysis
d	nominal diameter of meter plate in Eq. (E-37) for uncertainty analysis (m)
d_i	inner diameter of guard plate (mm)
d_o	outer diameter of meter plate (mm)
d_s	diameter of guarded-hot-plate test specimen (mm)
f	functional relationship between measurand and input quantities
f_{mp}	geometrical factor in Eq. (E-15) (m)
i	index (dimensionless)
I	electric current (A)
ID	identification
j	index (dimensionless)
k	coverage factor for uncertainty (dimensionless)
l_i	linear dimensions (length, width) of insulation panel (mm), i = 1, 2, 3, 4, 5, 6
L	in-situ thickness of guarded-hot-plate test specimen (mm)
L_0	in-situ thickness of guarded-hot-plate test specimen at room temperature (mm)
L_{av}	average (in-situ) specimen thickness in Eq. (18) (m)
$L_{corr.}$	thickness correction due to thermal expansion/contraction effects (mm)
L_{datum}	reference setting for the in-situ thickness measurement system (mm)
L_{gage}	dimensional measurements from dial indicator (mm)
L_{gb}	gage block length at temperature t in Eq. (D-5) (mm)
L_i	thickness dimensions of insulation panel (mm), i = 1, 2, 3, 4, 5, 6, 7, 8
L_p	(average) thickness of insulation panel (mm)
L_q	length of fused-quartz rod in Eq. (E-22) (mm)
L_s	thickness dimension of 500 mm diameter specimen (mm)
$L_{uncorr.}$	uncorrected in-situ thickness measurement (mm)
$L(T_m)$	in-situ thickness measurement corrected for thermal expansion effects (mm)
m_0	initial mass of the insulation panel (specimen) at time t_0 in Eq. (4) (kg)
m_c	thickness of thermometry cold plate in Eq. (E-22) (mm)
m_h	thickness of hot plate in Eq. (E-22) (mm)
m_s	mass of the guarded-hot-plate test specimen (kg)
$m(t)$	mass of the insulation panel (specimen) as a function of time (kg)
n	number of independent observations (dimensionless)

p	atmospheric (barometric) pressure (kPa)
p_a	axial clamping pressure (Pa)
q	heat flow rate through a surface of unit area perpendicular to the direction of heat flow ($W \cdot m^{-2}$)
Q	axial heat flow rate through meter area of guarded-hot-plate test specimen (W)
Q_e	lateral heat flow rate across the plate perimeter to the edge guard (W)
Q_g	lateral (i.e., radial) heat flow rate across the guard gap (W)
Q_{HPCG}	lateral heat flow rate across the hot plate connection guard (W)
Q_m	input power to meter-plate resistance heater in Eq. (E-1) (W)
Q_{SPRT}	input power from standard platinum resistance thermometer (W)
r	number of replicates per day in Eq. (E-29) (dimensionless)
r_h	radius of hole in Eq. (E-41) (mm)
r_i	inner radius of guard plate (mm)
r_o	outer radius of meter plate (mm)
R	thermal resistance ($m^2 \cdot K \cdot W^{-1}$)
R_s	electrical resistance of standard resistor (Ω)
s	standard deviation
s_a	standard deviation of daily averages in Eq. (E-29) (mm)
s_d	pooled within-day standard deviation in Eq. (E-29) (mm)
s_p	standard deviation of process
s_{pool}	pooled standard deviation
SIM	Inter-American Metrology System
SPC	statistical process control
SPRT	standard platinum resistance thermometer
SRM	Standard Reference Material
t	surface plate temperature for thermal expansion correction in Eq. (D-5) (°C)
t_0	initial time, $t = 0$ (s)
t-value	estimate (e.g., slope) divided by standard uncertainty of estimate (dimensionless)
T_a	chamber air temperature (K)
T_c	(average) cold-plate surface temperature (K)
T_{eg}	edge guard temperature (K)
T_h	hot-plate surface temperature (K)
T_m	mean specimen temperature in Eq. (19) (K)
T_r	reference temperature of 293.5 K in Eq. (E-22) (K)
T_{WJ}	water jacket temperature (K)
u_c	combined standard uncertainty ($k = 1$)
$u_{c,\,bal}$	combined standard uncertainty ($k = 1$) of digital weighing balance (kg)
$u_{c,r}$	relative combined standard uncertainty (k = 1) (dimensionless)
$u_{c,\,gage\#1}$	combined standard uncertainty ($k = 1$) for height gage #1 (mm)
$u_{c,\,gage\#2}$	combined standard uncertainty ($k = 1$) for height gage #2 (mm)
u_i	standard uncertainty for quantity X_i
u_{plate}	standard uncertainty for plate flatness (mm)
u_s	standard uncertainty for calibration artifact

U	expanded uncertainty ($k = 2$)
U_r	relative expanded uncertainty (k = 2) (dimensionless)
V_m	voltage difference across meter-plate resistance heater (V)
V_s	voltage difference across standard resistor (V)
x_i	input estimate (x-value for graphical analysis)
x_{i-1}	previous x-value for graphical analysis
x_j	input value (coded as –1 or +1) for imbalance model in Eq. (E-7)
X_1	output from inboard length gage (mm)
X_2	output from outboard length gage (mm)
X_i	input quantity
α	coefficient of thermal expansion (K^{-1})
β_{ji}	regression coefficients for imbalance model in Eq. (E-7)
$\delta\rho$	difference in bulk density of insulation panel and 500 mm diameter specimens (%)
δL	change in combined reading of length gages relative to 293.15 K (mm)
$\delta T_{corr.}$	temperature correction due to SPRT location at midplane of plate (K)
δT_s	hot plate spatial (lateral) temperature variation (K)
ΔL	change in the average thickness of the specimen pair in Eq. (E-20) (mm)
ΔL_{gb}	length correction of gage block in Eq. (D-5) (mm)
ΔL_q	change in length of fused-quartz rod due to thermal expansion/contraction (mm)
Δm_c	change in thickness of the thermometry cold plate due to thermal expansion/contraction (mm)
Δm_h	change in thickness of hot plate due to thermal expansion/contraction (mm)
ΔQ	change in meter-plate heater power due to imbalance condition expressed in Eq. (E-7) (W)
Δt	elapsed time in Eq. (4) (s)
ΔT	surface-to-surface temperature difference across guarded-hot-plate test specimen (K), $\Delta T = (T_h - T_c)$
ΔT_{av}	average temperature difference in Eq. (18) (K)
ΔT_{gap}	temperature difference across the guard gap in Fig. 17 (K)
ΔT_{HPCG}	temperature difference across the hot plate connection guard (W)
ΔT_{mp}	change in meter plate temperature from room conditions (K)
ρ	bulk density ($kg \cdot m^{-3}$)
ρ_{av}	average in-situ bulk density of a specimen pair ($kg \cdot m^{-3}$)
ρ_p	bulk density of insulation panel in Eq. (10) ($kg \cdot m^{-3}$)
ρ_s	bulk density of guarded-hot-plate test specimen in Eq. (1) and Eq. (16) ($kg \cdot m^{-3}$)
λ	thermal conductivity ($W \cdot m^{-1} \cdot K^{-1}$)
λ_0	baseline (balanced) case for imbalance model in Eq. (E-7) ($W \cdot m^{-1} \cdot K^{-1}$)
λ_a or k_a	apparent thermal conductivity ($W \cdot m^{-1} \cdot K^{-1}$)
λ_{exp}	experimental thermal conductivity in Eq. (18) ($W \cdot m^{-1} \cdot K^{-1}$)
λ_{pred}	predicted thermal conductivity for imbalance model in Eq. (E-7) ($W \cdot m^{-1} \cdot K^{-1}$)
λ_{Ni}	thermal conductivity of nickel in Eq. (E-15) ($W \cdot m^{-1} \cdot K^{-1}$)

Additional subscripts

1	denotes inboard cold plate/specimen relative to the vertical vacuum baseplate
2	denotes outboard cold plate/specimen relative to the vertical vacuum baseplate
av	denotes average value for a quantity associated with the specimen pair
A	denotes Type A standard uncertainty evaluation
B	denotes Type B standard uncertainty evaluation
Ni	denotes nickel or nickel 201 alloy

Additional superscript

‾	denotes sample mean
^	denotes predicted

1. Introduction

The National Institute of Standards and Technology (NIST) issues Standard Reference Materials® (SRMs)[1] for insulating materials having certified value assignments for thermal conductivity or thermal resistance. Thermal insulation SRMs are intended specifically for application in standardized steady-state methods employing test apparatus with experimental arrangements either having flat plates or conditioning chambers, or both [1-3]. These primary standards support metrology and traceability for insulation testing communities in industry, academia, and government as an integral component of their quality assurance systems. In the United States, these SRMs can also assist insulation manufacturers in complying with federal requirements for labeling and advertising of home insulation commonly known as the U.S. Federal Trade Commission R-value Rule [4].

The thermal transmission properties of insulating SRMs are characterized as functions of bulk density, mean temperature, and, for SRM 1450e, atmospheric air pressure. Since it is impractical to measure the thermal conductivity of every specimen, the characterization is realized by batch certification. The benefit of batch certification is production of a large quantity of units that are economical and available on demand for several years. A minor disadvantage is that the uncertainty statement contains a component, usually small, due to the material lot variability. The measurement plan involves a statistically based sampling strategy for selecting specimens from the candidate material lot for testing in a guarded-hot-plate apparatus. The analysis of the thermal conductivity data of the sample sub-lot is used for certification of the SRM lot.

Value assignments for NIST thermal insulation SRMs are developed by means of the guarded-hot-plate apparatus [1]. The instrument is an absolute method since the resultant thermal transmission properties are determined directly from basic measurements of electrical power, temperature, length, and area. The measurement technique establishes steady-state heat flow through flat homogeneous slabs – the surfaces of which are in contact with adjoining parallel boundaries (i.e., plates) maintained at constant temperatures. By accurately monitoring the plate separation, temperature difference, and knowing the geometric shape factor for the heat flow, the steady-state heat transmission properties of the specimen are determined using Fourier's law of heat conduction. Influence quantities such as ambient temperature, plate clamping pressure, and plate emittance, among others, are controlled during the measurement.

This report provides supplemental documentation for the SRM 1450e Certificate on the following topics:

- overview and historical background;
- standard terminology for reference materials, thermal insulation, and measurement uncertainty;
- certification project plan;
- measurement methods for the bulk density and thermal conductivity;
- uncertainty analysis; and,
- certification.

[1] The term "Standard Reference Material" and the diamond-shaped logo which contains the term "SRM," are registered with the United States Patent and Trademark Office.

2. Overview

The renewal process for SRM 1450e involves three major phases (Fig. 1): 1) material fabrication and acquisition; 2) batch certification by a NIST technical laboratory; and, 3) distribution by the NIST Office of Reference Materials (ORM).

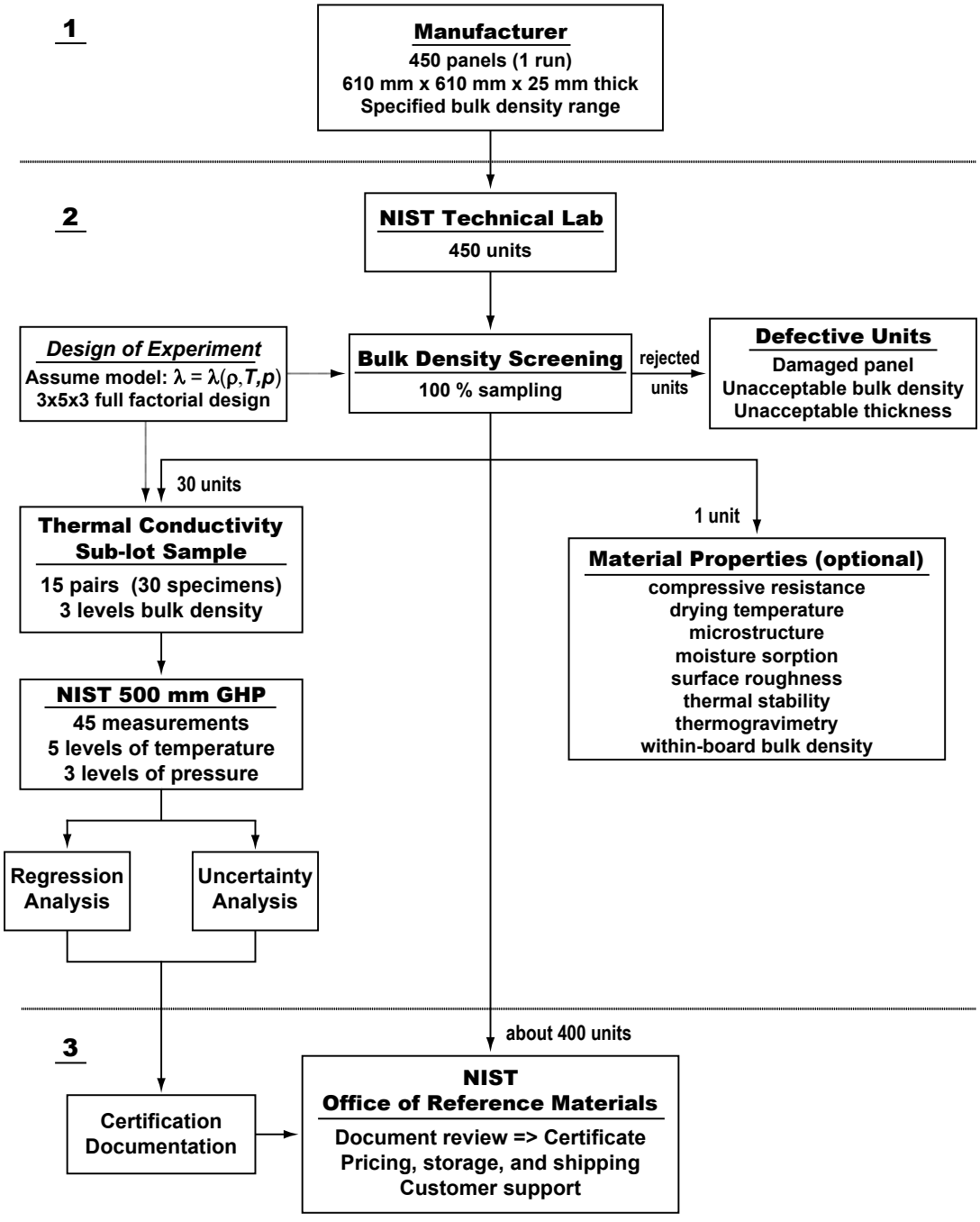

Fig. 1. Production of SRM 1450e.

2.1. Development and Production

In Phase 1, the NIST technical laboratory, as part of its planning and research, assesses the needs and priorities of U.S. industry with regard to thermal insulation reference materials. Based on industry input, the laboratory prepares the technical requirements for procurement of the insulating material. Acquisition is accomplished via a contract with an approved vendor. Execution of Phase 1 generally requires one year from initiation to completion.

For Phase 2, the technical lab proceeds with production and certification of the renewal after delivery of the material. Execution of the steps below to measure the properties for certification typically requires two years.

1) First and foremost, development of a statistically justified sampling and measurement plan;
2) Measurements of bulk density for homogeneity screening of the material lot (100 % sampling);
    a. rejection of anomalous and/or damaged panels (i.e., units);
    b. selection of a stratified sub-sample of 15 pairs of specimens containing low (5 pairs), mid (5 pairs), and high (5 pairs) bulk density strata;
3) Thermal conductivity measurements of a statistical sub-sample using the NIST 500 mm guarded-hot-plate apparatus; and,
4) Analysis of data leading to batch certification.

Phase 3, undertaken by the NIST Office of Reference Materials (ORM), encompasses all final administrative functions including document review and approval, pricing, storage, shipping, publicity, and customer support. The production costs of the renewal are recovered, under current Congressional authorization, through the sale of the SRM to end users.

Figure 1 also depicts an optional compilation of supplemental material properties that have been previously investigated by NIST researchers for various lots of 1450 materials [5]. The primary purpose of these investigations is to determine what, if any, are the effects of other (secondary) factors on the certified properties of thermal conductivity and thermal resistance. In contrast to a NIST Certified Value (Sec. 3), these investigations provide informative data of interest and are noted as such when included in the certificate. Standard Reference Material 1450e does not incorporate any of the supplemental measurements depicted in Fig. 1 and, thus, does not include NIST Information Values.

2.2. Historical Progress

Standard Reference Material 1450e, like previous 1450 lots, is a semi-rigid, high-density molded fibrous-glass board commercially manufactured from a single run. Table 1 reviews the chronology of the 1450 Series and includes information for year acquired, year issued, bulk density, temperature, references on the technical development (where available), and laboratory facility for each SRM. When an SRM lot is exhausted, the renewal (i.e., replacement lot) retains the original number designation and a lower-case letter (a, b, c, etc.) is appended to denote the new lot. Revisions to the certificates due to modifications, corrections, or other changes are noted on the Certificate Revision History and, in this report, are denoted by a Roman numeral (I, II, etc.).

The SRM approach for thermal insulating materials was recommended in 1977 by a working group [6] under ASTM Subcommittee C16.30 on Thermal Measurement as part of a larger mission to establish a national accreditation program for thermal insulation. In response, NIST (formerly the National Bureau of Standards[2] (NBS)) established SRM 1450 in 1978 using materials obtained previously for an internal NBS calibration program.

Table 1. Chronology of SRM 1450, Fibrous Glass Board.

SRM	Year acquired	Year issued	Bulk density ($kg \cdot m^{-3}$)	Temperature (K)	Ref.	NIST facility
1450	1961	1978[a]	100 to 180	255 to 330	[7-8]	[b]
1450a	1958	1979[a]	60 to 140	255 to 330	[7-8]	[b]
1450b(I)	1981	1982	110 to 150	260 to 330	---	[b]
1450b(II)	1980, 1981	1985	110 to 150	100 to 330	[9]	[b, c, d]
1450c(I)	1996	1997	150 to 165	280 to 340	[10]	[e]
1450c(II)	1996	2010	150 to 165	280 to 340	---	[e]
1450d	2009	2011	114 to 124	280 to 340	[11]	[e]
1450e	2017	2020	110 to 154	280 to 360		[f]

[a] Issued initially under an internal NBS calibration program.
[b] NBS 200 mm square guarded-hot-plate apparatus, Gaithersburg, Maryland.
[c] NBS 300 mm diameter guarded-hot-plate apparatus, Gaithersburg, Maryland.
[d] NBS 200 mm diameter guarded-hot-plate apparatus, Boulder, Colorado.
[e] NIST 1016 mm diameter guarded-hot-plate apparatus, Gaithersburg, Maryland.
[f] NIST 500 mm diameter guarded-hot-plate apparatus, Gaithersburg, Maryland.

Table 1 footnotes identify the five guarded-hot-plate facilities utilized for the thermal characterization of 1450 and ensuing renewals. The renewal for 1450b was cooperatively characterized by aggregating data from the NBS Center for Chemical Engineering in Boulder, Colorado and the NBS Center for Building Technology in Gaithersburg, Maryland. In 1982, 1450b(I) was issued with certified values over a limited temperature range and informational values below 255 K. After low-temperature measurements were conducted at Boulder, Colorado, NBS re-issued 1450b(II) with certified values from 100 K to 330 K. Standard Reference Material 1450c(I) was initially issued in 1997 and was re-issued in 2010 with revised certification values for thermal resistance (1450c(II)).

Although the SRM approach for insulation materials was established in 1978, NBS initiated a formal calibration program [7] for thermal insulation in 1958. The program provided customers with individual calibration measurements of high-density molded fibrous glass insulation board. From 1958 to 1978, NBS provided over 300 pairs [8] of calibrated reference specimens selected from one of four lots of fibrous-glass board, designated by the year of their acquisition (1958, 1959, 1961, and 1970) using the NBS 200 mm guarded-hot-plate apparatus located in Gaithersburg, Maryland. In 1978, the remaining supply of boards was used to establish SRMs 1450 and 1450a [8]. Due to limited stockpiles, 1450 and 1450a were rapidly depleted and two new lots were acquired in 1980 and 1981 for the development of SRM 1450b [9].

[2] In 1901, Congress established the National Bureau of Standards (NBS) to support industry, commerce, scientific institutions, and all branches of government. In 1988, as part of the Omnibus Trade and Competitiveness Act, the name was changed to the National Institute of Standards and Technology (NIST) to reflect a broader mission for the agency. For historical accuracy, this report will use, where appropriate, NBS for events prior to 1988.

In 1995, the NIST Standard Reference Materials Program (SRMP) requested that the Building and Fire Research Laboratory initiate a research program to replenish 1450b with a new SRM lot, designated 1450c. Because 1450b had been characterized in the early 1980s, a questionnaire to re-assess requirements for a new SRM was disseminated to the user community. Based on the survey responses, NIST procured a new material lot of molded fibrous-glass insulation boards [10] having a nominal bulk density of 160 $kg \cdot m^{-3}$ (10 $lb \cdot ft^{-3}$). In contrast to previous 1450 lots, the procedures for acquisition, testing, and production of 1450c were modified as described below.

- 130 molded fibrous-glass boards (1220 mm by 1220 mm) from a single production run were acquired [10]. After completion of the thermal characterization, the units were cut by NIST SRMP to their final dimensions of 610 mm 610 mm.
- Under guidance from the NIST Statistical Engineering Division, a balanced experimental design for temperature and bulk density was developed and implemented for batch certification of the material lot [10].
- Additional measurements and statistical analyses were carried out to assess not only the between-board but also within-board variability for thickness and bulk density.

The planning and research phase for renewal of SRM 1450d began in 2007 when NIST acquired and evaluated two replacement candidates [12]. Additional technical information and requirements were obtained from SRM customers and from an ASTM C16.30 Reference Materials Task Group. Based on this response, the following characteristics for 1450d were established [11].

- The nominal bulk density for 1450d was specified to be 128 $kg \cdot m^{-3}$ (8 $lb \cdot ft^{-3}$), congruent with the 1450b version.
- A single production run of 450 units was stipulated and the vendor was required to trim the boards to a final panel size of 610 mm by 610 mm (24 in. by 24 in.).
- The 1450d experimental design was modified to individually certify the bulk density of each unit, necessitating 100 % sampling of the panels and assigning a unique identification number from 001 to 450 to each panel.

The planning phase for the renewal of SRM 1450e began in 2016 and the characteristics, based on 1450d, were established and summarized below. Details of the certification project design are explained in Sec. 4.

- The nominal bulk density for 1450e was the same as 1450d, 128 $kg \cdot m^{-3}$ (8 $lb \cdot ft^{-3}$).
- A single production run of 450 units was stipulated and the vendor was required to trim the boards to a final panel size of 610 mm by 610 mm (24 in. by 24 in.). For 100 % sampling of the panels, NIST assigned a unique identification number from 500 to 949 to individual panels (differentiating the 1450e lot from the 1450d numbering sequence).
- In an effort to extend the upper temperature certification, the thermal characterization was increased from 340 K to 360 K (Table 1). The technical approach for SRM 1450e also considered the effect of gas pressure on the thermal conductivity over a restricted range from 60 kPa to 100 kPa.

3. Terms and Definitions

3.1. Reference Materials

Section 3.1 provides definitions for reference materials, excerpted verbatim, from Refs. [13-14]. Additional SRM definitions are available at https://www.nist.gov/srm/srm-definitions.

Reference Material (RM): material, sufficiently homogeneous and stable with respect to one or more specified properties, which has been established to be fit for its intended use in a measurement process [14].

NOTE 1 RM is a generic term.
NOTE 2 Properties can be quantitative or qualitative, e.g. identity of substances or species.
NOTE 3 Uses may include the calibration of a measurement system, assessment of a measurement procedure, assigning values to other materials, and quality control.
NOTE 4 ISO/IEC Guide 99:2007 has an analogous definition (5.13), but restricts the term "measurement" to apply to quantitative values. However, Note 3 of ISO/IEC Guide 99:2007, 5.13 (VIM) specifically includes qualitative properties, called "nominal properties".

Certified Reference Material (CRM): Reference material (RM) characterized by a metrologically valid procedure for one or more specified properties, accompanied by an RM certificate that provides the value of the specified property, its associated uncertainty, and a statement of metrological traceability [14].

NOTE 1 The concept of value includes a nominal property or a qualitative attribute such as identity or sequence. Uncertainties for such attributes may be expressed as probabilities or levels of confidence.
NOTE 2 Metrologically valid procedures for the production and certification of RMs are given in, among others, *ISO Guides 34* and *35*.
NOTE 3 *ISO Guide 31* gives guidance on the contents of RM certificates.
NOTE 4 ISO/IEC Guide 99:2007 has an analogous definition (5.14).

NIST Standard Reference Material® (SRM): A CRM issued by NIST that also meets additional NIST-specified certification criteria and is issued with a certificate or certificates of analysis that reports the results of its characterizations and provides information regarding the appropriate use(s) of the material [13]. NOTE: An SRM is prepared and used for three main purposes: (1) to help develop accurate methods of analysis; (2) to calibrate measurement systems used to facilitate exchange of goods, institute quality control, determine performance characteristics, or measure a property at the state-of-the-art limit; and (3) to ensure the long-term adequacy and integrity of measurement quality assurance programs. The terms "Standard Reference Material" and the diamond-shaped logo which contains the term "SRM," are registered with the United States Patent and Trademark Office.

NIST Certified Value: A value reported on an SRM certificate or certificate of analysis for which NIST has the highest confidence in its accuracy in that all known or suspected sources of bias have been fully investigated or accounted for by NIST [13].

3.2. Thermal Insulation

Section 3.2 provides terms, symbols, definitions, and units pertaining to properties and measurements of thermal insulating materials, excerpted verbatim, from Refs. [1] and [15].

apparent thermal conductivity, λ_a or k_a: a thermal conductivity assigned to a material that exhibits thermal transmission by several modes of heat transfer resulting in property variation with specimen thickness, or surface emittance (*SI* units: $(W/m^2)/(K/m) = W \cdot m^{-1} \cdot K^{-1}$) [15].

NOTE 1 Thermal conductivity and resistivity are normally considered to be intrinsic or specific properties of materials and, as such, should be independent of thickness. When nonconductive modes of heat transfer are present within the specimen (radiation, free convection) this may not be the case. To indicate the possible presence of these phenomena (for example, thickness effect) the modifier "apparent" is used, as in apparent thermal conductivity.

NOTE 2 Test data using the "apparent" modifier must be quoted only for the conditions of the measurement. Values of thermal conductance and thermal resistance calculated from apparent thermal conductivity or resistivity, are valid only for the same conditions.

density, ρ: the mass per unit volume of material. (*SI* units: $kg \cdot m^{-3}$) [15].

NOTE 1 The metered section density, ρ_m, or the specimen density, ρ_s where metered section area density cannot be obtained, are to be reported as the average of the two pieces (excerpted from Ref. [1]). The equation for specimen density is the following:

$$\rho_s = \frac{m_s}{A_s \times L} \tag{1}$$

where:

m_s = mass of the specimen (kg),
A_s = area of the specimen (m^2), and
L = specimen thickness (m).

heat flow; heat flow rate, Q: the quantity of heat transferred to or from a system in unit time (W) [15].

NOTE 1 see **heat flux** for the areal dependence.

NOTE 2 This definition is different from that given in some textbooks, which may use $\dot{Q}$ or $\dot{q}$ to represent heat flow rate. The ISO definition uses Φ.

heat flux, q: the heat flow rate through a surface of unit area perpendicular to the direction of heat flow ($W \cdot m^{-2}$) [15].

fibrous glass: a synthetic vitreous fiber insulation made by melting predominantly silica sand and other inorganic materials, and then physically forming the melt into fibers [15].

NOTE 1 Commonly referred to as fiber glass.

NOTE 2 To form an insulation product, there are often other materials applied to the fibrous glass such as binders, oils, etc.

thermal conductivity, λ: the time rate of steady state heat flow through a unit area of a homogeneous material induced by a unit temperature gradient in a direction perpendicular to that unit area (*SI* units: $(W/m^2)/(K/m) = W \cdot m^{-1} \cdot K^{-1}$) [15].

NOTE 1 Thermal conductivity testing is usually done in one of two apparatus/specimen geometries: flat-slab specimens with parallel heat flux lines, or cylindrical specimens

with radial heat flux lines. The operational definition of thermal conductivity for flat-slab specimens is given as follows:

$$\lambda = \frac{Q\,L}{A\,\Delta T} \tag{2}$$

where:
Q = heat flow rate,
A = area through which Q passes, and
L = thickness of the flat-slab specimen across which the temperature difference ΔT exists
The $\Delta T/L$ ratio approximates the temperature gradient.

thermal resistance, *R*: the quantity determined by the temperature difference, at steady state, between two defined surfaces of a material or construction that induces a unit heat flow rate through a unit area.

$$R = \frac{\Delta T}{q} = \frac{L}{\lambda} \tag{3}$$

A resistance (R) associated with a material shall be specified as a material R. A resistance (R) associated with a system or construction shall be specified as a system R (R in SI units: $K/(W/m^2) = K{\cdot}m^2{\cdot}W^{-1}$ [15]

NOTE 1 Thermal resistance and thermal conductance are multiplicative reciprocals.

thermal transmission properties: those properties of a material or system that define the ability of a material or system to transfer heat such as thermal resistance and thermal conductivity, among others [1].

semi-rigid board insulation: qualitative property associated with the degree of suppleness (i.e., flexibility), particularly related to the geometrical dimensions and bulk density of the board.

3.3. Uncertainty

Section 3.3 provides definitions pertaining to measurement uncertainty, excerpted verbatim, from Refs. [16-17].

combined standard uncertainty, u_c: standard uncertainty of the result of a measurement when that result is obtained from the values of a number of other quantities, equal to the positive square root of a sum of terms, the terms being the variances or covariances of these other quantities weighted according to how the measurement result varies with changes in these quantities.

coverage factor, *k*: numerical factor used as a multiplier of the combined standard uncertainty in order to obtain an expanded uncertainty.

NOTE 1 A coverage factor, k, is typically in the range 2 to 3.

expanded uncertainty, *U*: quantity defining an interval about the result of a measurement that may be expected to encompass a large fraction of the distribution of values that could be reasonably attributed to the measurand.

standard uncertainty, u_i: uncertainty of the result of a measurement expressed as standard deviation.

Type A evaluation (of uncertainty): method of evaluation of uncertainty by the statistical analysis of a series of observations

Type B evaluation (of uncertainty): method of evaluation of uncertainty by means other than the statistical analysis of a series of observations

4. Certification Project Design

Section 4 describes the project plan for certification of SRM 1450e beginning with the project definition and scope for intended use. Descriptions of the material, fabrication, and manufacturer controls are presented. The material preparation at NIST covers inspection, storage, and conditioning as part of the overall sampling plan. Lastly, the measurement methods for the homogeneity analysis, certification measurements, and uncertainty evaluation are described.

4.1. Project Definition and Scope for Intended Use

The certification project is defined as follows.

> The preparation of thermal insulation SRM 1450e (128 kg·m^{-3}) for thermal conductivity and thermal resistance measurements with expanded uncertainties (k = 2) associated with the certified values of less than or equal to 2 % over a mean temperature range of 280 K to 360 K and an atmospheric pressure range of 60 kPa to 100 kPa.

Standard Reference Material 1450e is intended for use as a proven check for the guarded-hot-plate apparatus [1], or other absolute thermal conductivity apparatus, and for calibration of a heat-flow-meter apparatus [2] over the temperatures 280 K to 360 K and barometric pressures from 60 kPa to 101.3 kPa (sea-level pressure). This report cannot exclude the use of SRM 1450e for other purposes, but the user is cautioned that other applications are not necessarily covered by the SRM 1450e Certificate or by this report. Additional usage issues are covered in Sec. 8 and in the SRM 1450e Certificate (under Instructions for Handling, Storage, And Use).

4.2. Material

The material is manufactured in board form consisting of discontinuous glass fibers bonded by a thermosetting resin, typically a phenolic binder formulation. The organic binder restricts the upper temperature of the material to 473 K [10]. Recent 1450 certificates, however, advise a precautionary upper value of 380 K.

4.2.1. Fabrication

The material lot was fabricated by Quiet Core Incorporated over a three-day period in August 2017 at their manufacturing facility in Bethlehem, Pennsylvania. Raw material consisting of uncured fibrous-glass insulation, nominally 20 kg·m^{-3}, was cut, compiled in multiple layers (i.e., pelts) between two metal platens, and molded into boards under pressure and heat. The thickness and bulk density of a board was controlled by the construction and number of pelts in a board. The glass fiber lay for an assembly is characteristically parallel to the long dimensions of the sheet (i.e., perpendicular to the direction of heat flow in application). After removal from the mold, the sheet was cooled and trimmed to finished panels each having a nominal size of 610 mm by 610 mm.

The technical information for the physical properties of the finished material lot is summarized below:

- production run time period: 3 days (August 14-16, 2017)
- target bulk density: 128 kg·m^{-3} ± 10 %
- target thickness: 25.4 mm
- trimmed panel size: 610 mm × 610 mm
- approximate mold size : 1321 mm × 2540 mm (52 in. × 100 in.)
- number of molded sheets: 57
- number of panels per sheet: 8
- number of panels: 450 (from one lot of material)
- panel color: amber

The number of requested panels was determined based on the number of units required to provide a 10-year inventory for the NIST Office of Reference Materials, plus 30 panels necessary for the thermal characterization of the candidate reference material (Fig. 1).

4.2.2. Production Control

The manufacturer implemented the following controls during the production of the material lot.

- Prior to fabrication, incoming uncured rolls having the same nominal density were selected at random and the gram mass per unit area sampled at six pre-determined locations. The mass average and range were computed and checked against required nominal values and range limits for acceptance.
- During the fabrication process, the molded sheets were monitored at regular intervals by control charting measured data for the thickness, mass, and density.
  - The control limits for the thickness average and range were determined for a subgroup of four measurements taken from each panel location within a sheet (8 panels × 4 measurements per panel = 32 measurements per sheet). The control limits for the thickness average and range were compared against a specified thickness of 25.4 mm and range of 0.8 mm, respectively.
  - The control limits for the mass and density were determined for each of the panels measured. The control limits for the density average and range were compared against the specified density of 128 kg·m^{-3} and tolerance of ±10 %.
- During the fabrication process, the individual sheets were inspected visually for any obvious material defects. After the cutting process, the panels were stacked and crated for protection during transport.

4.3. Delivery, Inspection, and Storage

The 450 finished panels, comprising the lot of material, were delivered to NIST in August, 2017. An inspection of each panel by NIST personnel revealed that 15 panels were substantially damaged and, later, removed from the lot (Sec. 5.3.6). During the review, an identification number from 500 to 949 was sequentially assigned to each panel, permanently marked in black on one edge with a spray-paint template. The material lot was stored for several months in a laboratory workspace at ambient conditions.

4.4. Measurement Methods

The bulk density study required 100 % sampling of the lot of material. The results of the study were used to select a stratified sub-sample for the thermal characterization of the reference material.

4.4.1. Sampling Procedure

The 450 panels were randomly divided into nine groups of 50 panels. Each group of 50 panels was processed through a three-day measurement procedure outlined below.

- *Day 1*: Convection oven, 100 °C
  - The group of 50 panels was placed in a convection oven and heat treated in air at 100 °C for approximately 19 h.
- *Day 2*: Mass measurements, 23 °C
  - Each panel was removed from the oven and weighed nine times every 20 s over three minutes at ambient conditions of 23 °C to establish a mass time history.
  - The completion of mass measurements for a group of 50 panels typically required 3.3 h.
- *Day 3*: Dimensional measurements, 24 °C
  - After weighing, the group of 50 panels was placed (in a different randomization sequence order) in another laboratory at ambient conditions of 24 °C for approximately 21 h.
  - The lateral dimensions (length and width) of each panel were measured by one operator and the thickness dimensions of each panel were measured concurrently by another operator.
  - The completion of lateral and thickness measurements of a group of 50 panels typically required 1.9 h and 2.7 h, respectively.

The entire measurement process for all nine groups of 50 panels (450 panels in total) required 36 days.

4.4.2. Bulk Density

The bulk density, which is defined in Sec. 3.2, was determined for each finished panel from established gravimetric and dimensional measurement procedures that are documented in Sec. 5. The objective of the bulk density study was to assess the homogeneity of the lot, that is, variability between insulation panels (i.e., material variability), thereby providing empirical data for the following:

- quantitative ranking of the material lot by bulk density;
- the upper and lower bulk density limits of the material lot; and,
- detection of any anomalous thermal insulation panels for possible exclusion.

4.4.3. Thermal Characterization

The steady-state thermal transmission measurements (i.e., thermal conductivity) were determined in accordance with ASTM Test Method C 177 [1] using the NIST 500 mm guarded-hot-plate apparatus [18]. In contrast to the 100 % sampling process for the homogeneity study, the thermal conductivity of SRM 1450e was batch certified. Sub-sampling of the insulation material lot was based on the demonstrated approach taken for the development of the previous version, SRM 1450d [11]. The SRM 1450e lot was sub-sampled at three levels of bulk density (low, mid, and high). Quantitative values for these rankings were defined using the results of the homogeneity study (Sec. 5.3). Detailed procedures of the thermal conductivity study and subsequent analysis of data are documented in Sec. 6 and Sec. 7, respectively.

5. Bulk Density Study

This section describes the mass and dimensional measurements, graphical analyses, and tabulated results for mass, panel area, thickness, and bulk density for the insulation panels.

5.1. Mass Measurements

The mass of an insulation panel was determined by the gravimetric method. The measurement station consisted of:

- digital weighing balance (32.1 kg range, 0.0001 kg resolution);
- foot switch for manual event activation; and,
- RS-232 serial interface for the digital balance and a desktop computer.

Following the sampling procedure in 4.4.1, 50 panels were placed in a large convection oven and conditioned at 100 °C for approximately 19 h. Each panel was removed and weighed as a function of elapsed time (Δt). The start time was synchronized with the specimen removal by means of a foot switch and the mass data, in kilograms, were repeatedly acquired from the digital balance every 20 s for 180 s using a computer program.

By measuring the panel mass at equal time intervals and establishing a mass history, the initial mass (m_0) for each panel at time zero (t_0) is determined by regression analysis, thus correcting for the small mass change with time. The mass data were fitted to Eq. (4) using three different computer analysis programs, cross-checked for complete consistency of results.

$$m(t) = m_0 + a(\Delta t) \tag{4}$$

Appendix B provides a graphical analysis of the mass measurements for all 450 insulation panels (500 through 949) and summarizes regression values for m_0 for each panel.

5.2. Dimensional Measurements

After completion of the mass measurements, the 50 panels were placed in a laboratory at ambient conditions of 24 °C for 21 h. The length, width, and thickness measurements of each group of 50 insulation panels were performed concurrently by two operators under ambient conditions of approximately 24 °C and 10 % to 30 % relative humidity. The dimensional measurements were derived from basic length measurements using electronic height gages with digital readouts. The datum plane was defined by a large granite surface plate. A touch probe, providing a consistent contact force, was brought in contact with a polished workpiece placed on the insulation panel. The acquired length value, in millimeters, was transferred to a desktop computer by a USB interface cable and recorded in an electronic spreadsheet.

5.2.1. Lateral Panel Dimensions – Length and Width

Figure 2 illustrates the essential features of the measurement station for the lateral measurements of a panel, consisting of the following instrumentation:

- granite surface plate (1.2 m by 1.8 m, unilateral flatness tolerance of 0.018 mm);
- electronic height gage with digital readout (635 mm range, 0.01 mm resolution);
- bi-directional touch probe (3 mm diameter carbide ball contact point, 0.4 N measuring force); and,

- statistical process control (SPC) data output cable with converter tool to USB communication cable for connection to a desktop computer.

The insulation panel was placed on the granite surface plate in a vertical position and clamped securely between an aluminum sheet and a right-angle support fixture (Fig. 2a). The fixture consisted of an aluminum jig plate (13 mm thick by 560 mm by 560 mm) attached to two right angles (200 mm by 125 mm). The right angles were precision ground square to within 0.051 mm (per 150 mm) and parallel to within 0.006 mm (per 150 mm). The touch probe measurements were carried out with a round polished gage block as the workpiece in contact with the insulation panel.

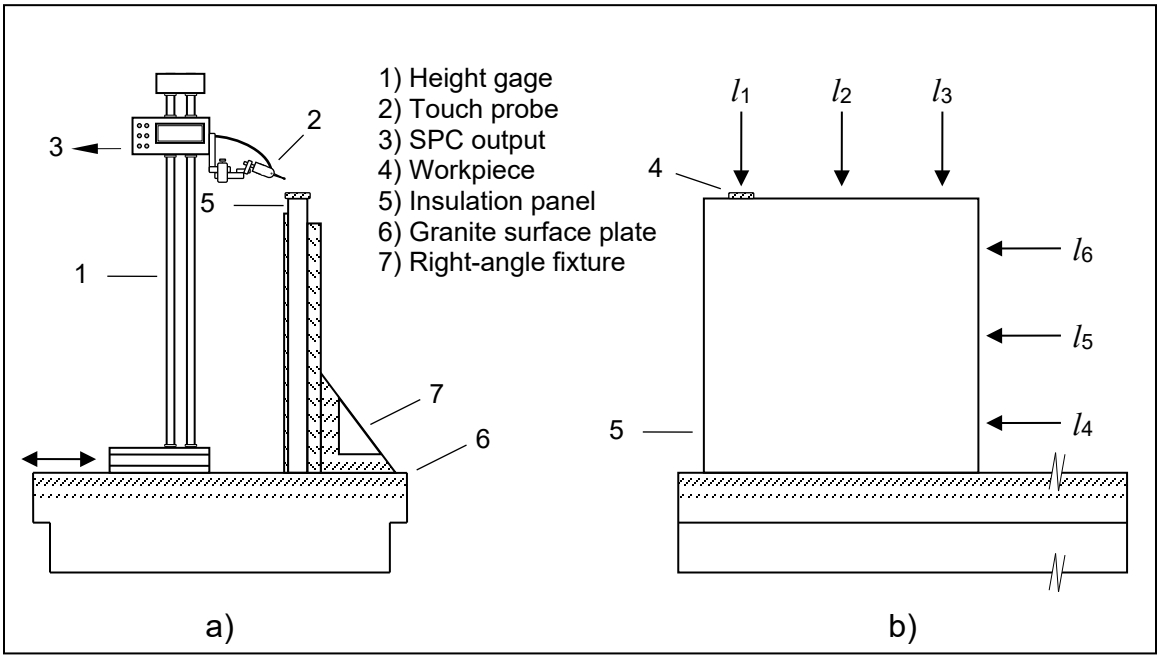

Fig. 2. a) Side view shows height gage and right-angle fixture with insulation panel clamped between the aluminum jig plate and aluminum sheet. b) Front view shows panel length measurements at locations l_1, l_2, l_3, l_4, l_5, and l_6 (clamp fixture and height gage are not shown).

Prior to measuring each panel, a zero-reference plane for the workpiece was established, and the measurement process was checked, at the beginning and end of the process, using a 609.6 mm gage standard consisting of two 304.8 mm (12 in.) gage blocks wrung together. The linear dimensions l_1, l_2, and l_3 in Fig. 2 were obtained by moving the height gage along the surface plate and contacting the workpiece at each location. Afterwards, the panel was unclamped, rotated 90° clockwise, and re-clamped to measure l_4, l_5, and l_6. Pilot testing indicated that data acquired from the two middle locations, l_2 and l_5, were sufficient for the determination of bulk density. As a check, however, one panel from each group was selected, at random, for measurements at all locations (l_1, l_2, l_3, l_4, l_5, and l_6).

For nine panels (IDs 542, 571, 619, 641, 684, 755, 759, 879, and 903), the area of the panel A_p was computed from Eq. (5).

$$A_{\mathrm{p}} = \left(\frac{l_1 + l_2 + l_3}{3} \right) \times \left(\frac{l_4 + l_5 + l_6}{3} \right) \tag{5}$$

The areas (A_{p}) of the other panels were computed from Eq. (6).

$$A_{\mathrm{p}} = l_2 \times l_5 \tag{6}$$

5.2.2. Thickness

Figure 3 illustrates the essential features of the measurement station for the thickness measurements of a panel. The measurement station was the same in function as the station for lateral dimensions except a different electronic height gage (330 mm range, 0.01 mm resolution), desktop computer, and connection cable were used. The insulation panel was placed horizontally on the granite surface plate (Fig. 3a). The thickness measurement locations (L_1, L_2, L_3, L_4, L_5, L_6, L_7, and L_8), each representing the geometric center of a 203 mm by 203 mm subdivision, are shown in Fig. 3b. The thickness and lateral dimensional measurements were conducted concurrently by two operators.

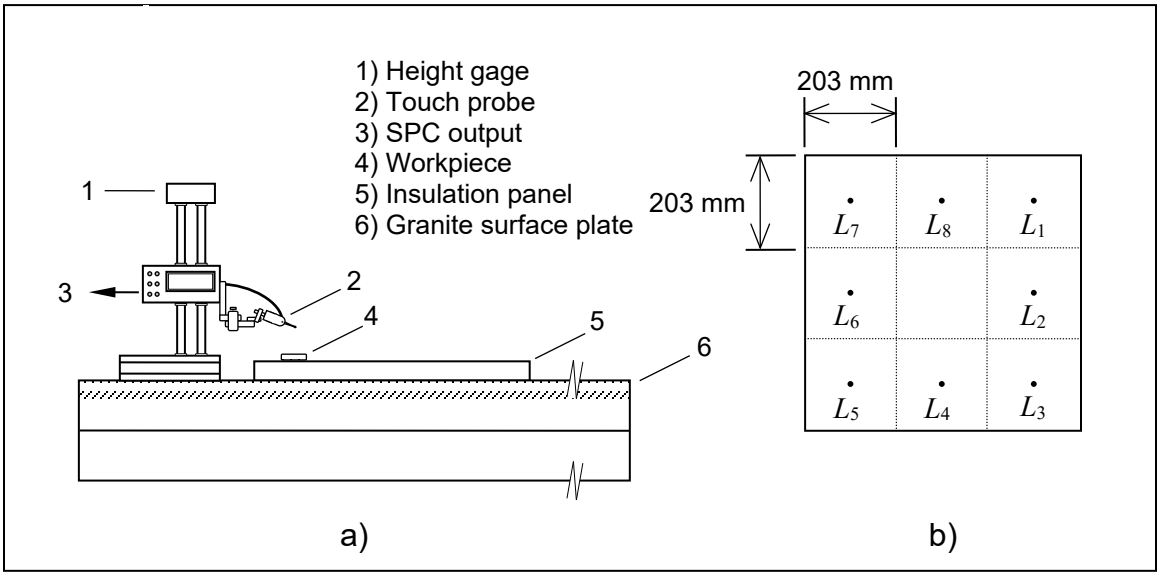

Fig. 3. a) Front view shows 305 mm height gage and insulation panel, with workpiece, on granite surface plate. b) Top view shows the eight measurement locations (L_1 through L_8) each in the geometric center of a 203 mm by 203 mm subdivision of the insulation panel.

Prior to measuring each panel, a zero-reference plane for the workpiece was established, and the measurement process was checked, at the beginning and end of the process, using a 25.4 mm (1 in.) gage block. For the thickness dimensions, the height gage was stationary, and the panel re-positioned so that the touch probe contacted the workpiece at each measurement location. Based on previous testing for 1450d [11], thickness measurements from four locations were sufficient for determination of the bulk density. For each group, one-half of the panels were measured at the corners (L_1, L_3, L_5, and L_7) and the other half, at the mid-centers (L_2, L_4, L_6, and L_8). The pattern was sequentially alternated from panel to

panel. As a check, one panel from each group was selected, at random, for measurements at locations L_1 through L_8.

For nine panels (IDs: 542, 571, 619, 641, 684, 755, 759, 879, and 903), the mean thickness of the panel was computed from Eq. (7). The thicknesses of the other panels were computed using either Eq. (8) or Eq. (9).

$$\bar{L}_p = \left(L_1 + L_2 + L_3 + L_4 + L_5 + L_6 + L_7 + L_8\right)/8 \tag{7}$$

$$\bar{L}_p = \left(L_1 + L_3 + L_5 + L_7\right)/4 \tag{8}$$

$$\bar{L}_p = \left(L_2 + L_4 + L_6 + L_8\right)/4 \tag{9}$$

Appendix C provides a graphical analysis of the thickness measurements for all 450 insulation panels.

5.3. Homogeneity Assessment

The bulk density for a panel (ρ_p) was determined from the gravimetric and dimensional measurements of the panel using Eq. (10)

$$\rho_p = \frac{m_0}{A_p \times \bar{L}_p} \tag{10}$$

where m_0 is the mass of the panel (kg) from Eq. (4); A_p is the area of the panel (m^2) from Eq. (5) or Eq. (6); and, $\bar{L}_p$ is the average panel thickness (m) from either Eq. (7), Eq. (8), or Eq. (9). The mass and dimensional measurements for the 450 panels (acquired in nine groups of 50 panels) were conducted over 36 days from February 28, 2018 to March 19, 2018. The following aggregate data were collected for the 450 panels.

- 4050 mass measurements (9 observations per panel × 450 panels)
- 936 lateral panel dimensions (2 observations per panel × 441 panels + 6 per panel × 9 panels)
- 1836 thickness dimensions (4 observations per panel × 441 panels + 8 per panel × 9 panels)

5.3.1. Tabulated Results

Table 2 summarizes the physical properties of Panel IDs 500 to 949 (450 panels) and includes the quantities: mass (m_0), length (l_2), width (l_5), area (A_s), thickness ($\bar{L}_p$), and bulk density (ρ_p). For the nine panels on which three measurements for length and width were acquired, the value for l_2 and l_5 in Table 2 represent the averages of the three measurements. The values of bulk density presented were rounded to the nearest whole number for certification purposes.

Table 2. Physical properties of SRM 1450e units (450 panels).

Panel ID	Mass (kg)	Length (mm)	Width (mm)	Area (m^2)	Thickness (mm)	Bulk density ($kg \cdot m^{-3}$)
500	1.2143	613.13	610.71	0.37445	25.17	129
501	1.2838	608.41	610.94	0.37170	25.19	137
502	1.3111	612.95	610.76	0.37437	25.05	140
503	1.1666	610.38	608.70	0.37154	25.24	124
504	1.0958	613.25	610.88	0.37462	25.14	116
505	1.2171	608.40	610.65	0.37152	25.13	130
506	1.2291	608.21	610.50	0.37131	25.31	131
507	1.2628	613.31	610.53	0.37444	25.14	134
508	1.1923	610.40	608.84	0.37164	25.08	128
509	1.2015	610.47	612.99	0.37421	25.24	127
510	1.2211	610.41	608.64	0.37152	25.40	129
511	1.1531	610.49	612.76	0.37408	25.17	122
512	1.1970	608.87	610.63	0.37179	25.51	126
513	1.0791	613.35	610.70	0.37457	25.21	114
514	1.2159	608.10	609.68	0.37075	25.26	130
515	1.1350	614.05	610.22	0.37471	25.14	120
516	1.2576	609.09	609.59	0.37130	25.23	134
517	1.1212	611.33	609.56	0.37264	25.04	120
518	1.1508	609.31	610.08	0.37173	25.25	123
519	1.2049	610.64	609.95	0.37246	25.35	128
520	1.2437	609.37	609.50	0.37141	25.30	132
521	1.0972	610.94	609.41	0.37231	25.18	117
522	1.2695	610.03	609.42	0.37176	25.56	134
523	1.0877	610.76	610.06	0.37260	25.42	115
524	1.2054	609.57	609.25	0.37138	25.12	129
525	1.0901	609.96	610.91	0.37263	25.03	117
526	1.1965	609.78	610.36	0.37219	25.56	126
527	1.1155	611.46	609.81	0.37287	25.16	119
528	1.0631	610.43	610.78	0.37284	25.24	113
529	1.2522	609.70	610.21	0.37205	25.28	133
530	1.2509	609.94	609.77	0.37192	25.45	132
531	1.1953	610.69	609.22	0.37205	25.14	128
532	1.0986	609.52	609.87	0.37173	25.25	117
533	1.2520	610.17	610.28	0.37238	25.46	132
534	1.1147	608.86	610.84	0.37192	25.06	120
535	1.2390	610.26	610.07	0.37230	25.47	131
536	1.0709	609.76	610.00	0.37195	25.16	114
537	1.2196	609.76	609.54	0.37167	25.13	131
538	1.0815	609.69	609.90	0.37185	25.26	115
539	1.0983	609.86	609.90	0.37195	25.28	117
540	1.1965	609.33	609.94	0.37166	25.47	126
541	1.1839	609.23	610.53	0.37195	25.66	124
542	1.1642	609.55	610.59	0.37219	25.22	124
543	1.2263	609.68	609.73	0.37174	25.08	132
544	1.2321	610.12	609.74	0.37202	25.38	130
545	1.0898	609.60	609.74	0.37170	25.33	116
546	1.2595	609.45	609.92	0.37172	25.70	132
547	1.2432	609.68	609.53	0.37162	25.44	131
548	1.0909	610.17	609.80	0.37208	25.10	117
549	1.1618	609.96	609.86	0.37199	25.18	124
550	1.1441	610.98	608.44	0.37175	25.02	123
551	1.1306	611.24	613.59	0.37505	25.10	120

Panel ID	Mass (kg)	Length (mm)	Width (mm)	Area (m^2)	Thickness (mm)	Bulk density ($kg \cdot m^{-3}$)
552	1.1481	608.67	610.59	0.37165	25.25	122
553	1.1913	613.16	610.74	0.37448	25.38	125
554	1.0954	610.72	608.70	0.37175	25.36	116
555	1.0810	610.19	613.08	0.37410	25.27	114
556	1.1959	611.24	608.93	0.37220	25.10	128
557	1.1077	611.02	612.99	0.37455	25.03	118
558	1.1311	610.68	608.57	0.37164	25.08	121
559	1.2140	610.40	613.30	0.37436	25.17	129
560	1.1908	610.72	608.57	0.37167	25.56	125
561	1.1269	610.60	612.82	0.37419	25.30	119
562	1.1860	611.15	608.71	0.37201	25.47	125
563	1.1067	613.10	610.92	0.37456	25.21	117
564	1.2095	611.15	608.21	0.37171	25.03	130
565	1.1710	610.26	613.78	0.37457	25.14	124
566	1.2270	609.45	610.31	0.37195	25.15	131
567	1.0811	609.17	609.91	0.37154	25.12	116
568	1.2395	609.33	608.97	0.37106	25.14	133
569	1.1797	609.07	611.35	0.37236	25.04	127
570	1.0837	609.96	610.27	0.37224	25.05	116
571	1.0499	609.94	609.39	0.37169	25.22	112
572	1.1072	609.02	609.66	0.37130	25.00	119
573	1.1919	609.15	610.82	0.37208	25.04	128
574	1.1038	609.96	610.32	0.37227	25.18	118
575	1.2340	610.07	609.40	0.37178	25.30	131
576	1.2042	609.48	609.04	0.37120	25.12	129
577	1.1363	609.14	611.48	0.37248	25.03	122
578	1.2629	609.87	609.28	0.37158	25.22	135
579	1.1390	609.53	610.84	0.37233	25.05	122
580	1.1113	609.39	610.07	0.37177	25.31	118
581	1.2331	610.29	610.15	0.37237	25.43	130
582	1.2621	609.53	609.33	0.37141	25.39	134
583	1.1200	609.33	610.64	0.37208	25.22	119
584	1.2206	609.44	610.17	0.37186	25.39	129
585	1.1042	609.48	610.37	0.37201	24.99	119
586	1.2757	609.64	609.68	0.37169	25.27	136
587	1.1068	610.29	610.06	0.37231	25.08	119
588	1.1941	609.33	609.50	0.37139	25.32	127
589	1.2431	609.86	609.52	0.37172	25.28	132
590	1.1189	609.58	610.72	0.37228	25.13	120
591	1.1318	609.68	610.79	0.37239	25.21	121
592	1.1063	610.20	610.15	0.37231	25.24	118
593	1.1944	609.97	609.74	0.37192	25.55	126
594	1.2049	611.24	609.46	0.37253	25.16	129
595	1.1196	609.70	609.71	0.37174	25.16	120
596	1.2328	610.01	608.52	0.37120	25.35	131
597	1.0667	610.00	611.22	0.37284	25.06	114
598	1.1132	609.71	609.88	0.37185	24.95	120
599	1.2325	610.63	609.90	0.37242	25.09	132
600	1.1839	611.34	609.39	0.37254	25.36	125
601	1.1245	610.93	612.76	0.37435	25.26	119
602	1.0834	610.97	609.01	0.37209	25.15	116
603	1.2356	611.07	613.20	0.37471	25.23	131
604	1.2163	613.85	610.70	0.37488	25.41	128
605	1.1009	608.27	611.07	0.37170	25.24	117

Panel ID	Mass (kg)	Length (mm)	Width (mm)	Area (m^2)	Thickness (mm)	Bulk density ($kg \cdot m^{-3}$)
606	1.1269	608.93	611.00	0.37206	25.00	121
607	1.1974	612.96	610.90	0.37446	25.15	127
608	1.1333	611.06	613.32	0.37478	25.27	120
609	1.2127	610.56	608.74	0.37167	25.56	128
610	1.1830	610.61	608.77	0.37172	25.27	126
611	1.0681	610.64	612.64	0.37410	25.22	113
612	1.2048	609.42	610.70	0.37217	25.11	129
613	1.1222	612.42	610.99	0.37418	25.12	119
614	1.0838	609.01	610.67	0.37190	24.93	117
615	1.2133	612.92	610.77	0.37435	25.07	129
616	1.0739	610.04	609.65	0.37191	24.91	116
617	1.2220	609.97	610.12	0.37216	25.19	130
618	1.2166	609.64	609.29	0.37145	25.21	130
619	1.1462	609.58	610.86	0.37237	25.04	123
620	1.1967	610.14	609.77	0.37205	25.30	127
621	1.1995	609.98	609.85	0.37200	25.44	127
622	1.2408	609.50	609.70	0.37161	25.26	132
623	1.1873	609.63	610.61	0.37225	25.18	127
624	1.2334	609.82	609.78	0.37186	25.32	131
625	1.0681	610.18	609.89	0.37214	25.23	114
626	1.2083	610.31	610.12	0.37236	25.50	127
627	1.2090	609.84	610.01	0.37201	25.28	129
628	1.2655	609.58	610.11	0.37191	25.42	134
629	1.1139	609.96	609.98	0.37206	25.16	119
630	1.1798	609.99	609.71	0.37192	25.65	124
631	1.1458	610.11	610.22	0.37230	25.41	121
632	1.1690	609.32	609.65	0.37147	25.07	126
633	1.1131	608.58	610.69	0.37165	25.16	119
634	1.1969	609.24	609.94	0.37160	25.16	128
635	1.1516	608.89	610.49	0.37172	25.13	123
636	1.2124	609.66	609.98	0.37188	25.26	129
637	1.1165	609.57	610.52	0.37216	25.06	120
638	1.2292	611.30	610.13	0.37297	25.16	131
639	1.0821	609.74	609.74	0.37178	25.02	116
640	1.1022	609.58	610.72	0.37228	25.12	118
641	1.2236	609.94	609.65	0.37185	25.09	131
642	1.1348	610.81	609.94	0.37256	24.99	122
643	1.2552	610.43	609.73	0.37220	25.47	132
644	1.1348	610.77	609.99	0.37256	25.22	121
645	1.1900	609.85	610.07	0.37205	25.10	127
646	1.1848	610.00	610.19	0.37222	25.35	126
647	1.0461	609.94	609.35	0.37167	25.15	112
648	1.1125	609.93	609.74	0.37190	25.05	119
649	1.2090	609.81	610.44	0.37225	25.13	129
650	1.0931	609.17	610.78	0.37207	25.07	117
651	1.2037	612.86	610.89	0.37439	25.27	127
652	1.2684	608.49	611.24	0.37193	25.60	133
653	1.1543	611.71	613.62	0.37536	25.42	121
654	1.0428	611.08	609.73	0.37259	25.24	111
655	1.2361	612.65	611.56	0.37467	25.34	130
656	1.2216	612.92	610.89	0.37443	25.63	127
657	1.1126	609.00	611.14	0.37218	25.06	119
658	1.2353	610.82	612.66	0.37423	25.53	129
659	1.1370	609.19	610.79	0.37209	25.03	122

Panel ID	Mass (kg)	Length (mm)	Width (mm)	Area (m^2)	Thickness (mm)	Bulk density ($kg \cdot m^{-3}$)
660	1.2473	610.23	609.15	0.37172	25.29	133
661	1.0686	610.61	612.56	0.37404	24.95	114
662	1.0688	607.78	610.70	0.37117	25.10	115
663	1.2894	614.05	610.96	0.37516	25.28	136
664	1.0987	608.90	611.06	0.37207	25.35	116
665	1.2091	613.26	611.08	0.37475	25.77	125
666	1.1794	609.37	610.01	0.37172	25.43	125
667	1.0792	610.03	609.83	0.37202	25.29	115
668	1.2438	609.04	610.05	0.37155	25.58	131
669	1.1472	610.65	610.02	0.37251	25.34	122
670	1.1958	609.27	609.34	0.37125	25.01	129
671	1.1507	609.01	611.28	0.37228	25.06	123
672	1.2397	609.98	609.54	0.37181	25.42	131
673	1.1142	609.77	610.34	0.37217	25.24	119
674	1.1842	609.51	609.19	0.37131	25.08	127
675	1.0994	610.76	609.02	0.37197	25.21	117
676	1.1190	609.44	611.94	0.37294	25.10	120
677	1.2038	609.60	609.51	0.37156	25.09	129
678	1.1237	610.41	609.71	0.37217	25.29	119
679	1.2187	610.39	611.05	0.37298	25.36	129
680	1.2901	609.66	610.29	0.37207	25.39	137
681	1.1362	610.83	609.65	0.37239	25.15	121
682	1.1780	609.82	609.63	0.37177	25.62	124
683	1.0627	609.99	610.06	0.37213	25.34	113
684	1.2352	609.99	609.23	0.37162	25.52	130
685	1.0946	609.85	610.81	0.37250	25.21	117
686	1.2398	609.65	610.21	0.37202	25.76	129
687	1.1251	610.29	609.96	0.37225	25.26	120
688	1.2351	610.14	609.74	0.37203	25.36	131
689	1.0795	610.78	610.06	0.37261	25.17	115
690	1.2155	609.67	610.19	0.37202	25.58	128
691	1.0785	610.18	610.96	0.37280	25.31	114
692	1.2003	610.21	610.05	0.37226	25.63	126
693	1.1143	609.14	609.69	0.37139	25.40	118
694	1.1163	610.18	609.96	0.37219	25.63	117
695	1.2005	609.59	609.96	0.37183	25.91	125
696	1.2528	610.13	609.89	0.37211	25.49	132
697	1.1939	609.70	609.72	0.37175	25.26	127
698	1.1148	609.87	609.57	0.37176	25.28	119
699	1.1536	609.01	610.45	0.37177	25.17	123
700	1.2091	610.61	608.81	0.37175	24.98	130
701	1.1737	610.18	612.74	0.37388	24.98	126
702	1.0573	608.92	611.20	0.37217	25.00	114
703	1.1211	612.54	610.47	0.37394	25.01	120
704	1.1226	609.01	610.44	0.37176	24.99	121
705	1.1127	612.29	610.22	0.37363	25.13	119
706	1.1145	611.99	610.96	0.37390	25.39	117
707	1.0425	610.86	609.07	0.37206	25.48	110
708	1.1264	612.27	610.71	0.37392	25.43	118
709	1.1179	610.24	609.28	0.37181	25.19	119
710	1.1557	610.53	608.81	0.37170	25.02	124
711	1.1174	610.60	612.99	0.37429	25.13	119
712	1.2048	610.28	608.83	0.37156	24.94	130
713	1.2851	609.89	612.99	0.37386	24.98	138

Panel ID	Mass (kg)	Length (mm)	Width (mm)	Area (m^2)	Thickness (mm)	Bulk density ($kg \cdot m^{-3}$)
714	1.0779	610.17	608.56	0.37133	25.32	115
715	1.1336	610.00	612.85	0.37384	25.06	121
716	1.3193	610.30	608.75	0.37152	24.99	142
717	1.2909	610.14	613.07	0.37406	24.94	138
718	1.2011	610.58	609.13	0.37192	25.52	127
719	1.2355	609.67	612.26	0.37328	25.30	131
720	1.3767	609.95	608.83	0.37136	25.33	146
721	1.3284	609.99	612.38	0.37355	25.35	140
722	1.3607	610.40	609.15	0.37183	25.21	145
723	1.3262	609.84	613.73	0.37428	25.14	141
724	1.2809	610.81	608.49	0.37167	25.13	137
725	1.2735	612.97	610.21	0.37404	24.96	136
726	1.2297	610.46	608.83	0.37167	25.46	130
727	1.2821	610.19	612.60	0.37380	25.27	136
728	1.3980	610.10	609.27	0.37172	25.12	150
729	1.3592	609.99	611.97	0.37330	25.30	144
730	1.2834	610.55	608.93	0.37178	24.93	138
731	1.3623	609.78	613.46	0.37408	25.08	145
732	1.2800	610.60	608.54	0.37158	25.09	137
733	1.2888	610.02	613.31	0.37413	25.08	137
734	1.2475	610.20	608.76	0.37147	24.97	134
735	1.2737	610.49	613.74	0.37468	25.12	135
736	1.1874	610.26	608.85	0.37156	24.93	128
737	1.2705	610.22	614.47	0.37496	25.05	135
738	1.0391	610.59	608.77	0.37171	25.30	111
739	1.0890	609.96	612.85	0.37381	25.18	116
740	1.2216	610.43	608.24	0.37129	25.11	131
741	1.2260	610.44	614.17	0.37491	25.26	129
742	1.2465	608.49	610.16	0.37128	25.04	134
743	1.3513	610.09	612.69	0.37380	25.44	142
744	1.2295	608.93	610.30	0.37163	25.08	132
745	1.2321	613.39	610.29	0.37435	25.04	131
746	1.2026	611.00	608.91	0.37204	25.41	127
747	1.1931	610.98	612.68	0.37434	25.23	126
748	1.2373	610.78	608.87	0.37189	25.18	132
749	1.2021	610.67	612.56	0.37407	25.26	127
750	1.1349	613.45	610.48	0.37450	25.04	121
751	1.0192	609.97	613.12	0.37399	25.03	109
752	1.1031	610.04	609.24	0.37166	25.24	118
753	1.1877	611.67	609.91	0.37306	25.43	125
754	1.1816	610.14	609.00	0.37158	25.21	126
755	1.1721	612.25	610.34	0.37368	25.22	124
756	1.1368	608.72	611.12	0.37200	25.09	122
757	1.1510	612.53	610.41	0.37389	24.99	123
758	1.2298	609.24	612.05	0.37289	24.99	132
759	1.2094	610.90	612.55	0.37420	24.94	130
760	1.1261	609.99	609.19	0.37160	24.96	121
761	1.1938	610.03	611.81	0.37322	25.20	127
762	1.1065	610.25	608.50	0.37134	24.89	120
763	1.2032	610.54	612.93	0.37422	24.94	129
764	1.1914	609.04	610.10	0.37158	24.89	129
765	1.1415	610.88	612.35	0.37407	25.10	122
766	1.1561	609.17	610.67	0.37200	24.99	124
767	1.2363	609.96	612.90	0.37384	24.97	132

Panel ID	Mass (kg)	Length (mm)	Width (mm)	Area (m^2)	Thickness (mm)	Bulk density ($kg \cdot m^{-3}$)
768	1.1888	610.83	613.29	0.37462	25.06	127
769	1.1913	610.23	608.55	0.37136	25.02	128
770	1.2015	610.17	608.21	0.37111	25.04	129
771	1.2200	610.06	613.60	0.37433	25.03	130
772	1.2281	610.35	611.95	0.37350	25.29	130
773	1.2879	609.80	609.32	0.37156	25.09	138
774	1.2150	610.27	608.99	0.37165	25.34	129
775	1.2229	610.17	612.51	0.37374	25.12	130
776	1.1051	610.04	608.33	0.37111	25.00	119
777	1.1106	610.79	613.94	0.37499	25.25	117
778	1.2303	610.17	607.53	0.37070	25.00	133
779	1.2564	610.78	615.06	0.37567	25.05	134
780	1.0343	608.68	610.21	0.37142	25.26	110
781	1.0574	612.48	610.06	0.37365	25.10	113
782	1.2108	608.81	610.19	0.37149	25.19	129
783	1.2908	613.42	610.21	0.37432	25.15	137
784	1.2445	608.90	610.58	0.37178	25.10	133
785	1.2980	612.51	610.09	0.37369	25.16	138
786	1.2133	608.58	610.65	0.37163	25.15	130
787	1.2394	612.98	610.41	0.37417	25.09	132
788	1.2022	609.50	610.78	0.37227	25.37	127
789	1.1870	611.86	610.48	0.37353	25.32	126
790	1.3524	609.06	610.37	0.37175	25.35	144
791	1.3348	612.43	611.22	0.37433	25.46	140
792	1.2958	610.88	609.04	0.37205	25.44	137
793	1.2516	610.61	612.45	0.37397	25.29	132
794	1.3047	610.45	608.85	0.37167	25.15	140
795	1.3238	610.57	613.51	0.37459	25.18	140
796	1.2453	610.29	608.86	0.37158	25.14	133
797	1.3166	610.43	612.83	0.37409	25.38	139
798	1.2845	610.48	608.88	0.37171	25.20	137
799	1.2752	610.20	612.96	0.37403	25.15	136
800	1.2899	612.53	610.18	0.37375	25.22	137
801	1.3899	610.06	609.10	0.37159	25.30	148
802	1.2870	610.42	608.82	0.37164	25.10	138
803	1.2950	612.39	609.89	0.37349	25.14	138
804	1.2792	610.24	608.79	0.37151	25.35	136
805	1.3505	612.14	610.17	0.37351	25.90	140
806	1.2853	610.46	608.94	0.37173	25.16	137
807	1.3453	610.39	612.82	0.37406	25.32	142
808	1.3367	608.69	610.38	0.37153	25.24	143
809	1.3542	610.18	612.62	0.37381	25.06	145
810	1.4003	607.84	610.52	0.37110	25.94	145
811	1.1939	610.09	609.10	0.37161	25.01	128
812	1.2989	610.80	614.00	0.37503	25.11	138
813	1.1945	612.65	610.13	0.37380	25.04	128
814	1.1711	612.27	610.22	0.37362	25.11	125
815	1.0955	609.20	609.99	0.37161	25.14	117
816	1.1274	612.35	610.44	0.37380	25.11	120
817	1.0940	609.08	610.12	0.37161	25.05	118
818	1.3089	608.42	610.38	0.37137	25.02	141
819	1.2944	612.92	609.98	0.37387	25.06	138
820	1.2559	608.33	610.30	0.37126	25.14	135
821	1.2649	612.88	610.28	0.37403	24.95	136

Panel ID	Mass (kg)	Length (mm)	Width (mm)	Area (m^2)	Thickness (mm)	Bulk density ($kg \cdot m^{-3}$)
822	1.3512	612.97	610.12	0.37399	25.27	143
823	1.2054	608.81	610.32	0.37157	25.34	128
824	1.2529	612.08	610.10	0.37343	25.18	133
825	1.3781	608.51	609.66	0.37098	25.23	147
826	1.3418	610.01	609.05	0.37153	25.14	144
827	1.2697	610.44	612.16	0.37369	25.26	135
828	1.3427	609.98	608.57	0.37122	25.09	144
829	1.3096	610.49	612.88	0.37416	25.09	140
830	1.2117	608.81	610.84	0.37189	25.38	128
831	1.2701	612.31	609.80	0.37339	25.32	134
832	1.3045	609.07	610.27	0.37170	25.12	140
833	1.2640	612.47	610.02	0.37362	25.09	135
834	1.2637	613.49	610.52	0.37455	25.17	134
835	1.1826	610.53	608.12	0.37128	25.37	126
836	1.3120	612.89	610.44	0.37413	24.96	140
837	1.2818	610.38	608.69	0.37153	25.09	138
838	1.2634	608.47	610.16	0.37126	25.02	136
839	1.2320	612.80	610.04	0.37383	25.30	130
840	1.2474	610.48	612.74	0.37407	25.26	132
841	1.2663	608.28	610.21	0.37118	25.15	136
842	1.2642	608.46	610.51	0.37147	25.21	135
843	1.3231	610.21	612.72	0.37389	25.13	141
844	1.2549	610.58	608.79	0.37172	24.92	135
845	1.2709	610.39	609.14	0.37181	25.05	136
846	1.2566	609.10	610.12	0.37162	25.14	134
847	1.3084	610.45	612.68	0.37401	25.01	140
848	1.2754	611.29	610.42	0.37314	25.28	135
849	1.2886	612.77	611.73	0.37485	25.04	137
850	1.1986	609.91	608.93	0.37139	25.12	128
851	1.2540	612.17	610.27	0.37359	25.36	132
852	1.1572	609.84	608.82	0.37128	25.42	123
853	1.1283	612.01	610.08	0.37338	25.10	120
854	1.2418	608.81	610.19	0.37149	25.09	133
855	1.2963	610.40	612.52	0.37388	25.09	138
856	1.2013	609.08	610.20	0.37166	25.24	128
857	1.2644	610.44	612.30	0.37377	25.37	133
858	1.3213	609.98	608.91	0.37142	25.23	141
859	1.3770	612.42	610.47	0.37386	25.39	145
860	1.2756	610.14	608.10	0.37103	25.44	135
861	1.2280	612.96	609.83	0.37380	25.29	130
862	1.0286	610.58	609.05	0.37187	25.15	110
863	1.1286	608.73	610.42	0.37158	25.16	121
864	1.1171	612.84	610.38	0.37407	25.00	119
865	1.0910	608.82	610.45	0.37165	24.99	117
866	1.1855	608.89	609.91	0.37137	25.28	126
867	1.1416	612.46	610.20	0.37372	25.01	122
868	1.2851	612.96	610.48	0.37420	25.03	137
869	1.2729	608.70	610.09	0.37136	25.08	137
870	1.2275	608.94	610.24	0.37160	24.89	133
871	1.2473	612.65	610.27	0.37388	24.94	134
872	1.3339	609.06	609.80	0.37141	25.06	143
873	1.3321	612.06	610.00	0.37336	25.17	142
874	1.2848	608.91	610.06	0.37147	25.30	137
875	1.2625	612.24	610.36	0.37369	25.05	135

Panel ID	Mass (kg)	Length (mm)	Width (mm)	Area (m^2)	Thickness (mm)	Bulk density ($kg \cdot m^{-3}$)
876	1.2221	610.84	608.79	0.37187	25.29	130
877	1.2248	609.84	612.54	0.37355	25.21	130
878	1.3193	610.28	609.26	0.37182	25.08	141
879	1.2783	611.02	612.73	0.37439	25.27	135
880	1.2573	608.68	609.94	0.37126	24.96	136
881	1.2818	613.57	610.22	0.37441	25.10	136
882	1.2651	609.85	610.24	0.37216	25.19	135
883	1.2899	612.46	610.01	0.37361	25.07	138
884	1.3084	613.53	610.29	0.37443	25.01	140
885	1.2040	608.50	610.35	0.37140	24.97	130
886	1.2444	607.97	610.04	0.37089	25.09	134
887	1.2800	613.76	610.46	0.37468	24.96	137
888	1.0696	610.14	607.81	0.37085	25.20	114
889	1.1423	610.28	613.14	0.37419	25.16	121
890	1.2725	610.02	608.46	0.37117	25.03	137
891	1.2792	610.40	612.80	0.37405	25.22	136
892	1.2252	613.22	610.85	0.37459	25.13	130
893	1.2924	609.19	610.66	0.37201	25.01	139
894	1.2903	612.81	610.96	0.37440	25.07	137
895	1.2758	611.65	608.97	0.37248	25.11	136
896	1.2493	610.92	612.52	0.37420	25.42	131
897	1.2487	610.55	609.37	0.37205	25.24	133
898	1.2564	610.56	612.62	0.37404	25.35	133
899	1.2515	610.24	609.15	0.37173	25.03	134
900	1.2305	608.68	610.35	0.37151	25.08	132
901	1.2677	609.95	609.09	0.37151	25.12	136
902	1.2202	612.10	610.28	0.37355	25.35	129
903	1.2468	610.09	608.83	0.37144	25.10	134
904	1.3496	612.19	610.26	0.37360	25.15	144
905	1.2547	610.42	608.98	0.37173	25.09	135
906	1.3728	612.37	610.44	0.37382	25.17	146
907	1.2670	610.34	608.82	0.37159	25.19	135
908	1.2836	610.10	608.69	0.37136	25.34	136
909	1.3282	612.53	610.28	0.37382	25.54	139
910	1.2517	610.17	608.49	0.37128	25.44	133
911	1.1908	610.38	613.69	0.37458	25.16	126
912	1.1459	610.70	612.50	0.37405	25.13	122
913	1.1798	612.48	610.35	0.37383	25.03	126
914	1.2010	608.86	610.30	0.37159	25.19	128
915	1.1716	610.67	612.45	0.37401	25.08	125
916	1.1999	610.45	611.96	0.37357	25.32	127
917	1.1939	610.57	609.05	0.37187	25.50	126
918	1.1892	611.74	610.29	0.37334	25.29	126
919	1.3409	610.06	609.13	0.37161	25.26	143
920	1.2255	611.90	610.51	0.37357	25.36	129
921	1.2762	608.97	610.26	0.37163	25.15	137
922	1.2639	608.52	610.02	0.37121	25.25	135
923	1.2104	610.58	612.78	0.37415	25.34	128
924	1.1051	608.96	609.82	0.37136	25.31	118
925	1.2767	610.41	612.38	0.37380	26.42	129
926	1.2763	610.69	612.11	0.37381	25.31	135
927	1.2131	612.48	610.41	0.37386	25.19	129
928	1.2186	612.61	610.43	0.37396	25.19	129
929	1.3198	608.76	611.28	0.37212	25.38	140

Panel ID	Mass (kg)	Length (mm)	Width (mm)	Area (m^2)	Thickness (mm)	Bulk density ($kg \cdot m^{-3}$)
930	1.3328	612.63	610.88	0.37424	25.32	141
931	1.2586	608.75	610.22	0.37147	25.37	134
932	1.2841	613.18	611.19	0.37477	25.30	135
933	1.2448	610.15	608.99	0.37158	25.05	134
934	1.1353	608.85	610.15	0.37149	25.29	121
935	1.2008	610.30	612.70	0.37393	25.17	128
936	1.2372	608.99	610.06	0.37152	25.25	132
937	1.2058	612.69	610.77	0.37421	25.24	128
938	1.1966	610.19	609.00	0.37161	25.40	127
939	1.2365	608.50	610.21	0.37131	25.02	133
940	1.2506	608.81	610.07	0.37142	25.13	134
941	1.2717	610.66	612.14	0.37381	25.20	135
942	1.2540	609.00	610.00	0.37149	25.20	134
943	1.2197	610.46	612.06	0.37364	25.24	129
944	1.3372	610.14	608.18	0.37108	25.75	140
945	1.2320	608.89	610.08	0.37147	25.19	132
946	1.1883	612.91	610.56	0.37422	25.08	127
947	1.2586	608.98	610.47	0.37176	25.35	134
948	1.1452	610.50	612.83	0.37413	25.19	122
949	1.2661	613.53	610.57	0.37460	25.15	134

5.3.2. Graphical Analyses

The quantities in Table 2 – mass, length, width, area, thickness, and bulk density – were subjected to a four step graphical analysis to investigate the homogeneity of the material lot (i.e., between-panel results). For each set of data, the graphical analysis verified the underlying assumptions [19] of an ideal measurement process: a) stability, that is, fixed location and variation, b) randomness, and c) normality. It should be noted that initial diagnostic checks, using similar graphical data analyses (not presented), were applied to each group (50 panels) of data immediately after measurement completion to verify that measurement process was in control.

Figures 4 through 9 illustrate the four step graphical analysis [20] for panel mass (m_0), length (l_2), width (l_5), area (A_p), thickness (L_p), and bulk density (ρ_p), respectively, for the 450 panels. Each figure consists of 4 plots: a) run-sequence plot; b) lag plot; c) histogram; and d) normality plot. The four-step method was applied for verification of the four characteristics indicating statistical control of a process.

1) Run sequence plot plots values in the order obtained versus a sequence surrogate index (x_i versus i) and checks for systematic and random changes.
2) Lag plot plots adjacent values (x_i versus x_{i-1}) and also checks for randomness (specifically, lack of autocorrelation).
3) A histogram of values (x_i) checks the frequency distribution.
4) Normal probability plot of values (of x_i) checks the normality assumption.

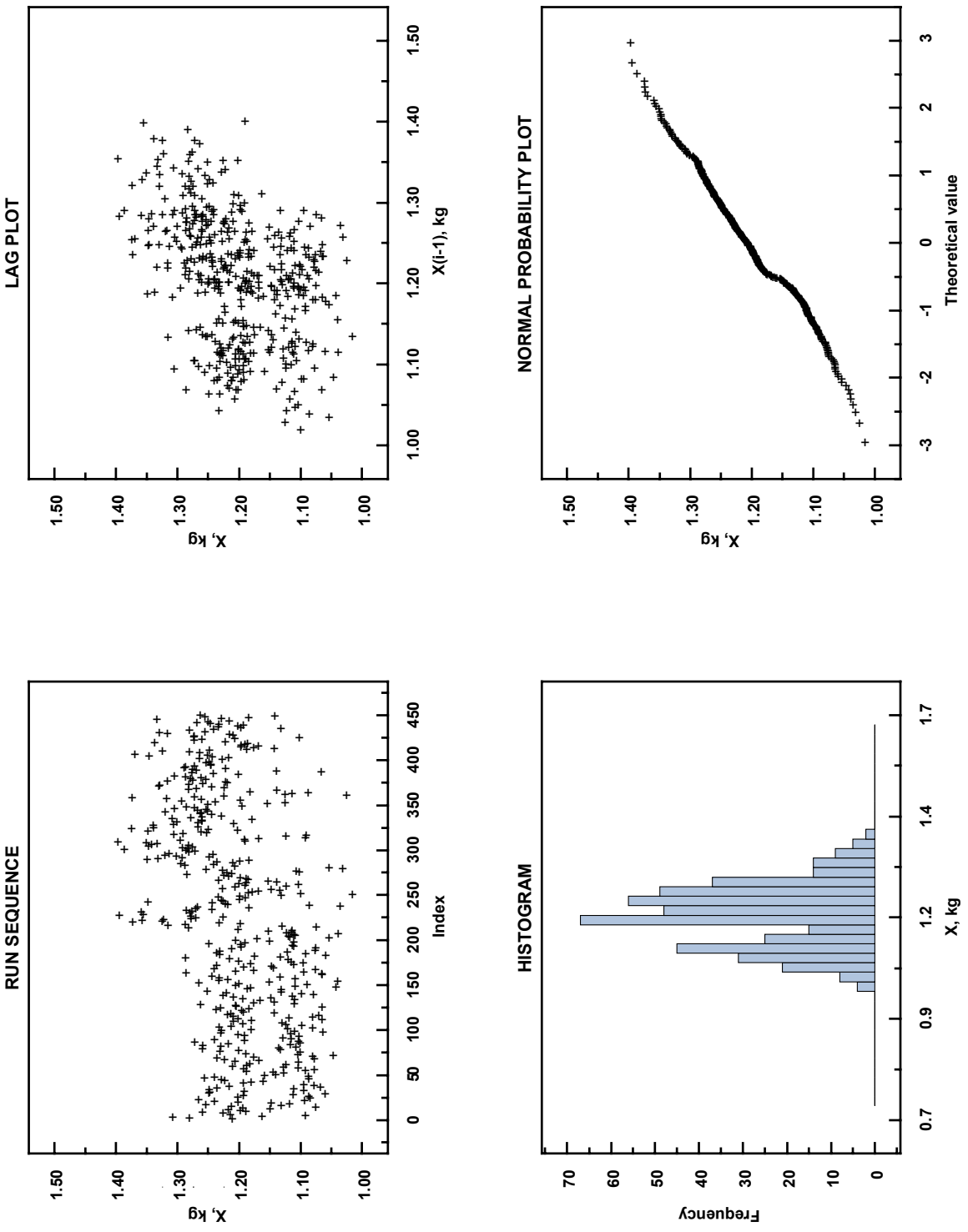

Fig. 4. a) Graphical analysis of panel mass (n = 450): (a) run sequence plot, (b) lag plot, (c) histogram, (d) normal probability plot (normality index). Summary statistics: mean = 1.2059 kg, standard deviation = 0.0784 kg, range = 0.3811 kg.

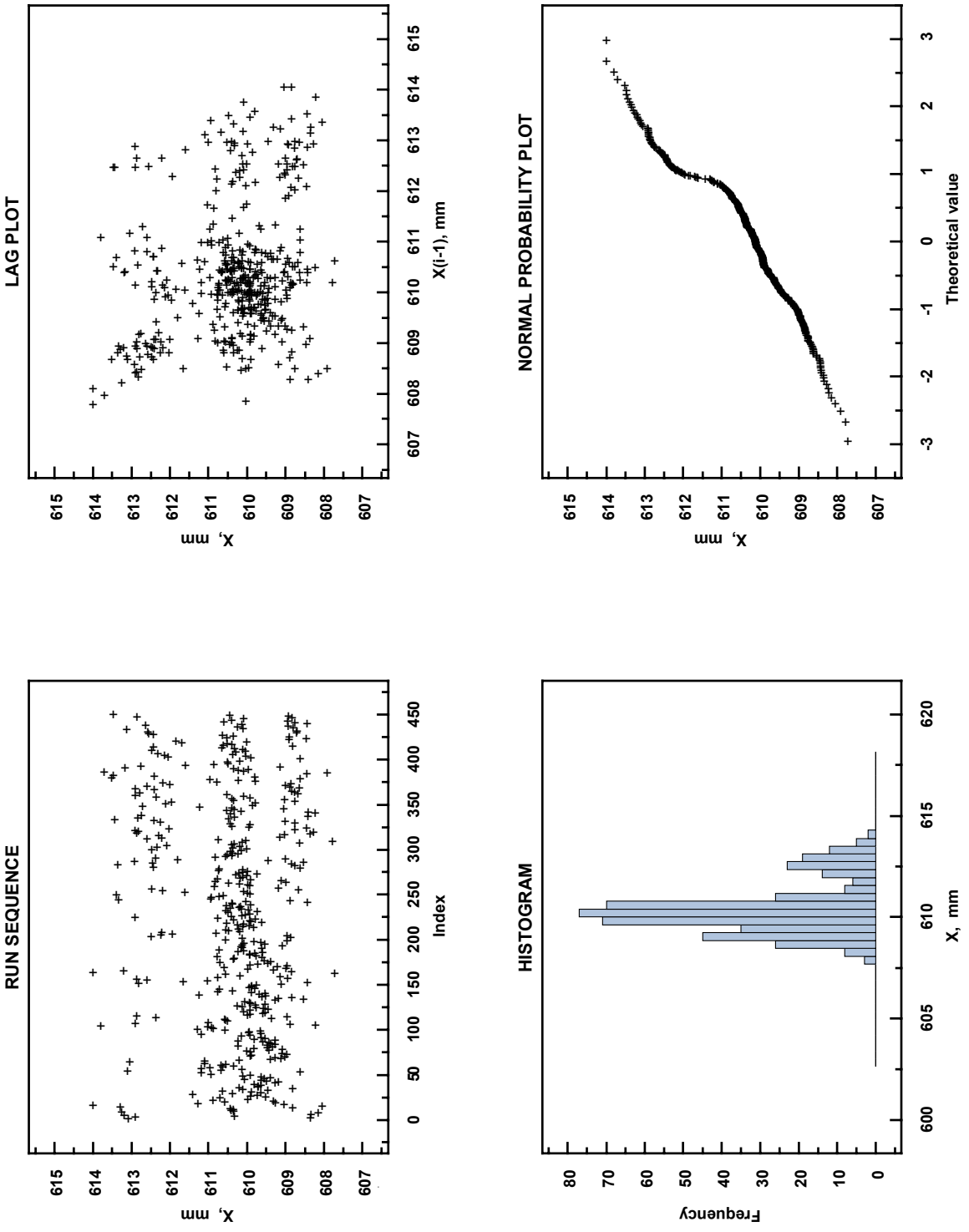

Fig. 5. a) Graphical analysis of panel length (n = 450): (a) run sequence plot, (b) lag plot, (c) histogram, (d) normal probability plot (normality index). Summary statistics: mean = 610.40 mm, standard deviation = 1.30 mm, range = 6.27 mm.

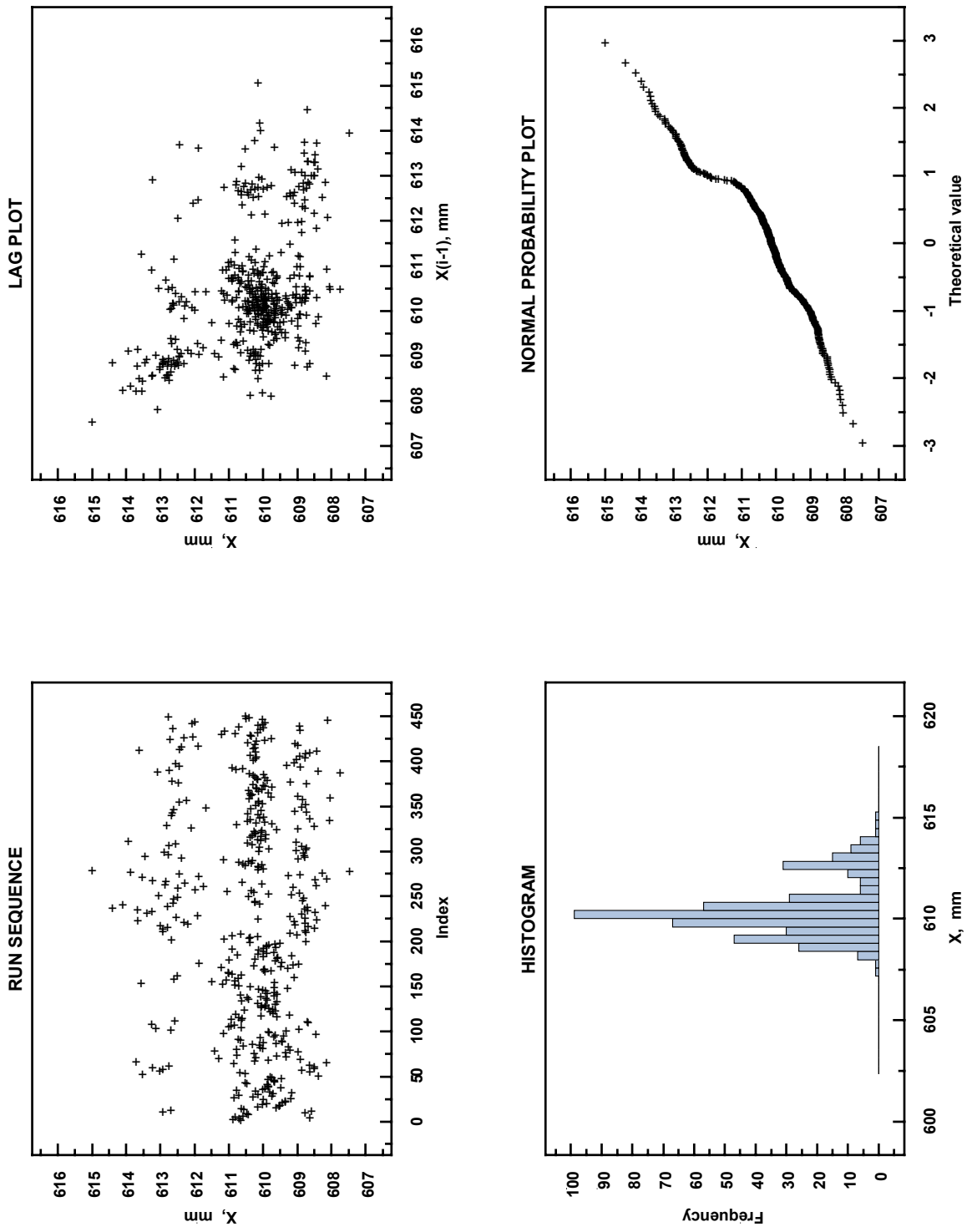

Fig. 6. a) Graphical analysis of panel width (n = 450): (a) run sequence plot, (b) lag plot, (c) histogram, (d) normal probability plot (normality index). Summary statistics: mean = 610.42 mm, standard deviation = 1.35 mm, range = 7.53 mm.

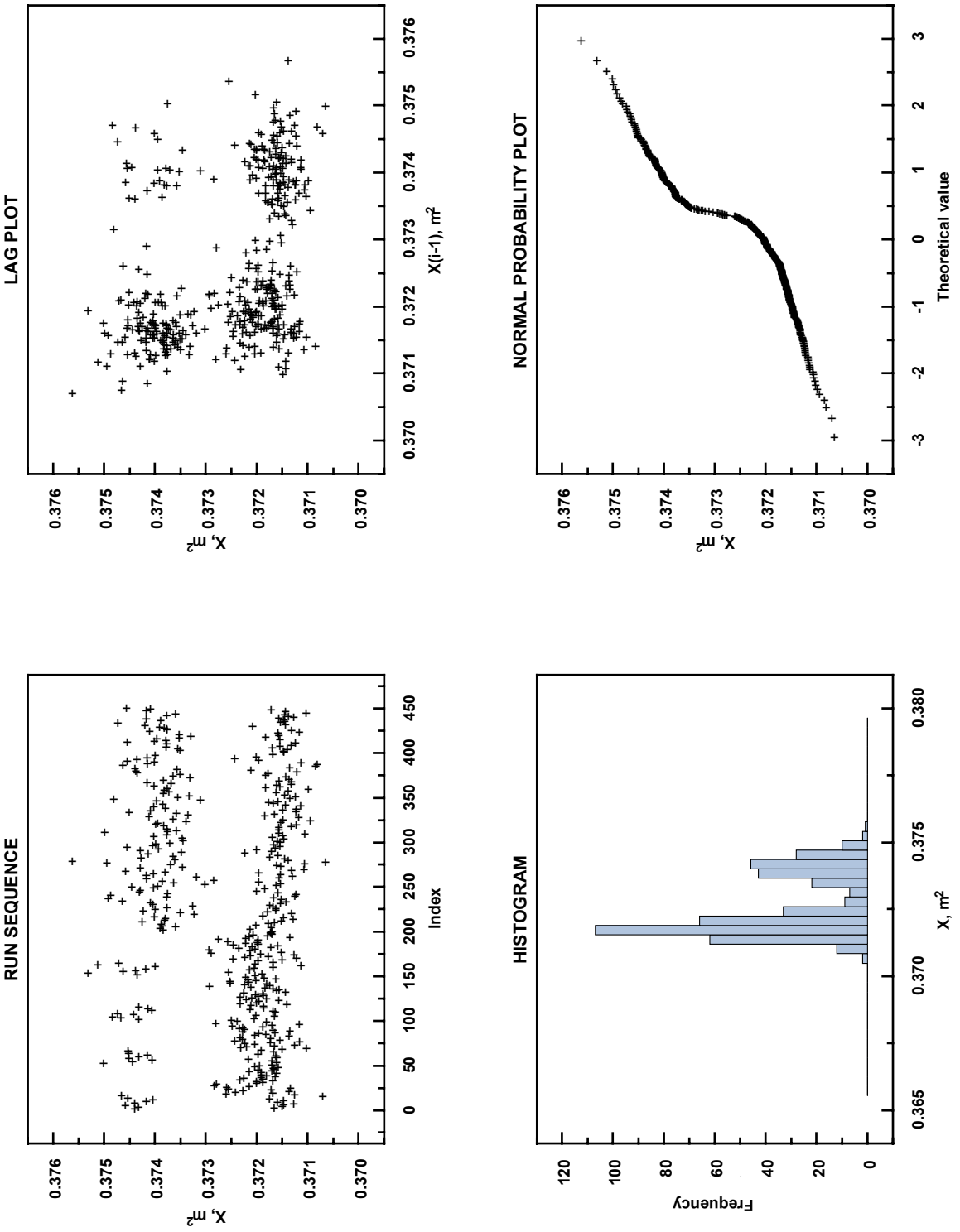

Fig. 7. a) Graphical analysis of panel area (n = 450): (a) run sequence plot, (b) lag plot, (c) histogram, (d) normal probability plot (normality index). Summary statistics: mean = 0.37260 m^2, standard deviation = 0.00118 m^2, range = 0.00497 m^2.

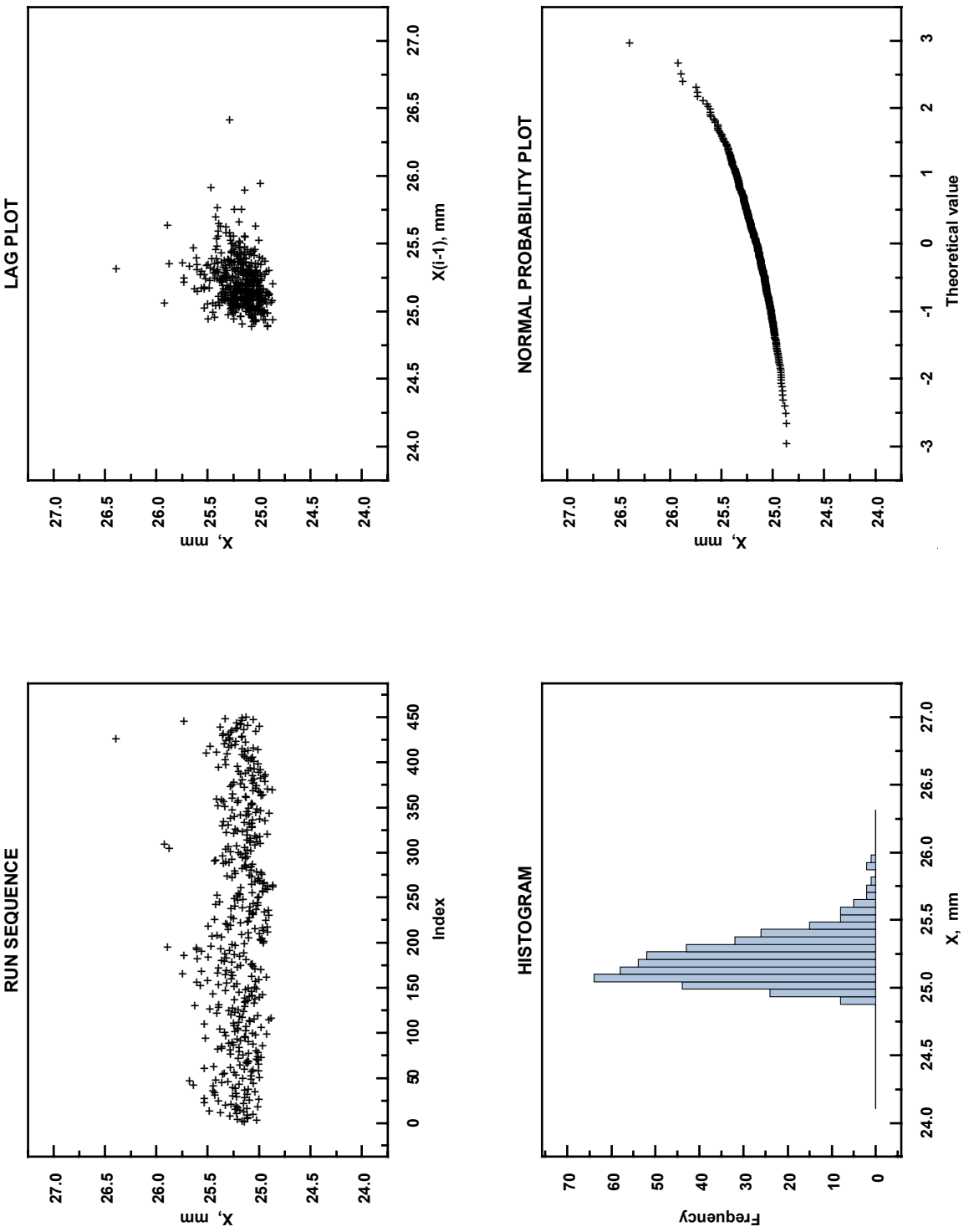

Fig. 8. a) Graphical analysis of panel thickness (n = 450): (a) run sequence plot, (b) lag plot, (c) histogram, (d) normal probability plot (normality index). Summary statistics: mean = 25.21 mm, standard deviation = 0.18 mm, range = 1.53 mm.

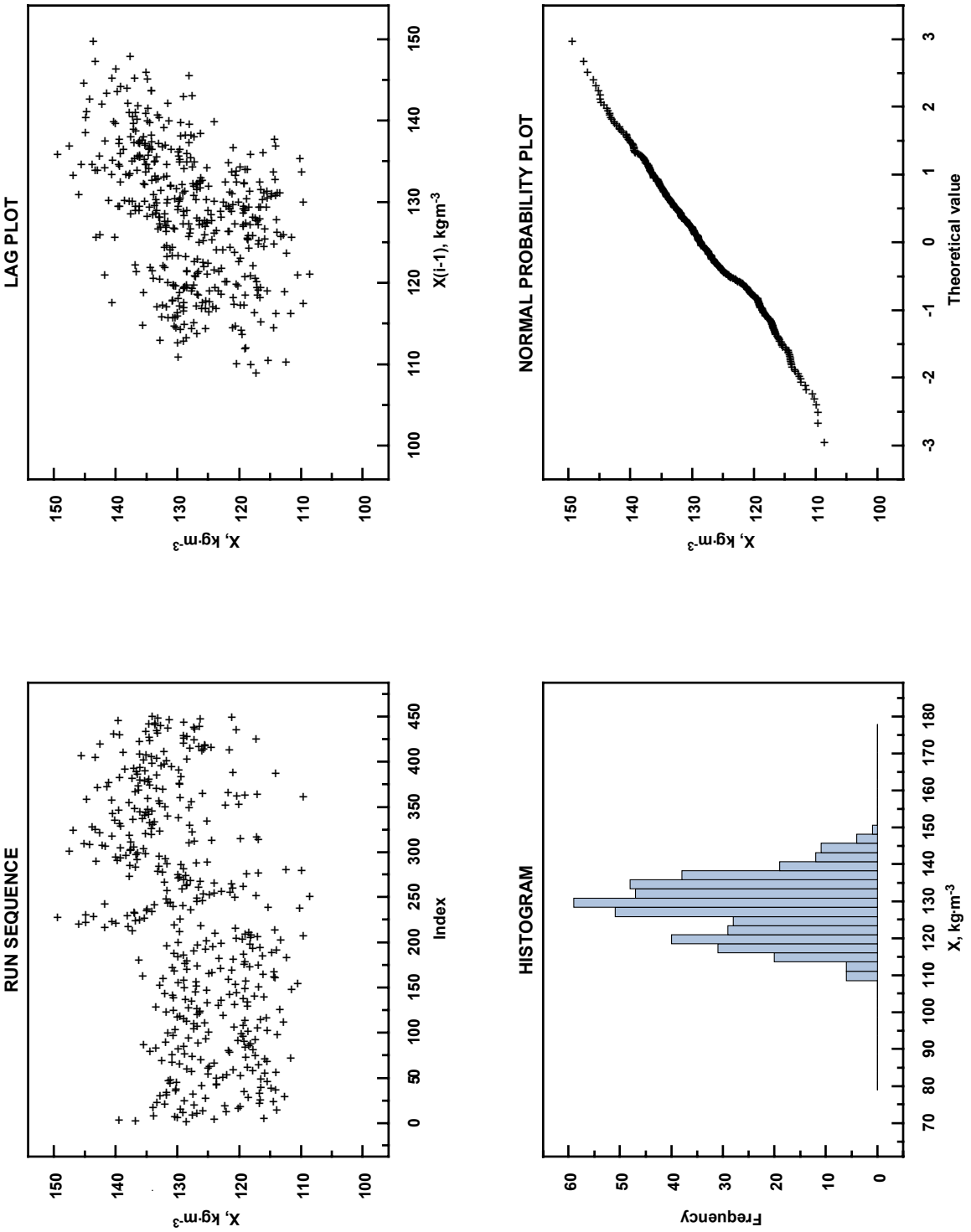

Fig. 9. a) Graphical analysis of panel bulk density (n = 450): (a) run sequence plot, (b) lag plot, (c) histogram, (d) normal probability plot (normality index). Summary statistics: mean = 128.4 kg·m^{-3}, standard deviation = 8.2 kg·m^{-3}, range = 40.9 kg·m^{-3}.

Diagnostic plots of the forms shown in Fig. 4 through 9, the so-called 4-plots, and in Appendix B and Appendix C, were done throughout the data logging stages of the experiment to check the integrity of the data as the data were being taken, to check for outlying points or entire outlying samples, and to check that values of m_0, l_2, l_5, A_p, $\overline{L}_p$, and the resultant ρ_p were within their anticipated ranges.

5.3.2.1. Panel Mass (m_0)

In Fig. 4 (m_0), there is indication of bimodality, that is, two underlying populations of masses. This quality is evident in the histogram (directly visible), the normal probability plot (two line segments with comparable slopes but different intercepts conjoined in a single plot), and the run sequence plot (high/low excursions from the mean values). The normal (Gaussian) probability plot is compatible with a normality assumption for the data, with the possible exception of just a few of the tail (extreme end) points, which are routinely observed with empirical data. The most probable source of variation in panel mass is from the manufacturing process itself.

5.3.2.2. Panel Length and Width (l_2 and l_5)

In Fig. 5 and Fig. 6 (l_2 and l_5, respectively), there are suggestions of multimodality, that is, two or more underlying populations of lengths and widths, respectively. This quality is evident in the histograms (directly visible), the normal probability plots (multiple line segments with comparable slopes but different intercepts conjoined in a single plot), and the run sequence plots (high/low excursions from the mean values). The presence of multi-modes is almost certainly due simply to the fact that the panels are not quite square, so that pairs of sides do not match exactly in length. The lag sequence plots are not suggestive of any autocorrelation, or systematic departure from randomness.

5.3.2.3. Panel Area (A_p)

In Fig. 7 (A_p), both the histogram and normal probability plots are strongly suggestive of underlying bimodality, viz. two underlying populations. However, the difference in the histogram peaks of approximately 0.5 % is not considered significant. While not suggestive of autocorrelation, the patterned heavy overstrike in the lag plot is apparent.

5.3.2.4. Panel Thickness (L_p)

In Fig. 8 (L_p), the histogram and normal probability plots are well-behaved, with the exception of some obvious outlying tail observations (common with empirical data, as mentioned in Sec. 5.3.2.1 for Fig. 4). The flywheel appearance of the lag plot is attributable to only a small subset of the overall set of measurements and is not indicative of systematic behavior. The obvious, approximately contiguous, high-lying and low-lying points in the run sequence plot may be the cause of these linear excursions from the random mass at the center of the lag plot.

5.3.2.5. Panel Bulk Density (ρ_p)

In Fig. 9 (ρ_p), the plots are well-behaved, meaning that the measurement process for ρ_p was in statistical control. It is interesting to note that much of the bi-modality present in the mass and area plots (Fig.4 and Fig. 7, respectively) does not appear in the density plots due, in part, to stronger contributions from thickness (Fig. 8).

5.3.3. Summary Statistics

Table 3 provides summary statistics for mass, length, width, area, thickness, and bulk density of the 450 panels. Overall, the mean values for length and width are within acceptable limits. A few panels that have linear dimensions greater than 613 mm (Figs. 5 and 6) could necessitate further trimming by the customer for installation in a heat-flow-meter apparatus [2]. The mean thickness of 25.21 mm is very near the target of 25.4 mm and the mean bulk density of 128.4 kg·m^{-3} is nearly the same as the target density of 128 kg·m^{-3}. The small standard deviation for thickness (0.18 mm) indicates that most of the panels are near the mean thickness. Unfortunately, the large range (1.53 mm) indicates that some of the panels are unacceptably thin or thick, as discussed in Sec. 5.3.4. The exceptionally large range for bulk density (40.9 kg·m^{-3}) is more than three times larger than the requested tolerance of 12.8 kg·m^{-3} (10 %) in Sec. 4.2.1.

Table 3. Summary statistics for the SRM 1450e production run (450 panels)

Statistic	Mass (kg)	Length (mm)	Width (mm)	Area (m^2)	Thickness (mm)	Bulk density (kg·m^{-3})
Mean	1.2059	610.4	610.4	0.37260	25.21	128.4
Std. dev. (*s*)	0.0784	1.3	1.3	0.00118	0.18	8.2
Range	0.3811	6.3	7.5	0.00497	1.53	40.9
Minimum	1.0192	607.8	607.5	0.37070	24.89	108.9
Maximum	1.4003	614.1	615.1	0.37567	26.42	149.8
Rel. std. dev. (%)	6.5 %	0.2 %	0.2 %	0.3 %	0.7 %	6.4 %

5.3.4. Between- and Within-Panel Thickness Variations

Figures 10a and 10b plot the individual panel thickness mean and standard deviation, respectively, for the 450 panels. Each plot is rank ordered from lowest to highest value (indexed from 1 to 450).

5.3.4.1. Between-Panel Variation

Figure 10a shows graphically that the mean panel thickness ranges from 24.89 mm to 26.42 mm. There are five panels outside the upper limit equal to the grand mean plus three times the standard deviation (+3*s*). These five panels (665, 695, 805, 810, and 925) were removed from the material lot. There are no panels outside the lower limit equal to the grand mean minus three times the standard deviation (–3*s*).

5.3.4.2. Within-Panel Variation

Figure 10b plots the standard deviation of the thickness measurements for each panel indicating the range of panel thickness variation. The individual panel variation ranges from 0.02 mm to approximately 1.6 mm. From Fig. 10b, an upper limit cutoff of 0.55 mm was selected to remove the extreme outlying data points. The eleven panels outside this limit (546, 560, 656, 658, 665, 753, 805, 810, 857, 910, and 925) were removed from the material lot. Four of the panels (665, 805, 810, and 925) were previously identified for removal due to unacceptable thickness (Sec. 5.3.4.1). For most of the data, the variation is less than 0.35 mm, or about 1 % of the grand mean panel thickness given in Table 3.

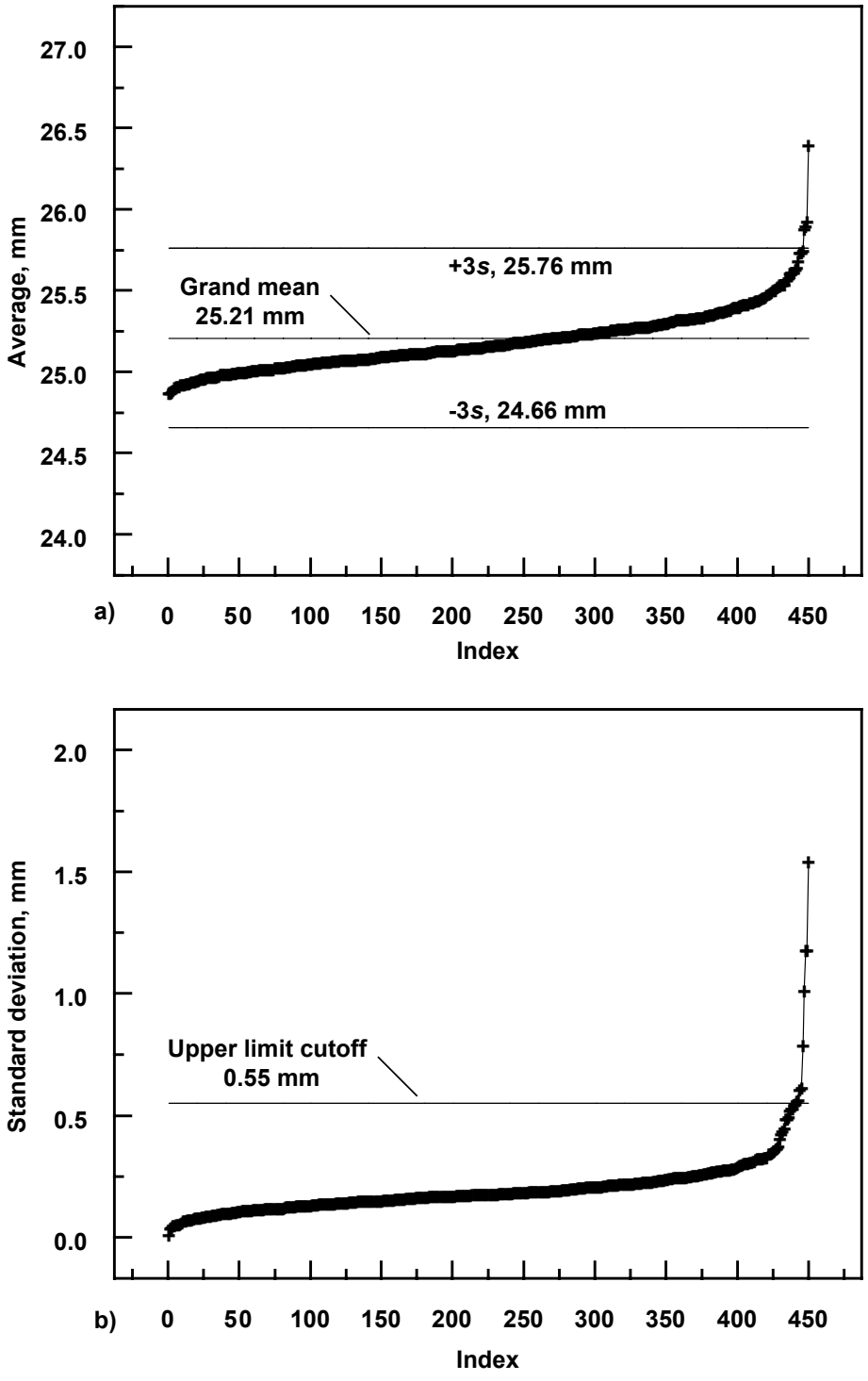

Fig. 10. a) Graphical analysis of between-panel thickness variation represented by the means of the individual panel thickness measurements. Panels outside the control limits of three times the standard deviation (±3*s*, where *s* equals 0.18 mm from Table 3) were removed. b) Graphical analysis of within-panel thickness variation represented by the standard deviations of the individual panel thickness measurements. The upper limit cutoff of 0.55 mm was selected arbitrarily.

5.3.5. Between-Panel Bulk Density Variations

Figure 11 plots the individual panel bulk density for all 450 panels, rank ordered from lowest to highest value.

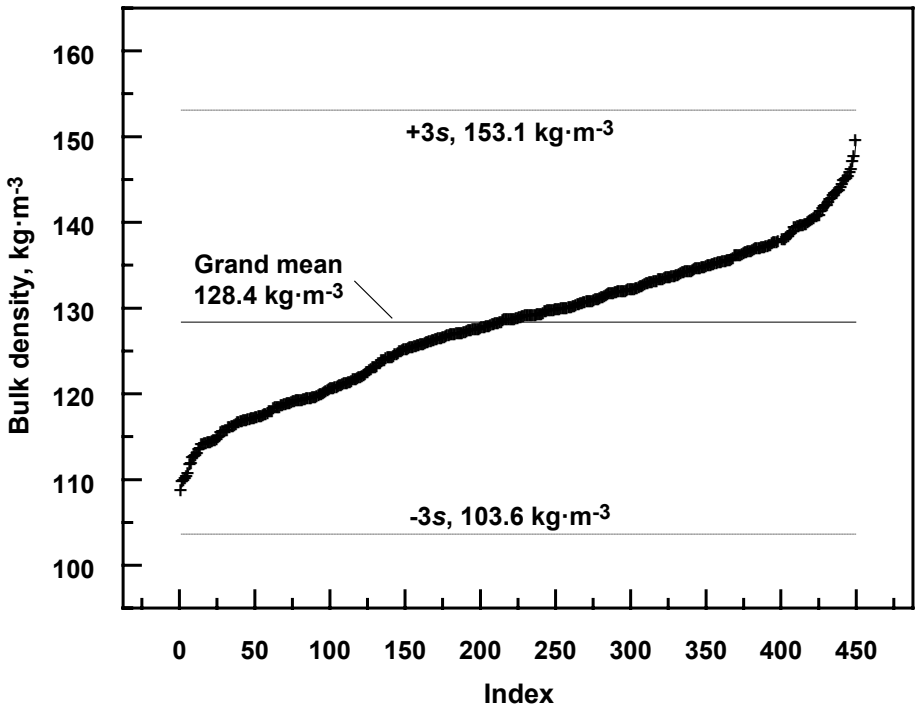

Fig. 11. Graphical analysis of between-panel bulk density variation.

5.3.6. Rejected Panels

There were 27 panels rejected from the material lot for the reasons stated below. The excluded panels represented 6 % (27 of 450) of the material lot (423 panels were accepted, or 94 %).

- Unacceptable thickness (1.1 %): 665, 695, 805, 810, and 925
- Unacceptable thickness variation (1.6 %): 546, 560, 656, 658, 753, 857, 910
- Material defect (1.8 %): 547, 574, 686, 699, 764, 819, 895, 944
- Damaged during shipping (1.6 %): 674, 741, 742, 744, 745, 849, 949

5.4. Uncertainty Assessment Panel Density

Substituting Eq. (6) for the area term (A_p) in Eq. (1) and utilizing the terminology described for measured mass and thickness yields Eq. (11).

$$\rho_p = \frac{m_0}{l_2 \times l_5 \times L_p} \tag{11}$$

For the simple multiplicative expression in Eq. (11), the relative uncertainties associated with each component are combined in quadrature.

$$u_{c,\mathrm{r}}\left(\rho_{\mathrm{p}}\right)=\frac{u_c\left(\rho_{\mathrm{p}}\right)}{\rho_{\mathrm{p}}}=\sqrt{\left(\frac{u\left(m_0\right)}{m_0}\right)^2+\left(\frac{u\left(l_2\right)}{l_2}\right)^2+\left(\frac{u\left(l_5\right)}{l_5}\right)^2+\left(\frac{u\left(L_{\mathrm{p}}\right)}{L_{\mathrm{p}}}\right)^2} \quad (12)$$

Substituting the standard uncertainties for m_0, l_2, l_5, and, L_{p} derived in Appendix D and the minimum quantity estimates from Table 3 yields the following relative uncertainty estimate for bulk density.

$$u_{c,\mathrm{r}}\left(\rho_{\mathrm{p}}\right)=\sqrt{\left(\frac{0.000397}{1.0192}\right)^2+\left(\frac{0.315}{607.8}\right)^2+\left(\frac{0.315}{607.5}\right)^2+\left(\frac{0.186}{24.89}\right)^2}\ =\ 0.00752 \quad (13)$$

The relative expanded uncertainty, $U_{\mathrm{r}}(\rho)$, is defined for a coverage factor of $k = 2$ in Eq. (14).

$$U_{\mathrm{r}}\left(\rho_{\mathrm{p}}\right)=k u_{\mathrm{c,r}}=2\,u_{\mathrm{c,r}}\left(\rho_{\mathrm{p}}\right)=0.015 \quad (14)$$

Expressed as a percent (× 100), $U_{\mathrm{r}}\left(\rho_{\mathrm{p}}\right)$ is equal to 1.5 %.

5.5. Bulk Density Metrological Traceability

Table 4 summarizes the calibration information for the electronic balance, gage blocks, and surface plate used to carry out the bulk density measurements. The calibration uncertainties were included in the extended uncertainty analysis (Appendix D). Internal checks (Items 2, 5, and 6) were conducted by the operators during the measurement process. The check of the Mettler balance (Item 2) was conducted before and after the mass measurements of each group of 50 panels. The digital height gages (Items 5 and 6) were checked before and after the dimensional measurements of each group of 50 panels.

Table 4. Calibration information for the bulk density measurements.

Item	Equipment Calibrated	Description of standard	Calibration		
			Organization	Date	Cert. Number
1	Mettler balance SG32001DL	Weight set 632 traceable to NIST	Mettler Toledo	2017	020218-133-032317
2	Mettler balance check	1 kg and 500 g masses	732.03		
3	1 in. gage block EBW1	Standards of the United States	NIST	2018	290351-18
4	12 in. gage blocks L4M041 & L4M042	Standards of the United States	NIST	2018	290351-18
5	Mitutoyo 0 to 300 mm height gage 192-670-10	1 in. gage block	732.03		
6	Mitutoyo 0 to 600 mm height gage 192-672-10	24 in. gage block	732.03		
7	Starrett surface plate	Traceable to NIST	LTI Metrology	2017	NIS001-10-41425-1
8	Troemner E/B weight set 4000010240	Reference masses traceable to NIST (684/289871-17)	Troemner LLC	2017	967451-1

6. Thermal Conductivity Study

This section describes the experimental design, specimens, guarded-hot-plate measurements, and determinations of thermal conductivity.

6.1. Experimental Design

The experimental design for the determination of thermal conductivity (λ) was based on the assumed model for bulk density (ρ), temperature (T_m), and air pressure (p) given in Eq. (15).

$$\lambda = (\rho, T, p) = a_0 + a_1\rho + a_2 T_m + a_3 p \tag{15}$$

where ρ is the bulk density of the 500 mm diameter specimen (discussed in Sec. 6.2.4), T_m, is the mean temperature, and p is the atmospheric pressure. The settings selected for each variable in Eq. (15) are given below:

- ρ 3 levels (low, mid, and high);
- T_m 5 levels (280 K, 300 K, 320 K, 340 K, 360 K); and,
- p 3 levels (60 kPa, 80 kPa, 100 kPa).

6.2. Specimens

For thermal characterization, a stratified density sample of 30 panels was selected from the lot of 450 panels (Table 2), excluding the rejected panels in Sec. 5.3.6. Because bulk density is a material property of a panel, this factor cannot be set as precisely as the other factors – temperature (T_m) and pressure (p).

6.2.1. Bulk Density Settings

The bulk densities of the 450 panels in Table 2 were ranked from lowest to highest and the following panels were selected.

- Low range: 107 kg·m^{-3} to 114 kg·m^{-3}
  ID: 751, 707, 862, 780, 738, 654, 647, 571, 683, and 781 (10 panels having the smallest bulk density)
- Mid-range: 126 kg·m^{-3} to 133 kg·m^{-3}
  ID: 634, 856, 736, 769, 914, 830, 811, 850, 627, and 594 (10 panels having a bulk density near the lot average)
- High range: 144 kg·m^{-3} to 152 kg·m^{-3}
  ID: 729, 828, 809, 859, 722, 731, 906, 720, 825, and 801 (10 panels having the largest bulk density)

6.2.2. Preparation

The specimens were hand-cut into 500 mm diameter discs for testing in the NIST 500 mm Guarded-Hot-Plate Apparatus using a sharp blade and a metal cutting template manufactured by the NIST Instrument Shop (Fig. 12). Each 500 mm diameter specimen was labeled with the same 3-digit identification number assigned to the panel (Table 2).

6.2.3. Conditioning

The 500 mm diameter specimens were placed in a large test chamber (Fig. 13) and were conditioned at 100 °C for 17.5 h.

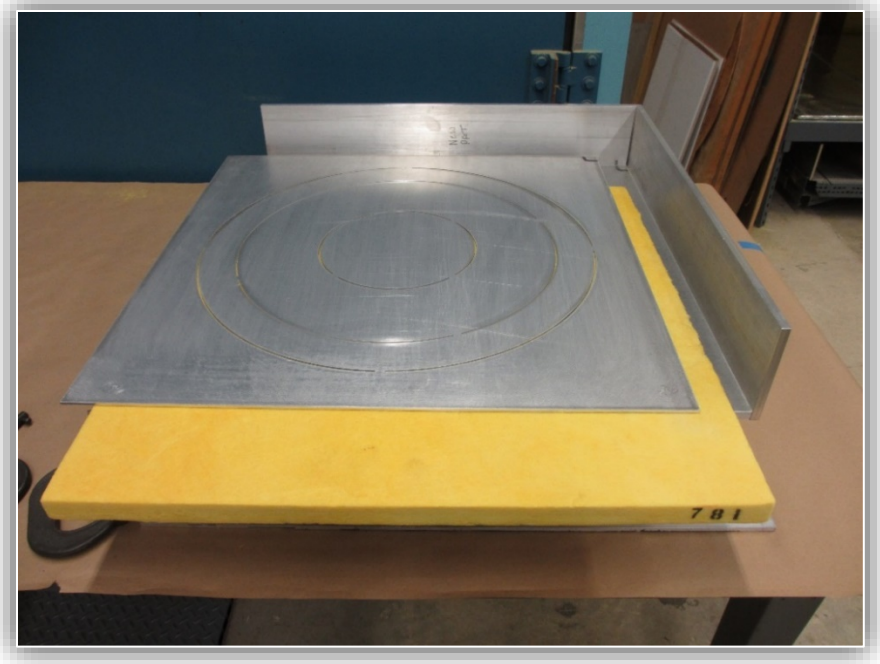

Fig. 12. Panel 781 placed in metal cutting template.

Fig. 13. Test specimens (500 mm diameter) in a large conditioning chamber.

6.2.4. Selection

The bulk densities of the 30 specimens were determined to corroborate the preceding results obtained for the panels (Table 2). The measurements of mass (m_0) and thickness (L),

with minor modifications, were conducted as described in Sec. 5.1 and Sec. 5.2, respectively. The specimen diameters ($\bar{d}_s$) were obtained from the average of two measurements using a precision steel rule having a resolution of 0.05 cm. The bulk densities of the round test specimens were computed from Eq. (16).

$$\rho_s = \frac{m_0}{\pi\left(\frac{\bar{d}_s}{2}\right)^2 \times L_s} \tag{16}$$

The bulk densities for the 30 test specimens are ranked from low to high and summarized in Table 5. The last column yields the 15 pairs of test specimens.

Table 5. Ranked bulk densities of the 30 test specimens.

ID	Mass (kg)	Thickness (mm)	SD (mm)	Diameter (cm)	Area (m^2)	Density ($kg \cdot m^{-3}$)	Pair
707	0.5431	25.5250	0.1215	50.200	0.19792	107.50	1
751	0.5354	25.1225	0.0900	50.175	0.19773	107.78	
780	0.5465	25.3750	0.1271	50.350	0.19911	108.17	2
862	0.5457	25.2200	0.1329	50.300	0.19871	108.89	
571	0.5523	25.2925	0.0793	50.350	0.19911	109.67	3
654	0.5505	25.2550	0.0785	50.300	0.19871	109.69	
738	0.5546	25.3400	0.1294	50.375	0.19931	109.82	4
683	0.5556	25.3975	0.0939	50.325	0.19891	109.98	
781	0.5685	25.1350	0.0858	50.350	0.19911	113.60	5
647	0.5696	25.1900	0.0852	50.250	0.19832	114.02	
736	0.6278	24.9950	0.1261	50.350	0.19911	126.15	6
914	0.6334	25.2250	0.1443	50.325	0.19891	126.23	
850	0.6389	25.2525	0.1266	50.350	0.19911	127.06	7
634	0.6388	25.1750	0.1453	50.400	0.19950	127.19	
594	0.6429	25.2000	0.1530	50.350	0.19911	128.13	8
769	0.6404	25.1050	0.1797	50.325	0.19891	128.25	
830	0.6526	25.4900	0.1042	50.300	0.19871	128.85	9
811	0.6469	25.1700	0.1759	50.225	0.19812	129.72	
856	0.6544	25.2750	0.2138	50.350	0.19911	130.04	10
627	0.6699	25.3900	0.0716	50.300	0.19871	132.79	
809	0.7198	25.1775	0.1247	50.350	0.19911	143.59	11
828	0.7196	25.1225	0.1666	50.375	0.19931	143.71	
729	0.7301	25.4500	0.1581	50.400	0.19950	143.79	12
859	0.7294	25.4775	0.1212	50.325	0.19891	143.92	
722	0.7326	25.2450	0.1741	50.275	0.19852	146.18	13
731	0.7361	25.2350	0.1399	50.350	0.19911	146.50	
720	0.7509	25.4100	0.1296	50.350	0.19911	148.41	14
906	0.7518	25.2550	0.1756	50.200	0.19792	150.40	
825	0.7624	25.2850	0.1041	50.375	0.19931	151.29	15
801	0.7679	25.4275	0.2777	50.275	0.19852	152.14	

The percent differences ($\delta\rho$) between the panels (ρ_p) and 500 mm diameter specimens (ρ_s) were computed from Eq. (17).

$$\delta\rho = \frac{\rho_p - \rho_s}{\rho_p} \times 100 \tag{17}$$

Figure 14 plots values of $\delta\rho$ for the 30 specimens ranked from low to high within each subrange of bulk density. The changes for individual specimens ranged from –3.3 % to +2.4% indicating a small within-panel density variation. However, on average, each group of ten specimens (corresponding to low-, mid-, and high-ρ) changed by only ±1 %.

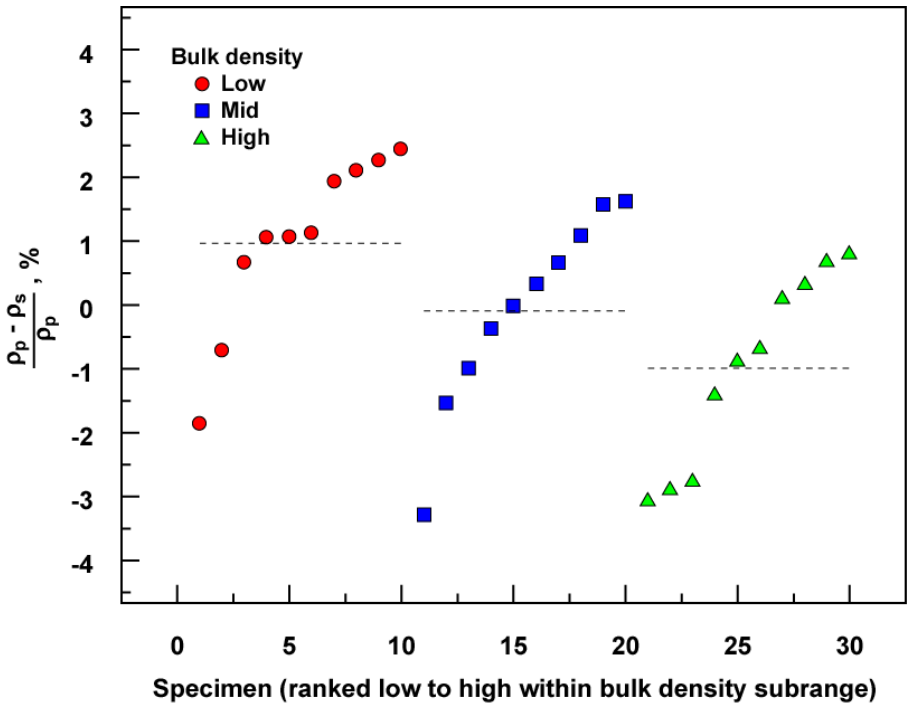

Fig. 14. Percent change in bulk density for the 500 mm diameter specimens.

6.3. Model Inputs

This section describes the final settings for the input parameters (ρ, T_m, and p) in Eq. (15).

6.3.1. Temperature and Bulk Density

Based on recent renewals of 1450 [5], temperature and bulk density, in that order, are the main factors affecting λ. Figure 15 plots the full factorial design for the three levels of ρ from Table 5 and the five (settable) levels of T_m (based on material and equipment limitations). This design checks the adequacy of Eq. (15) and also allows checking for the necessity of quadratic terms for both ρ and T_m. Each set of two data points, identified by their assigned IDs, represents a pair of specimens from Table 5. The benefit of testing a unique pair of specimens at each combined level of temperature and density is that independent information is obtained at each such level. The experimental design given in Fig. 15 is balanced in the sense that an equivalent amount of information is obtained at each setting of the independent variables. If either extra information had been obtained at some of the

settings, or worse, critical information omitted at one setting, the design would be unbalanced, and the resulting statistical analysis would suffer.

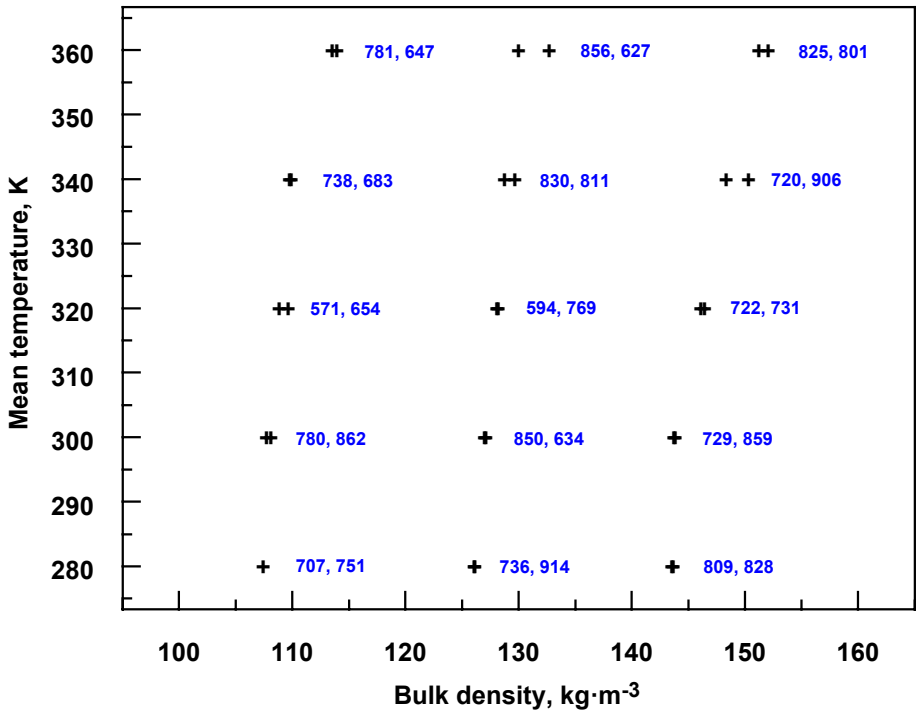

Fig. 15. Model inputs for mean temperature and bulk density.

6.3.2. Atmospheric Pressure

Previous NIST thermal conductivity data [21-22] for SRMs 1450b and 1450c revealed a gas pressure dependency for fibrous-glass board, particularly below 20 kPa. For SRM 1450e, the effect of gas pressure dependency at higher settings was reassessed to support thermal conductivity measurements at national metrology laboratories in the Inter-American Metrology System (SIM). SIM currently has 34 members and the elevations of these laboratory facilities range from sea level to nearly 4000 m (IBMETRO, La Paz, Bolivia).

Figure 16 plots the pressure for the NACA standard (lower) atmosphere [23] from an altitude of 0 m to 6000 m. The range of interest for the SIM national metrology institutes is sea-level, essentially 0 m, to 4000 m corresponding to an atmospheric pressure range of 101.3 kPa to 61.6 kPa [23]. Based on the results of Fig. 16, three pressure levels of 60 kPa, 80 kPa, and 100 kPa were selected for input to Eq. (15). Because of practical test limitations, these levels were not input independently to the model in Eq. (15). Rather, the three pressure levels of 60 kPa, 80 kPa, and 100 kPa were randomly input for each (T, ρ) data point in Fig. 15.

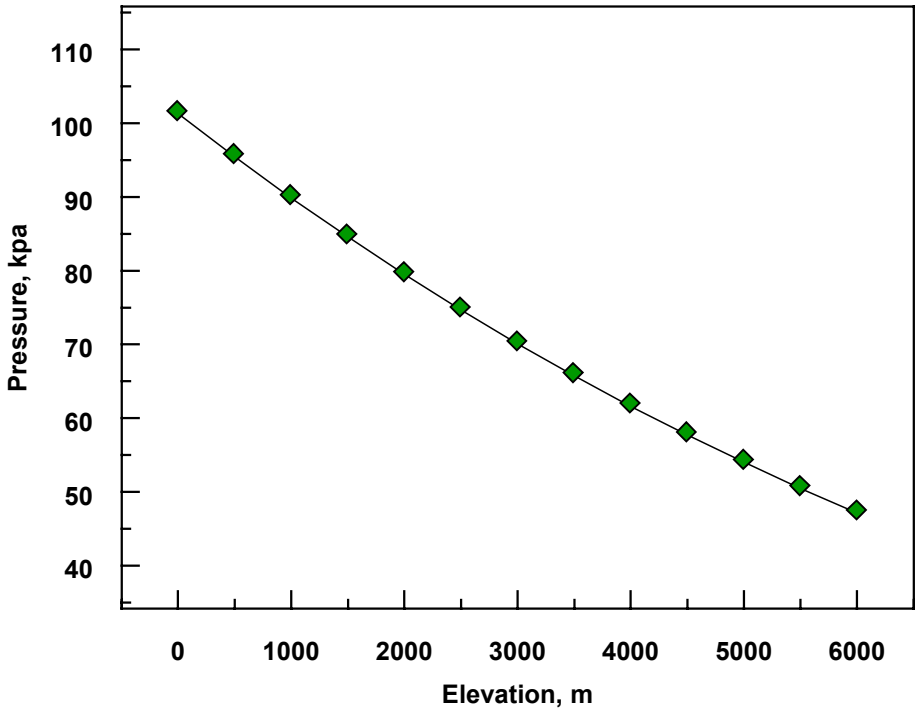

Fig. 16. Atmospheric pressure as a function of elevation (NACA standard [23]).

6.3.3. Supplementary Quantities

Other measurement quantities that were considered "nuisance" or influence parameters were either fixed at specified levels during testing in the guarded-hot-plate apparatus or recorded. The following parameters were fixed, or varied (slightly) with temperature, during the test.

- The direction of heat flow across the thickness of the specimens was fixed in the horizontal direction for the double-sided mode of operation.
- The temperature difference (ΔT) across the specimen was fixed at 25 K and followed standard practice for selecting test temperatures [24].
- The clamping pressure (p_a) on the specimens was manually applied at a nominal value of 500 Pa for all tests.
- The average temperature (T_{eg}) of the primary edge guards (inboard and outboard) were controlled to within 0.1 K, or less, of the mean temperature (T_m).
- The supply air to the chamber was maintained at a dewpoint of 213 K (–60 °C), or less, by a purge gas generator supplied by NIST compressed air. In general, however, the supply airline was manually closed during testing.

6.4. Test Arrangement and Settings

Table 6 re-ranks the specimens listed in Table 5 by input temperature (T_m) and by bulk density (ρ_s) within each temperature setting. Each specimen pair was tested at three randomized levels of pressure (p). The second column assigns a randomized test sequence for the guarded-hot-plate measurements. The test sequence outlined in Table 6 involved a total of 45 (=3×5×3) runs.

Table 6. Random test sequence and settings for the 15 pairs of test specimens.

Index	Test Sequence	Specimen ID	ρ_s (kg·m^{-3})	T_m (K)	p_1 (kPa)	p_2 (kPa)	p_3 (kPa)
1	1	707	107.50	280	100	80	60
		751	107.78				
2	3	736	126.15	280	80	100	60
		914	126.23				
3	2	809	143.59	280	80	60	100
		828	143.71				
4	6	780	108.17	300	60	100	80
		862	108.89				
5	10	850	127.06	300	100	80	60
		634	127.19				
6	7	729	143.79	300	80	100	60
		859	143.92				
7	8	571	109.67	320	100	60	80
		654	109.69				
8	9	594	128.13	320	100	80	60
		769	128.25				
9	4	722	146.18	320	80	100	60
		731	146.50				
10	14	738	109.82	340	60	80	100
		683	109.98				
11	5	830	128.85	340	100	80	60
		811	129.72				
12	13	720	148.41	340	60	80	100
		906	150.40				
13	15	781	113.60	360	80	60	100
		647	114.02				
14	12	856	130.04	360	100	80	60
		627	132.79				
15	11	825	151.29	360	60	80	100
		801	152.14				

6.5. Guarded-Hot-Plate Method

Figure 17 illustrates the main components of a guarded-hot-plate apparatus designed for horizontal heat flow through the specimens. The typical arrangement utilizes parallel flat plates as constant temperature heat sources and sinks in contact with the surfaces of homogeneous specimens to establish a steady-state heat flux across the thickness dimension of the specimen. The central heating element of the apparatus (e.g., meter plate) is encompassed by a primary guard designed to promote one dimensional heat flow (Q) perpendicular to the plate surface in the central volume of the adjoining test specimens. The physical

separation between the meter plate and guard plate components is designated the guard gap, or gap for short, and consists of an airspace.

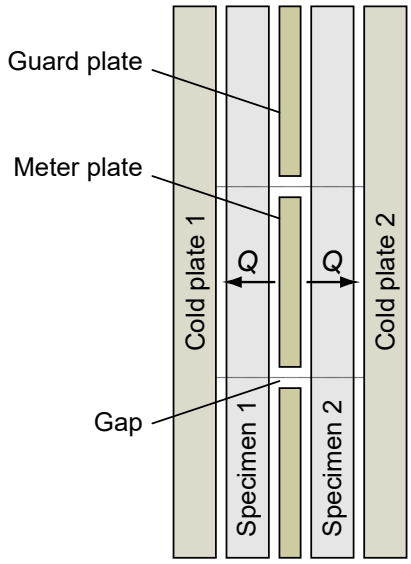

Fig. 17. Schematic illustration of a guarded-hot-plate apparatus (vertical plates) with a specimen pair installed. The numbers "1" and "2" refer to inboard and outboard locations relative to the hot plate.

The double-sided mode requires that the cold plates operate at the same temperature; thus, the heat flow Q represents the measurement for the pair of specimens (Fig. 17). The guard plate is independently operated at the same temperature as the hot plate to minimize lateral heat flows. The governing equation for the guarded-hot-plate method employs an algebraic form of the Fourier heat conduction equation slightly modified from the definition given in Eq. (2) in Sec. 3.2. The thermal transmission calculations, based on heat flux measurements from the guarded-hot-plate apparatus, are implemented in accordance with Eq. (18) for double-sided operation.

$$\lambda_{\text{exp}} = \frac{Q\, L_{\text{av}}}{2A\,\Delta T_{\text{av}}} \tag{18}$$

The terms L_{av} and ΔT_{av} in Eq. (18) represent the average values associated with the pair of specimens 1 and 2 in Fig. 17. The $2A$ term in Eq. (18) represents heat flow through two surfaces of the metered area. Values of λ_{exp} are reported at the mean specimen temperature, T_m, given by Eq. (19).

$$T_m = \frac{T_h + T_c}{2} = \frac{T_h + \left(T_{c1} + T_{c2}\right)/2}{2} \tag{19}$$

The thermal transmission properties of heat insulators determined from standard test methods typically include multiple mechanisms of heat transfer, including conduction, radiation, and possibly convection. For that reason, some experimentalists will include the adjective "apparent" when describing the thermal conductivity of insulating materials (Sec. 3.2). However, for brevity, the term thermal conductivity will be used in this report.

6.6. NIST Guarded-Hot-Plate Facility

Figure 18 shows the NIST 500 mm diameter guarded-hot-plate apparatus (with the edge of an outboard SRM 1450e specimen visible) and the vacuum bell jar. Under operation, the specimen pair, plates, guards, and peripheral equipment are enclosed by the vacuum bell jar. The plates are commercially pure nickel and the working surfaces have been treated with a black ceramic coating to have a surface total emittance of 0.8. The surfaces in contact with the specimens' metering area are flat to within 0.1 mm. The hot plate and cold plates are suspended from overhead rails and translate in the horizontal direction during installation of the specimen pair. A clamping force is transmitted axially to each cold plate by manual application, and an in-line load cell measures the applied loading (i.e., clamping pressure) during the test. The apparatus is described by Zarr et al. [18].

The hot plate is a monolithic assembly, 16.0 mm thick, consisting of a meter plate 200 mm in diameter and a co-planar, concentric guard plate 500 mm in diameter. The circular gap separating the meter plate and guard plate is 0.92 mm wide at the plate surface. The cross-sectional profile of the gap is diamond shaped to minimize lateral heat flow [18]. The temperature difference across the gap is measured by combining the outputs from two Type K twelve-junction thermopiles. Each thermopile is embedded on opposing surfaces of the hot plate.

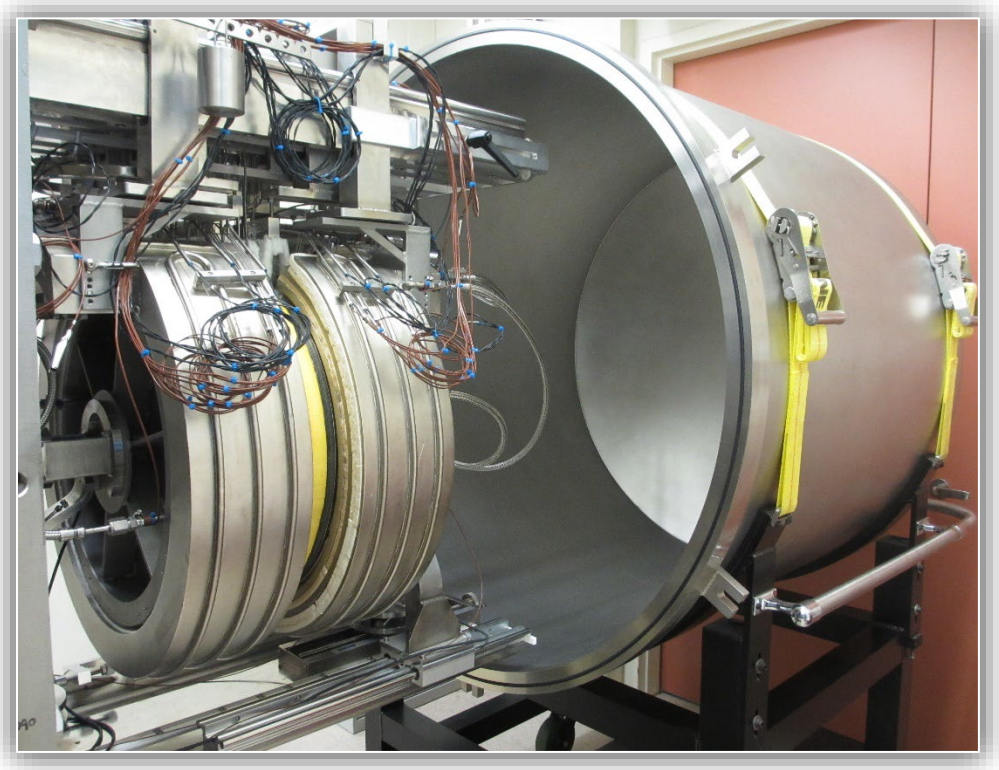

Fig. 18. NIST 500 mm diameter guarded-hot-plate apparatus: plates and edge guard (foreground), vacuum bell jar (background). The edge guards are partially separated revealing an amber SRM 1450e insulation specimen.

The metal-sheathed heaters for the hot plate are 3.2 mm in diameter and were custom manufactured using an internal bifilar design of nickel wires butt welded to gold (99.99 % nominal purity) wire leads. The heaters were formed such that the nickel-gold weld terminations were within 3 mm (or less) of the plate edge and the 2-to-4 wire transition of the meter-plate heater was within 1 mm of the centerline of the guard gap. After forming, the heaters were vacuum brazed in serpentine patterns at the midplane of the plate [18]. The electrical resistance of the meter-plate heater at room temperature is approximately 3.3 Ω.

Each cold plate system, shown schematically in Fig. 17 as a single layer, is in fact a multilayered assembly consisting of the following components: thermometry plate; woven glass fabric; heater plate; microporous insulation; coolant plate; rigid alumina insulation; and, water-cooled back plate. Active cooling of each cold plate system was accomplished by circulation of a chilled liquid through the coolant plate (described in Sec. 6.6.1). Temperature control of the thermometry plate was provided by the adjoining heater plate.

The primary temperature sensors installed in each plate for the determination of T_h, T_{c1}, and T_{c2} in Eq. (19) are long-stem standard platinum resistance thermometers (SPRTs). The sensors have a 4-wire sensing element located within the first 50 mm of the sheath tip. The SPRT is placed in a well that is brazed at the midplane of the plate so that the sensing region resides in the geometric center of the plate. To check temperature uniformity of a plate, six Type N metal sheathed thermocouples, 1.6 mm in diameter, were brazed in the surface of each plate at the locations described in Appendix E (E1.2).

6.6.1. Heating and Cooling Equipment

There are 16 separate heating circuits for controlling the temperatures of the apparatus components. Table 7 summarizes their (On/Off) status for each heater (items 1 through 16) at each mean temperature setting used during the development of SRM 1450e. The meter plate and cold plate heaters are items 1, 5, and 6, respectively. The primary guard (plate) heater for the meter plate is item 2. The remaining active heaters (items 3, 4, 9, 10, 11 through 16) function as secondary guards. The subscripts (1) and (2) in Table 7 refer to inboard and outboard components depicted in Fig. 17. The inactive guard heaters (items 3, 7, 8, 13, and 14) were not required for the temperature range of interest for thermal characterization of SRM 1450e. All active electrical heaters were energized by DC power supplies that were under proportional-integral-derivative (PID) computer control during testing [22].

There are four separate active cooling arrangements for the apparatus – specifically, the inboard and outboard coolant and water-jacket systems (items 17 through 20 in Table 7). The temperature for each system was maintained by a designated refrigerated circulation bath. At 280 K, low-temperature chillers, circulating ethanol, were installed. At other temperatures, the chillers were replaced by refrigerated baths circulating a mixture of ethanol and distilled water (volume fraction of 50 %). For all tests, the water jackets were operated with distilled water at a baseline temperature of 20 °C. All external thermal surfaces of the apparatus were protected by these constant-temperature water-jacket systems (Fig. 18). Table 8 summarizes the bath setpoints, in °C, for below- and near-ambient operation at each mean temperature setting used during the thermal characterization of SRM 1450e.

Table 7. Status of heating and cooling equipment.

Item	Description	280 K	300 K	320 K	340 K	360 K
1	Meter plate	On	On	On	On	On
2	Guard plate	On	On	On	On	On
3	Hot plate rim	Off	Off	Off	Off	Off
4	Hot plate connection	On	On	On	On	On
5	Cold plate$_1$	On	On	On	On	On
6	Cold plate$_2$	On	On	On	On	On
7	Cold plate$_1$ rim	Off	Off	Off	Off	Off
8	Cold plate$_2$ rim	Off	Off	Off	Off	Off
9	Cold plate$_1$ connection	On	On	On	On	On
10	Cold plate$_2$ connection	On	On	On	On	On
11	Edge guard	On	On	On	On	On
12	Edge guard	On	On	On	On	On
13	Edge guard$_1$ auxiliary	Off	Off	Off	Off	Off
14	Edge guard$_2$ auxiliary	Off	Off	Off	Off	Off
15	Edge guard$_1$ arch	On	On	On	On	On
16	Edge guard$_2$ arch	On	On	On	On	On
17	Coolant bath$_1$	[a]	[b]	[b]	[b]	[b]
18	Coolant bath$_2$	[a]	[b]	[b]	[b]	[b]
19	Water jacket$_1$	On	On	On	On	On
20	Water jacket$_2$	On	On	On	On	On
21	Mass flow controller	Off	Off	Off	Off	Off

[a] Low-temperature circulation bath
[b] Refrigerated circulation bath

Table 8. Bath temperature setpoints.

Item	Description	280 K	300 K	320 K	340 K	360 K
17	Coolant bath$_1$	–30°C	–5 °C	15 °C	20 °C	20 °C
18	Coolant bath$_2$	–30°C	–5 °C	15 °C	20 °C	20 °C
19	Water jacket$_1$	20 °C	20 °C	20 °C	20 °C	20 °C
20	Water jacket$_2$	20 °C	20 °C	20 °C	20 °C	20 °C

6.6.2. Vacuum Equipment

Atmospheric pressure control at 60 kPa, 80 kPa, and 100 kPa was achieved with a small diaphragm pump, vacuum controller, and vacuum gauge with an air admittance solenoid valve. The equipment is not shown in Fig. 18 but is described by Zarr and Thomas [22].

6.6.3. Specimen Installation and Operation

Each pair of test specimens was installed in the NIST 500 mm guarded-hot-plate apparatus at, or near, room conditions following a standard operating procedure. Before installation, the datum for the thickness display (Heidenhain ND 231B) was set with a fixture of 25.4 mm (1 in.) diameter precision spheres under an applied loading of 133 N to 178 N (30 lb_f to 40 lb_f). The specimen pair was installed under the same range of applied loading.

After enclosing the apparatus with the vacuum bell jar, the cooling, vacuum, and heating equipment were energized (in that order). Computer control of the apparatus was accomplished using a visual graphical programming language. The test data (including T_h, T_c, L, and Q) were collected each minute during a 4 h steady-state period (n = 240 observations per parameter) using a computer-controlled data acquisition system [22].

6.7. Guarded-Hot-Plate Measurements

The guarded-hot-plate measurements for production of SRM 1450e commenced on February 25, 2019 and concluded on May 8, 2019. The test facility was shut down for a site-wide maintenance outage from April 10 to April 16, 2019. A check standard consisting of a pair of SRM 1450d specimens (107, 155) was utilized at the beginning, end, and between Tests #3 and #4 (Table 6) to check the operation of the apparatus as testing progressed. At the conclusion of the production run, specimens 594 and 769 (from Table 6) were selected for subsequent validation measurements from 280 K to 360 K.

6.7.1. Data Summary (Tabular Format)

Table 9 summarizes the main experimental results – specimen information, input estimates, and the output estimate for measured thermal conductivity (λ_{exp}) – for the 15 specimen pairs specified in the experimental design (Table 6). The rows of data in Table 9 are grouped by T_m from 280 K to 360 K and, within each level of T_m, the average specimen densities (ρ_{av}) are arranged from lowest to highest value. Within each level of ρ_{av}, the data are ranked by air pressure (p) from 60 kPa to 100 kPa.

The subscript notations ($_1$) and ($_2$) for ID in Table 9 denote the inboard and outboard specimen, respectively; where inboard refers to the specimen location nearest to the vertical vacuum baseplate of the apparatus. The bulk density ρ_{av} is the average of ρ_1 and ρ_2 for the specimen pair (ID_1 and ID_2) under test. The heat flux, q, is equal to the heat flow rate (Q) divided by the metering area (A). Estimates for A were corrected for thermal expansion effects of the meter-plate radius (Appendix E). The output estimates for λ include an extra digit to reduce rounding errors.

During testing, the specimens were compressed slightly under load, thereby decreasing the in-situ specimen thickness (L) and increasing the bulk density. The densities (ρ_s) in Table 7 were adjusted by Eq. (20).

$$\rho = \rho_s \left(\frac{L_s}{L} \right) \tag{20}$$

where ρ is the in-situ bulk density during testing and L_s was the specimen thickness as determined on the granite surface plate (Sec. 4.3). No adjustments were made for changes in the specimen lateral surface area or mass. Values of ρ increased from 0.7 % to 1.5 %.

Table 9. SRM 1450e sub-sample thermal conductivity data.

ID_1	ID_2	ρ_{av} ($kg \cdot m^{-3}$)	T_m (K)	ΔT_{av} (K)	p (kPa)	L_{av} (m)	q ($W \cdot m^{-2}$)	λ_{exp} ($W \cdot m^{-1} \cdot K^{-1}$)
707	751	110.0	280.001	25.002	59.8	0.02496	60.98	0.03044
707	751	110.0	280.002	25.000	80.0	0.02497	61.08	0.03050
707	751	110.0	280.005	25.003	100.7	0.02497	61.16	0.03053
736	914	128.4	280.001	24.999	59.9	0.02485	61.61	0.03062
736	914	128.4	280.001	25.000	80.0	0.02485	61.74	0.03069
736	914	128.4	280.001	25.001	100.0	0.02485	61.80	0.03071
809	828	146.1	280.001	25.001	59.9	0.02488	62.84	0.03127
809	828	146.1	280.002	25.001	80.0	0.02488	62.96	0.03133
809	828	146.3	280.001	25.000	100.3	0.02486	63.04	0.03135
780	862	110.8	300.000	25.000	60.1	0.02496	65.04	0.03247
780	862	110.9	300.000	24.999	80.0	0.02494	65.10	0.03248
780	862	110.9	300.000	25.001	100.0	0.02495	65.14	0.03250
634	850	129.0	300.000	25.000	59.9	0.02501	65.85	0.03293
634	850	129.0	300.000	24.999	80.0	0.02501	65.92	0.03297
634	850	129.0	300.000	24.999	99.9	0.02501	65.96	0.03299
729	859	146.3	300.000	25.001	59.9	0.02520	66.38	0.03346
729	859	146.2	300.003	25.007	79.9	0.02521	66.54	0.03354
729	859	146.3	300.001	25.001	99.9	0.02520	66.54	0.03354
571	654	112.1	319.999	24.996	59.9	0.02490	69.93	0.03482
571	654	112.2	320.000	25.000	80.0	0.02489	69.97	0.03482
571	654	112.1	320.003	25.005	99.8	0.02490	69.99	0.03484
594	769	129.9	320.000	25.000	59.9	0.02498	70.06	0.03501
594	769	129.9	320.000	25.000	80.0	0.02498	70.11	0.03503
594	769	129.9	320.001	25.003	99.9	0.02499	70.14	0.03504
722	731	149.1	320.000	24.999	59.9	0.02492	71.05	0.03542
722	731	149.1	320.003	25.003	80.0	0.02493	71.17	0.03548
722	731	149.1	320.000	25.000	99.0	0.02492	71.16	0.03547
683	738	111.9	340.000	25.000	59.8	0.02512	73.80	0.03708
683	738	111.9	340.000	25.000	79.9	0.02511	73.76	0.03705
683	738	111.9	340.000	25.000	99.9	0.02510	73.74	0.03702
811	830	131.7	340.000	24.999	59.9	0.02503	74.14	0.03711
811	830	131.7	340.000	24.999	80.0	0.02502	74.16	0.03711
811	830	131.7	340.001	25.003	99.9	0.02503	74.13	0.03710
720	906	151.4	340.000	25.000	59.9	0.02516	75.03	0.03775
720	906	151.5	340.001	25.001	80.0	0.02515	75.05	0.03774
720	906	151.5	340.001	25.003	99.8	0.02515	75.02	0.03772
647	781	116.0	360.000	25.000	60.0	0.02489	78.84	0.03925
647	781	116.0	360.000	24.999	80.0	0.02489	78.75	0.03920
647	781	116.0	360.001	25.001	100.0	0.02489	78.63	0.03913
627	856	133.3	360.000	25.000	59.9	0.02515	79.32	0.03990
627	856	133.3	360.000	25.000	80.0	0.02515	79.29	0.03988
627	856	133.3	360.000	25.000	100.1	0.02515	79.23	0.03986
801	825	154.4	360.000	25.000	59.9	0.02509	79.40	0.03984
801	825	154.4	360.001	25.001	80.0	0.02508	79.36	0.03980
801	825	154.5	360.001	25.002	99.5	0.02507	79.22	0.03972

6.7.2. Secondary Factors

Table 10 summarizes test data for seven important secondary factors that were either fixed or merely monitored during the test. The order of presentation is the same as that in Table 9. The factors include the specimen clamping pressure (p_a), primary guard temperature difference (ΔT_{gap}), secondary edge guard temperatures (T_{eg1}, T_{eg2}), chamber air temperature (T_a), and water jacket temperatures (T_{WJ1}, T_{WJ2}) at their respective plate inlets. The data for these quantities are examined below.

The clamping pressure (p_a) was manually set at the beginning of each test (Sec. 6.6.3) by the operator. The average value of p_a was 0.526 kPa but, unfortunately, as evident in Table 10, the values ranged from 0.47 kPa to 0.60 kPa, or about 25 % due to changes in mean temperature (T_m). Although the variation in p_a was relatively large, the effect on measurements of λ was expected to be small.

A major factor affecting the measurement of λ is the temperature difference across the guard gap (ΔT_{gap}), determined by two 12-junction Type K thermopiles arranged in a circumferential zig-zag pattern across the guard gap. Ideally, ΔT_{gap} is maintained at, or near, zero kelvin to minimize detrimental lateral heat flows that would affect the measurement of the specimen heat flow (Q). A previous sensitivity study [25] for a pair of SRM 1450d specimens (ΔT of 25 K) showed that an imbalance of ΔT_{gap} equal to ±250 mK affected the measurement of λ by ±5 %. The absolute values of ΔT_{gap} in Table 10 are on the order of 0.7 mK, or less, except for one test where ΔT_{gap} was approximately 1.4 mK.

The temperatures of the inboard and outboard edge guards (T_{eg1}, T_{eg2}, respectively) were determined from the averages of six Type N thermocouples brazed in the inner ring of each guard system. Comparison of the edge guard temperatures in Table 10 with the mean temperatures (T_m) in Table 9 shows that the differences were 10 mK, or less. The sensitivity study [25] showed that an imbalance in T_{eg1} and T_{eg2} of ±2 K from T_m had a negligible effect on measured values of λ.

The water jacket temperatures (T_{WJ1}, T_{WJ2}) were measured by Type T thermocouples wrapped around the inlet piping to the cold plate system. As evident in Table 10, T_{WJ1} and T_{WJ2} varied slightly with T_m, ranging from 292 K to 294 K (19 °C to 21 °C). The sensitivity study [25] showed that an imbalance in T_{WJ1} and T_{WJ2} of ±2 K from T_m had a negligible effect on measured values of λ.

The ambient chamber air temperature (T_a) was uncontrolled and determined from the average of six Type T thermocouples placed at carefully chosen locations inside the vacuum bell jar. Table 10 shows that T_a ranged from 290.9 K to 301.5 K (difference of 10.6 K) for values of T_m from 280 K to 360 K. However, because T_{eg1} and T_{eg2} were maintained within a few millikelvin of T_m, the effect of T_a on measurements of λ was expected to be small.

Table 10. SRM 1450e sub-sample secondary test factors.

ID_1	ID_2	p_a (kPa)	ΔT_{gap} (K)	T_{eg1} (K)	T_{eg2} (K)	T_a (K)	T_{WJ1} (K)	T_{WJ2} (K)
707	751	0.55	0.00004	280.00	280.00	290.9	292.4	293.2
707	751	0.58	0.00004	280.00	280.00	291.5	292.4	293.3
707	751	0.58	-0.00036	280.01	280.00	290.9	292.4	293.2
736	914	0.48	0.00005	280.00	280.00	292.7	292.9	293.4
736	914	0.48	0.00004	280.00	280.00	291.0	292.8	293.3
736	914	0.48	-0.00002	280.00	280.00	292.1	292.9	293.3
809	828	0.49	0.00005	280.00	280.00	291.1	292.4	293.3
809	828	0.50	0.00004	280.00	280.00	291.1	292.4	293.2
809	828	0.48	0.00015	280.00	280.00	291.0	292.8	293.2
780	862	0.55	-0.00002	300.00	300.00	295.2	293.0	293.4
780	862	0.55	0.00000	300.00	300.00	295.4	293.0	293.4
780	862	0.55	-0.00008	300.00	300.00	295.0	293.0	293.4
634	850	0.50	0.00000	300.00	300.00	295.2	293.0	293.4
634	850	0.50	-0.00001	300.00	300.00	295.1	293.0	293.4
634	850	0.51	0.00006	300.00	300.00	294.9	293.0	293.4
729	859	0.54	0.00000	300.00	300.00	295.0	293.0	293.4
729	859	0.55	-0.00013	300.00	300.00	294.8	293.0	293.4
729	859	0.55	-0.00005	300.00	300.00	295.0	293.0	293.4
571	654	0.55	0.00015	320.00	320.00	297.9	293.1	293.5
571	654	0.55	-0.00001	320.00	320.00	298.3	293.2	293.5
571	654	0.55	0.00037	320.00	320.00	298.0	293.1	293.5
594	769	0.50	0.00000	320.00	320.00	298.3	293.2	293.5
594	769	0.51	0.00002	320.00	320.00	298.3	293.2	293.5
594	769	0.51	0.00016	320.00	320.00	298.1	293.1	293.5
722	731	0.58	0.00002	320.00	320.00	298.7	293.2	293.6
722	731	0.60	0.00144	320.00	320.00	297.8	293.1	293.5
722	731	0.59	0.00002	320.00	320.00	298.3	293.2	293.6
683	738	0.49	0.00001	340.00	340.00	298.2	293.1	293.5
683	738	0.50	-0.00001	340.00	340.00	298.4	293.1	293.5
683	738	0.51	-0.00004	340.00	340.00	298.7	293.1	293.5
811	830	0.53	0.00003	340.00	340.00	299.7	293.2	293.6
811	830	0.54	0.00004	340.00	340.00	300.0	293.2	293.6
811	830	0.54	0.00053	340.00	340.00	300.0	293.2	293.6
720	906	0.47	0.00033	340.00	340.00	299.8	293.2	293.6
720	906	0.47	-0.00005	340.00	340.00	300.0	293.2	293.6
720	906	0.48	0.00010	340.00	340.00	298.9	293.1	293.5
647	781	0.51	0.00003	360.00	360.00	299.1	293.1	293.5
647	781	0.52	0.00037	360.00	360.01	299.6	293.1	293.6
647	781	0.51	-0.00010	360.00	360.00	299.8	293.1	293.6
627	856	0.52	0.00001	360.00	360.00	301.0	293.2	293.6
627	856	0.53	0.00001	360.00	360.00	301.3	293.2	293.7
627	856	0.53	-0.00001	360.00	359.99	301.5	293.3	293.7
801	825	0.54	0.00066	360.00	360.00	300.5	293.2	293.6
801	825	0.55	-0.00007	360.00	360.00	301.1	293.2	293.7
801	825	0.55	0.00005	360.00	360.00	301.5	293.3	293.7

6.8. Check Standard Data

Table 11 summarizes the thermal conductivity measurement data for the SRM 1450d check standard (107, 155) described in Sec. 6.7. The average bulk density (ρ_{av}) for the specimen pair was 120 kg·m^{-3}.

Table 11. Thermal conductivity data for SRM 1450d check standard.

Date	T_m (K)	ΔT_{av} (K)	p (kPa)	L_{av} (m)	λ_{exp} (W·m^{-1}·K^{-1})
25 Feb 2019	300.00	25.01	100.2	0.02583	0.03248
12 Mar 2019	300.00	25.01	100.0	0.02596	0.03256
13 Mar 2019	300.01	25.01	99.4	0.02595	0.03253
12 May 2019	300.00	25.00	99.9	0.02593	0.03253

The mean value for λ_{exp} in Table 11 is 0.03252 W·m^{-1}·K^{-1} and the relative range (maximum value minus the minimum value divided by the mean) is 0.22 % indicating the that the measurement process was in a state of statistical control during the production run for SRM 1450e.

7. Analysis and Uncertainty Evaluation

Section 7 presents a graphical analysis of the thermal conductivity data for the SRM 1450e production run, final model determination, assessment of measurement uncertainties, and information on metrological traceability.

7.1. Data Screening (Graphical Analysis)

Figures 19, 20, and 21 plot values of λ_{exp} from Table 9 as a function of the input variables ρ, T_m, and p, respectively, for the design model given in Eq. (15). In each plot, the individual data points are plotted as filled circle, square, and triangle symbols (without error bars for clarity) corresponding to the three main levels selected for bulk density. For Figs. 19 and 21, the five levels of T_m from 280 K , 300 K, 320 K, 340 K, and 360 K are given for each profile.

The limits of the y-axis for each plot have been purposely fixed for a straightforward comparison of the effect of each input variable on the response variable λ_{exp}. A cursory review of the three plots strongly suggests that, in the range of ρ_s, T_m, and p covered for the 450 specimens comprising the current SRM, T_m, followed by ρ have the greatest effect on λ. The effect of p, for the range from 60 kPa to 100 kPa appears insignificant.

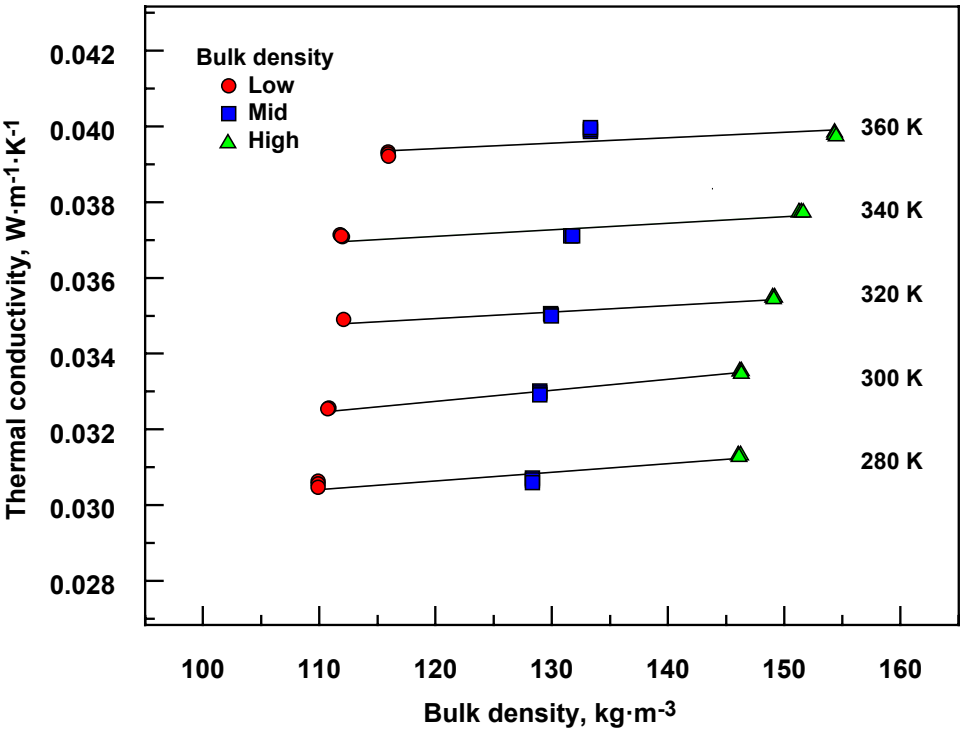

Fig. 19. Scatter plot of λ_{exp} versus ρ.

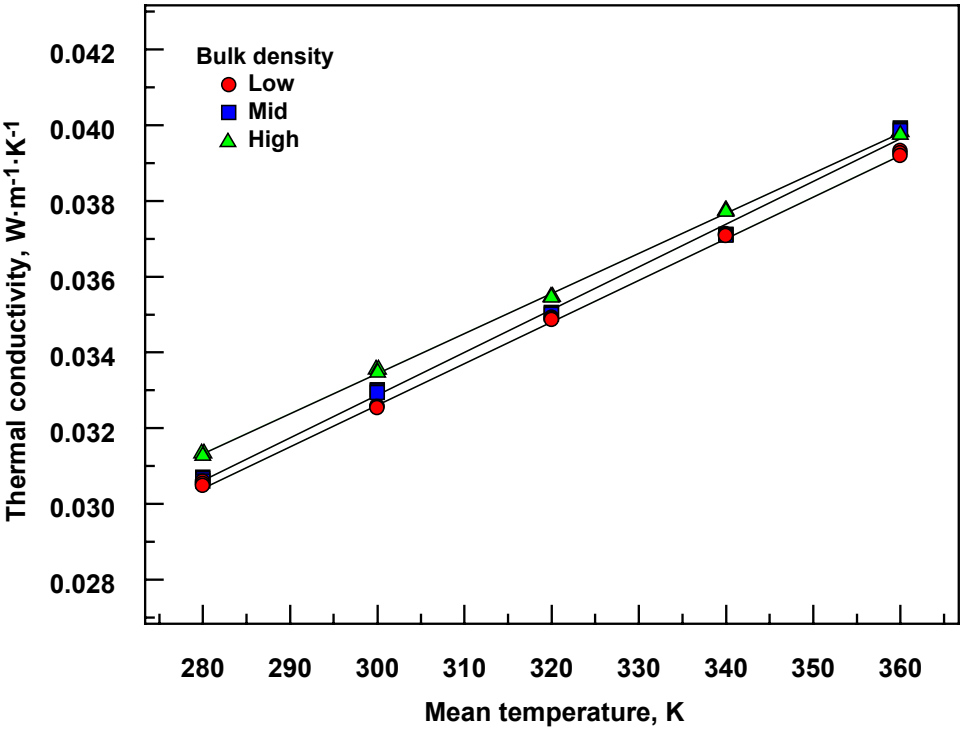

Fig. 20. Scatter plot of λ_{exp} versus T_m.

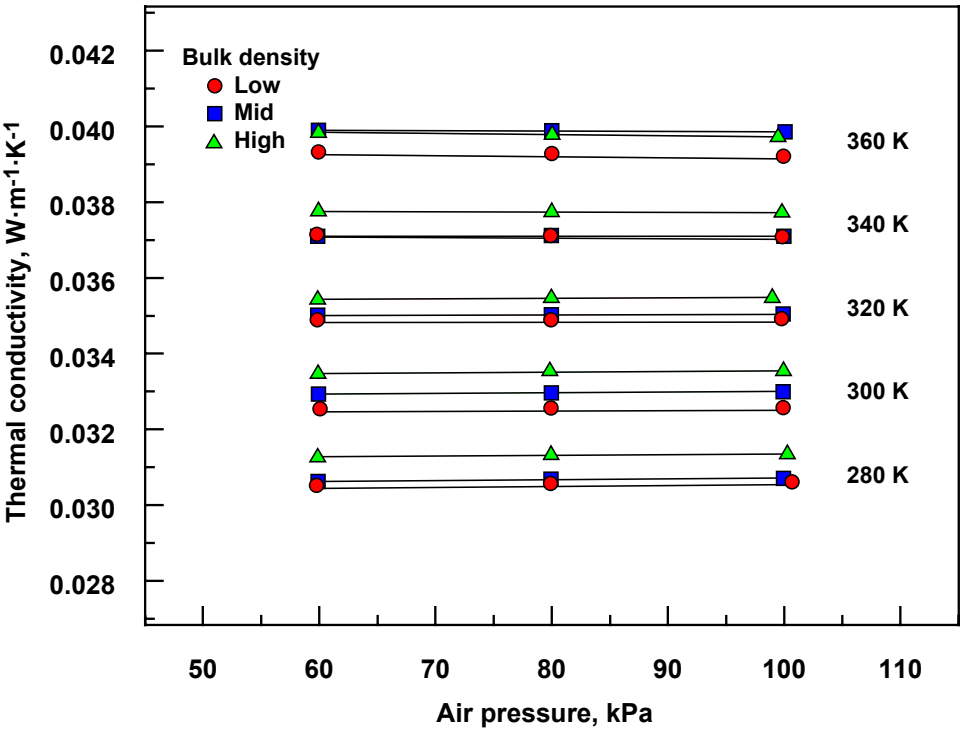

Fig. 21. Scatter plot of λ_{exp} versus p.

Table 12 summarizes the slopes of the lines shown in Fig. 19 and their corresponding t-values. For the five profiles (from 280 K to 360 K), the slopes are statistically significant ($|t| \geq 2$) at 95% confidence.

Table 12. Summary of linear profiles for λ_{exp} versus ρ (Fig. 19).

T_m (K)	Slope ($W \cdot m^2 \cdot K^{-1} \cdot kg^{-1}$)	t-value (dimensionless)
280	2.274×10^{-5}	7.6
300	2.905×10^{-5}	31.4
320	1.702×10^{-5}	13.1
340	1.745×10^{-5}	5.5
360	1.460×10^{-5}	3.0

Table 13 summarizes the slopes of the lines shown in Fig. 20 and their corresponding t-values. For the three profiles (low-, mid-, and high-ρ), the slopes are statistically significant ($|t| \geq 2$) at 95% confidence.

Table 13. Summary of linear profiles for λ_{exp} versus T_m (Fig. 20).

ρ-level	Slope ($W \cdot m^{-1} \cdot K^{-2}$)	t-value (dimensionless)
Low	1.099×10^{-4}	146
Mid	1.128×10^{-4}	64
High	1.058×10^{-4}	150

Table 14 summarizes the slopes of the lines shown in Fig. 21 and their corresponding *t*-values. In general, the slopes are small, one to two orders of magnitude smaller than the regression coefficients for bulk density (Table 12). Four of the profiles (shaded rows) are statistically indistinguishable from zero ($|t| \leq 2$) at 95% confidence. It is interesting to note that the slopes are positive from 280 K to 320 K and negative from 340 K to 360 K. The reason for the change in sign is not known at present.

Table 14. Summary of linear profiles for λ_{exp} versus p (Fig. 21).

T_m (K)	ρ-level	Slope ($W \cdot m^{-1} \cdot K^{-1} \cdot kPa^{-1}$)	*t*-value (dimensionless)
280	Low	23.5×10^{-7}	7.6
280	Mid	22.2×10^{-7}	3.8
280	High	19.5×10^{-7}	2.6
300	Low	8.33×10^{-7}	5.9
300	Mid	15.7×10^{-7}	8.4
300	High	20.2×10^{-7}	1.5
320	Low	3.85×10^{-7}	1.4
320	Mid	8.97×10^{-7}	10.0
320	High	13.8×10^{-7}	1.3
340	Low	-13.7×10^{-7}	-21.2
340	Mid	-2.32×10^{-7}	-1.2
340	High	-6.89×10^{-7}	-3.1
360	Low	-29.8×10^{-7}	-9.9
360	Mid	-11.2×10^{-7}	-19.4
360	High	-29.6×10^{-7}	-4.0

7.2. Final Model

Equation (21) gives the final model for SRM 1450e

$$\hat{\lambda} = -1.9731 \times 10^{-3} + 1.9923 \times 10^{-5}\, \rho + 1.0792 \times 10^{-4}\, T_m \qquad (21)$$

where $\hat{\lambda}$ is the predicted thermal conductivity ($W \cdot m^{-1} \cdot K^{-1}$), ρ is the bulk density ($kg \cdot m^{-3}$), and T_m is mean temperature (K). The residual standard deviation of the fit was 0.000158 $W \cdot m^{-1} \cdot K^{-1}$. The last digit of each regression coefficient in Eq. (21) is provided to reduce rounding errors. The pressure term in the design model (Eq. (15)) was determined not to be significant and was excluded from the final model. However, based on the empirical data, certified values of λ are valid for barometric pressures from 60 kPa to 101.3 kPa (sea-level pressure).

Figures 22 and 23 plot the deviations $(\lambda_{exp} - \hat{\lambda})/\hat{\lambda}$ in % versus ρ and T_m, respectively. As before, the data are color coded as shown in the legends. An additional temperature legend is included for Fig. 22. The deviations for both plots are randomly and interchangeably scattered (i.e., no discernible pattern) around zero.

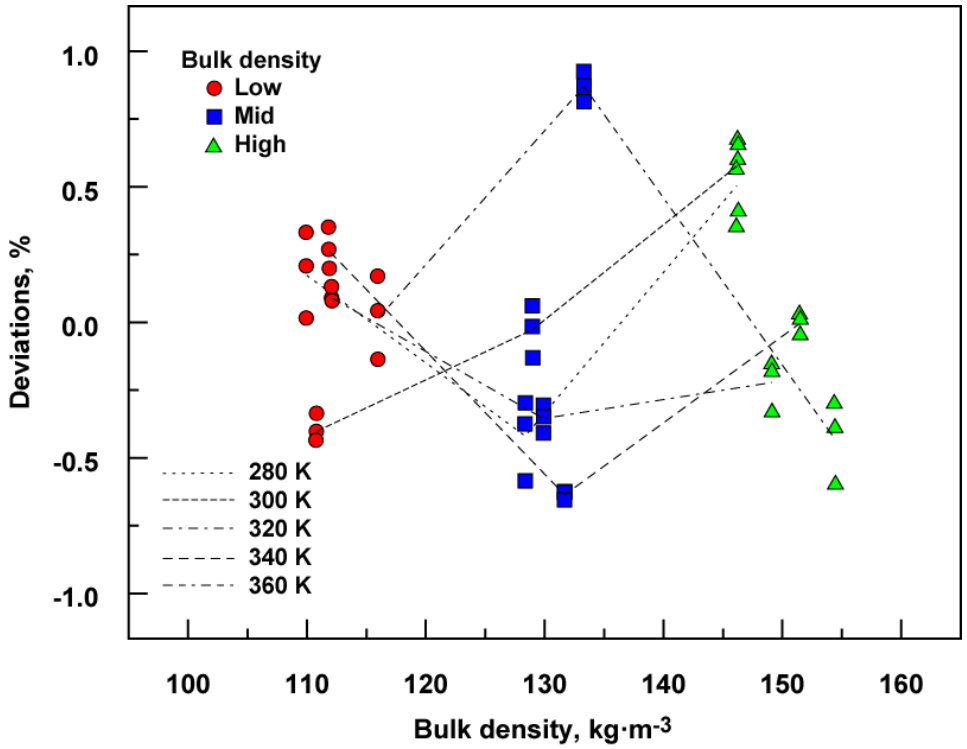

Fig. 22. Graphical analysis of deviations (in %) for the fit given in Eq. (21).

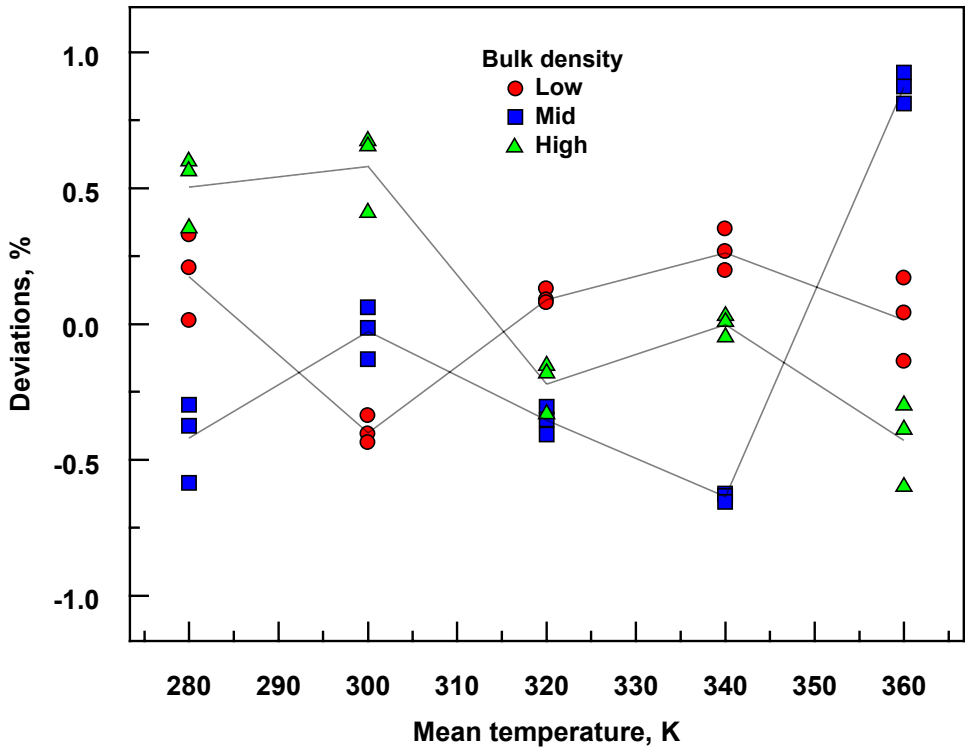

Fig. 23. Graphical analysis of deviations (in %) for the fit given in Eq. (21).

7.3. Model Validation

In addition to checking the model deviations as was done in Figs. 22 and 23, the final model given in Eq. (21) for SRM 1450e was validated by comparison with an independent set of thermal conductivity data. A series of supplemental thermal conductivity measurements were conducted for specimen pair (594, 769) having a bulk density of 130 kg·m^{-3}. These measurements were conducted sequentially from June 4, 2019 to June 12, 2019 at multiple temperatures from 280 K to 360K without removing the specimens from the guarded-hot-plate apparatus. Figure 24 plots the thermal conductivity data (diamond symbols) and the fitted line for the thermal conductivity data (Eq. (21)) versus mean temperature. It is observed that all the supplemental points in Fig. 24 fall very close to the final model given in Eq. (21).

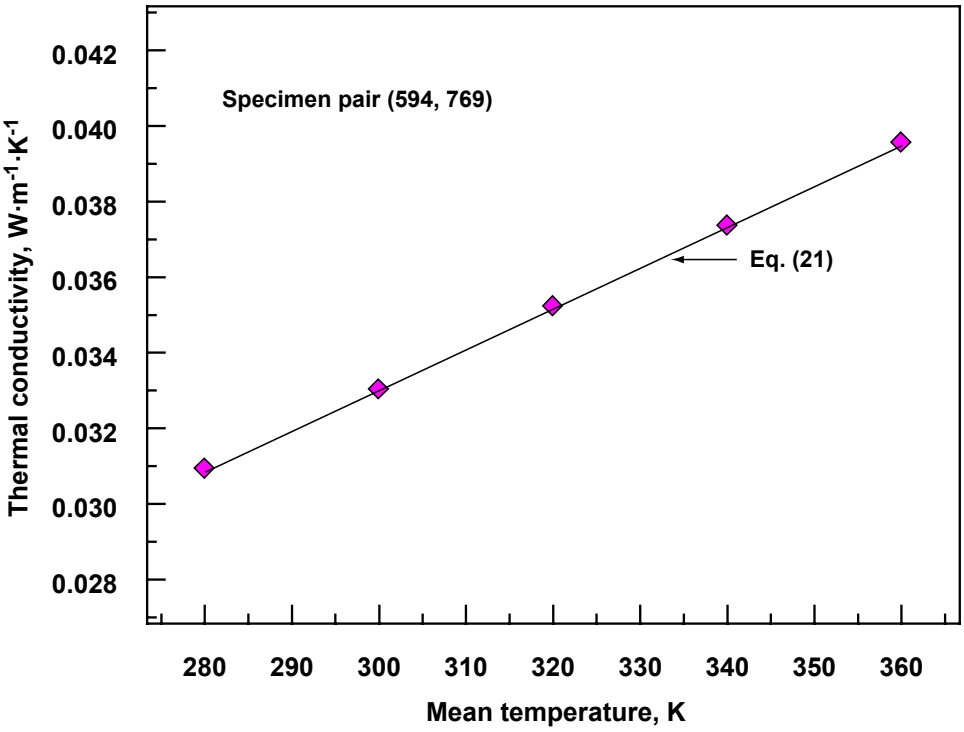

Fig. 24. Re-measured thermal conductivity versus mean temperature for specimen pair (594, 769). The solid line represents the fitted model given in Eq. (21), ρ = 130 kg·m^{-3}.

7.4. Thermal Conductivity Uncertainty Assessment

For the multiplicative expression in Eq. (2), the relative combined standard uncertainty in λ can be expressed as the relative uncertainties associated with each factor combined in quadrature.

$$u_{c,r}(\lambda) = \frac{u_c(\lambda)}{\lambda} = \sqrt{\left(\frac{u(Q)}{Q}\right)^2 + \left(\frac{u(\Delta T)}{\Delta T}\right)^2 + \left(\frac{u(L)}{L}\right)^2 + \left(\frac{u(A)}{A}\right)^2} \qquad (22)$$

The standard uncertainties and input quantities in Eq. (22) are derived in Appendix E. Table 15 summarizes the relative contributory, combined ($k = 1$), and expanded uncertainties ($k = 2$) for thermal conductivity as a function of mean temperature.

Table 15. Thermal conductivity uncertainty budget.

T_m (K)	$u_{c,r}$ (Q) (%)	$u_{c,r}$ (ΔT) (%)	$u_{c,r}$ (L) (%)	$u_{c,r}$ (A) (%)	$u_{c,r}$ (λ) (%)	U_r (λ) (%)
280	0.11	0.19	0.24	0.03	0.33	0.66
300	0.10	0.07	0.23	0.03	0.26	0.53
320	0.10	0.26	0.24	0.03	0.37	0.74
340	0.11	0.25	0.24	0.03	0.36	0.72
360	0.13	0.41	0.24	0.03	0.49	0.98

From Table 15, the maximum value of 0.98 % (at 360 K) was selected as a conservative estimate for the expanded uncertainty for thermal conductivity measurement. Rounded for convenience and expressed as a percent, $U_r(\lambda)$ is equal to 1.0 %. The major contributory uncertainties for SRM 1450e are due to the empirical determinations for specimen temperature difference (ΔT_{av}) and thickness (L_{av}). These findings are consistent with results from a previous guarded-hot-plate uncertainty analysis [26].

7.5. Thermal Conductivity Metrological Traceability

Table 16 summarizes the calibration information for the guarded-hot-plate equipment. The uncertainties due to calibration of the artifacts and equipment were included in the extended uncertainty analysis described in Appendix E.

Table 16. Calibration information for the thermal conductivity measurements.

Item	Equipment Calibrated	Description of standard	Calibration		
			Organization	Date	Cert. Number
1	Otto Wolff Model N85-7a7, S/N: 5350	Standards of the United States	NIST	2018	291216-18
2	Agilent 3458A, S/N: US28029523	see Certificate	Keysight Technologies	2018	1-9836320191-1
3	Rosemont Aerospace 163CE	Standards of the United States	NIST	2000	262640-00
4	MicroK 800, S/N: 08-P050 ITL28502/1	see Certificate	Isothermal Technology	2008	08-07-68
5	Tinsley Model 5685-A, S/N: 274591	Standards of the United States	NIST	2018	291216-18
6	ARI T-11N-39.3BN9B Type N TC, Tag: Start	By comparison w/SPRT	NIST	2002	267520D
7	ARI T-11N-39.3BN9B Type N TC, Tag: Middle	By comparison w/SPRT	NIST	2002	267520D
8	ARI T-11N-39.3BN9B Type N TC, Tag: End	By comparison w/SPRT	NIST	2002	267520D
9	Bal-tec™, Grade 25, 25.4 mm balls	Standards of the United States	NIST	2018	18-732-3079
10	Fused-silica	SRM 739	NIST		

11	Heidenhain MT12, S/N: 10315800D	Inspection Certificate	Heidenhain	2001	243602-01
12	Heidenhain MT12, S/N: 10315803D	Inspection Certificate	Heidenhain	2001	243602-01
13	Heidenhain ND231B, S/N: 9387273-A3	Bal-tec™, Grade 25, 25.4 mm balls	732.03		
14	Hot plate diameters	Standards of the United States	NIST	2006	274749-07
15	Transducer Techniques Load Cell 119216	Standards of the United States	NIST	2007	274030-06
16	Nor-Cal CDG091-100 w/APC-001, s/n:215008	Standards of the United States	NIST	2006	283622-06

8. Certification

Section 8 presents summary information on the properties of interest, values and uncertainty, statement of metrological traceability, and instructions for use for Standard Reference Material 1450e. This information is intended to provide supplementary documentation for the SRM 1450e Certificate.

8.1. Properties of Interest

Standard Reference Material 1450e is a high-density molded fibrous glass board certified for bulk density, ρ, and thermal conductivity, λ. Each SRM unit consists of a square panel of fine-glass fibers and phenolic binder molded into a semi-rigid board. The nominal dimensions of a unit are 610 mm by 610 mm by 25.2 mm (Table 3) and the bulk density ranges from 110 kg·m^{-3} to 154 kg·m^{-3} (Table 9).

8.2. Values and Uncertainties

Each unit of SRM 1450e is individually certified for bulk density, ρ (Table 3), and batch certified for thermal conductivity with Eq. (23):

$$\hat{\lambda} = -1.9731\times10^{-3} + 1.9923\times10^{-5}\,\rho + 1.0792\times10^{-4}\,T_m \qquad (23)$$

where $\hat{\lambda}$ is the predicted thermal conductivity (W·m^{-1}·K^{-1}), ρ is the bulk density (kg·m^{-3}), and T_m is the mean specimen temperature (K). Equation (23) is certified to be valid for ρ from 110 kg·m^{-3} to 154 kg·m^{-3}, specimen ΔT of 25 K, T_m from 280 K to 360 K, and p from 60 kPa to 101.3 kPa (sea-level pressure). The expanded uncertainty for λ values from Eq. (23) is 1 % with a coverage factor of approximately $k = 2$.

8.3. Statement of Metrological Traceability

The input quantities for the determination of bulk density and thermal conductivity are metrologically traceable to working references maintained at NIST as described in Sec. 5.5 and Sec. 7.4, respectively.

8.4. Instructions for Use

Standard Reference Material 1450e is intended for use as a proven check for the guarded-hot-plate apparatus (or other absolute thermal conductivity apparatus) and for calibration

of a heat-flow-meter apparatus over the temperature range of 280 K to 360 K and barometric pressures from 60 kPa to 101.3 kPa (sea-level pressure). NIST cannot exclude the use of SRM 1450e for other purposes, but the user is cautioned that other purposes are not sanctioned by the SRM 1450e Certificate.

8.4.1. Storage

For protection and identification, it is recommended that the reference material be stored in the original packaging in a clean, dry environment at temperatures between 15 °C and 30 °C.

8.4.2. Preparation and Conditioning Before Measurement

Prior to the thermal conductivity measurement, the reference material should be conditioned in laboratory conditions of 20 ° C to 25 °C and from 40 % RH to 65 % RH until the mass of the unit is stable (i.e., two successive measurements within 24 h are less than 1 % [1]).

8.4.3. Thermal Conductivity Measurement

Thermal conductivity measurements should be conducted in accordance with the appropriate ASTM Test Method C 177 [1], C 518 [2], or another similar international standard.

8.4.4. Guidelines and Precautions

The following guidelines and precautions are provided for the user.

- *Stacking*: Certified values of thermal conductivity are valid for a single unit and are invalid for stacked units.
- *Slicing*: Certified values of thermal conductivity are invalid for a unit where the thickness of the material has been modified by slicing.
- *Cutting*: It is possible to cut the reference material unit into smaller pieces. It is imperative to verify that bulk density of each piece is within the certified range of bulk density (Sec. 8.2).
- *Compression*: The SRM unit should not be compressed more than 10 % of original thickness.
- *Upper Temperature Limit*: The upper temperature limit for this reference material is limited to the decomposition point of the binder, approximately 473 K (200 °C) [10]. As a precaution, this reference material should not be heated above 380 K (107 °C). It should be noted that oven drying, as opposed to desiccant drying, can remove other volatiles and potentially affect chemical or physical properties of the material.
- *Lower Temperature Limit*: A lower temperature limit for SRM 1450e has not been established but, in principle, there is no known lower limit.
- *Atmospheric Pressure*: The effect due to changes in barometric pressure from 60 kPa to 101.3 kPa (sea-level pressure) is negligible for this material.

Acknowledgments

The authors appreciate the assistance provided by Jeffrey Cregger and Matthew Spencer in conducting the mass and dimensional measurements for bulk density.

References

[1] ASTM International (2019) *C177-19 – Test Method for Steady-State Heat Flux Measurements and Thermal Transmission Properties by Means of the Guarded-Hot-Plate Apparatus* (ASTM International, West Conshohocken, Pennsylvania).

[2] ASTM International (2019) *C518-17 – Test Method for Steady-State Thermal Transmission Properties by Means of the Heat Flow Meter Apparatus* (ASTM International, West Conshohocken, Pennsylvania).

[3] ASTM International (2019) *C1363-11 – Test Method for Thermal Performance of Building Materials and Envelope Assemblies by Means of a Hot Box Apparatus* (ASTM International, West Conshohocken, Pennsylvania).

[4] Federal Trade Commission (2019) *R-value Rule 16 CFR Part 460 – Labeling and Advertising of Home Insulation* (Electronic Code of Federal Regulations). https://www.ecfr.gov

[5] Zarr RR, Heckert NA, and Leigh SD (2014) Retrospective Analysis of NIST Standard Reference Material 1450, Fibrous Glass Board, for Thermal Insulation Measurements. *J. Res. Natl. Inst. Stand. Technol* 119: 296-370. http://dx.doi.org/10.6028/jres.119.012

[6] ASTM Subcommittee C16.30 (1978) Reference Materials for Insulation Measurement Comparisons. *Thermal Transmission Measurements of Insulation, ASTM STP 660*, ed Tye RP (ASTM International, West Conshohocken, Pennsylvania), pp 7-29.

[7] NBS (1959) Research Highlights of the National Bureau of Standards: Annual Report, Fiscal Year 1959. *Miscellaneous Publication 229*, p 88.

[8] Siu MCI (1980) Fibrous Glass Board as a Standard Reference Material for Thermal Resistance Measurement Systems. *Thermal Insulation Performance, ASTM STP 718*, eds McElroy DL and Tye RP, pp 343-360.

[9] Hust JG (1985) Standard Reference Materials: Glass Fiberboard SRM for Thermal Resistance. National Institute of Standards and Technology, *NBS Special Publication 260-98*.

[10] Zarr RR (1997) Standard Reference Materials: Glass Fiberboard, SRM 1450c, for Thermal Resistance from 280 K to 340 K. National Institute of Standards and Technology, *NIST Special Publication 260-130*.

[11] Zarr RR, Harris AC, Roller JF, Leigh SL (2011) Standard Reference Materials: SRM 1450d, Fibrous-Glass Board, for Thermal Conductivity from 280 K to 340 K. National Institute of Standards and Technology, *NIST Special Publication 260-173*.

[12] Zarr RR, Leber, DD (2010) Evaluation of Thermal Insulation Materials for NIST SRM 1450d, Fibrous-Glass Board. *Thermal Conductivity 30*, ed Gaal DS, Gall PS (DEStech Publications, Inc., Lancaster, Pennsylvania), 386-392.

[13] May W, Parris R, Beck C, Fassett J, Greenberg R, Guenther F, Kramer G, Wise S, Gills T, Colbert J, Gettings R, MacDonald B (2000) Standard Reference Materials®: Definitions of Terms and Modes Used at NIST for Value-Assignment of Reference

Materials for Chemical Measurements. National Institute of Standards and Technology, *NIST Special Publication 260-136*.

[14] International Organization for Standardization (2015) *ISO Guide 30:2015 – Reference materials – Selected terms and definitions* (International Organization for Standardization, Geneva, Switzerland).

[15] ASTM International (2019) *C 168-19 – Standard Terminology Relating to Thermal Insulation Annual Book of ASTM Standards* (ASTM International, West Conshohocken, Pennsylvania).

[16] International Bureau of Weights and Measures (2010) *JCGM 100:2008 – Evaluation of measurement data – Guide to the expression of uncertainty in measurement* (Joint Committee for Guides in Metrology, International Bureau of Weights and Measures, Paris, France). https://www.bipm.org/utils/common/documents/jcgm/JCGM_100_2008_E.pdf

[17] Taylor, BN, Kuyatt CE (1994) Guidelines for Evaluating and Expressing the Uncertainty of NIST Measurement Results. U.S. Department of Commerce, Washington, D.C. *NIST Technical Note 1297*. https://nvlpubs.nist.gov/nistpubs/Legacy/TN/nbstechnicalnote1297.pdf

[18] Zarr RR, Flynn DR, Hettenhouser JW, Brandenburg NJ, Healy WM (2006) Fabrication of a guarded-hot-plate apparatus for use over an extended temperature range and in a controlled gas environment. *Thermal Conductivity 28*, ed Dinwiddie RB, White MA, McElroy DL (DEStech Publications Inc. Lancaster, Pennsylvania), pp. 235-245.

[19] National Institute of Standards and Technology (2012) *NIST/SEMATECH e-Handbook of Statistical Methods*. https://www.itl.nist.gov/div898/handbook/eda/section2/eda21.htm

[20] National Institute of Standards and Technology (2012) *NIST/SEMATECH e-Handbook of Statistical Methods*. https://www.itl.nist.gov/div898/handbook/eda/section2/eda23.htm

[21] Smith DR, Hust JG (1983) Effective Thermal Conductivity of Glass-Fiber Board and Blanket Standard Reference Materials. *Thermal Conductivity 17*, ed Hust JG (Plenum, New York, New York), pp. 483-496.

[22] Zarr RR, Thomas WC (2013) Initial measurement results of the NIST 500 mm guarded-hot-plate apparatus under automated temperature and pressure control. *Thermal Conductivity 31*, ed Kiss LI, St-Georges L (DEStech Publications Inc. Lancaster, Pennsylvania), pp. 195-204.

[23] List RJ (1966) Smithsonian Meteorological Tables (Smithsonian Institution), 6th Ed., p. 267.

[24] ASTM International (2019) *C1058/C1058M-10(Reapproved 2015) – Practice for Selecting Temperatures for Evaluating and Reporting Thermal Properties of Thermal Insulation* (ASTM International, West Conshohocken, Pennsylvania).

[25] Zarr RR, Filliben JJ (2016) Sensitivity analysis for a guarded-hot-plate apparatus: A methodology based on orthogonal experiment designs. *Journal of Testing and Evaluation* 44(1): 102-127.

[26] Zarr RR (2010) Assessment of Uncertainties for the NIST 1016 mm Guarded-Hot-Plate Apparatus: Extended Analysis for Low-Density Fibrous-Glass Thermal Insulation. *J. Res. Natl. Inst. Stand. Technol.*, 115(1), 23-59. http://dx.doi.org/10.6028/jres.115.004
[27] Miller V (2002) Recommended guide for determining and reporting uncertainties for balances and scales. National Institute of Standards and Technology, Gaithersburg, Maryland, NISTIR 6919. https://www.nist.gov/system/files/documents/2017/04/28/NISTIR6919.pdf
[28] Doiron T, Stoup J (1997) Uncertainty and dimensional calibrations. *J. Res. Natl. Inst. Stand. Technol.*, 102(6): 647-676. http://dx.doi.org/10.6028/jres.102.044
[29] Flynn DR (2005) Design of a 500 mm Guarded Hot Plate Apparatus for Measuring Thermal Transmission Properties of Insulations from 90 to 900 K: Phase II. *NIST GCR 05-881*, pp. 101-102.
[30] Kollie TG (1977) Measurement of the thermal-expansion coefficient of nickel from 300 to 1000 K and determination of the power-law constants near the Curie temperature. *Physical Review B*, 16(11): 4872-4881.
[31] SRM 739 *Fused Silica Thermal Expansion*; National Institute of Standards and Technology; U.S. Department of Commerce: Gaithersburg, MD (27 December 1991).

Appendix A: Change Log

No revisions (April 2020).

Appendix B: Mass Plots (Panel ID: 500 through 949)

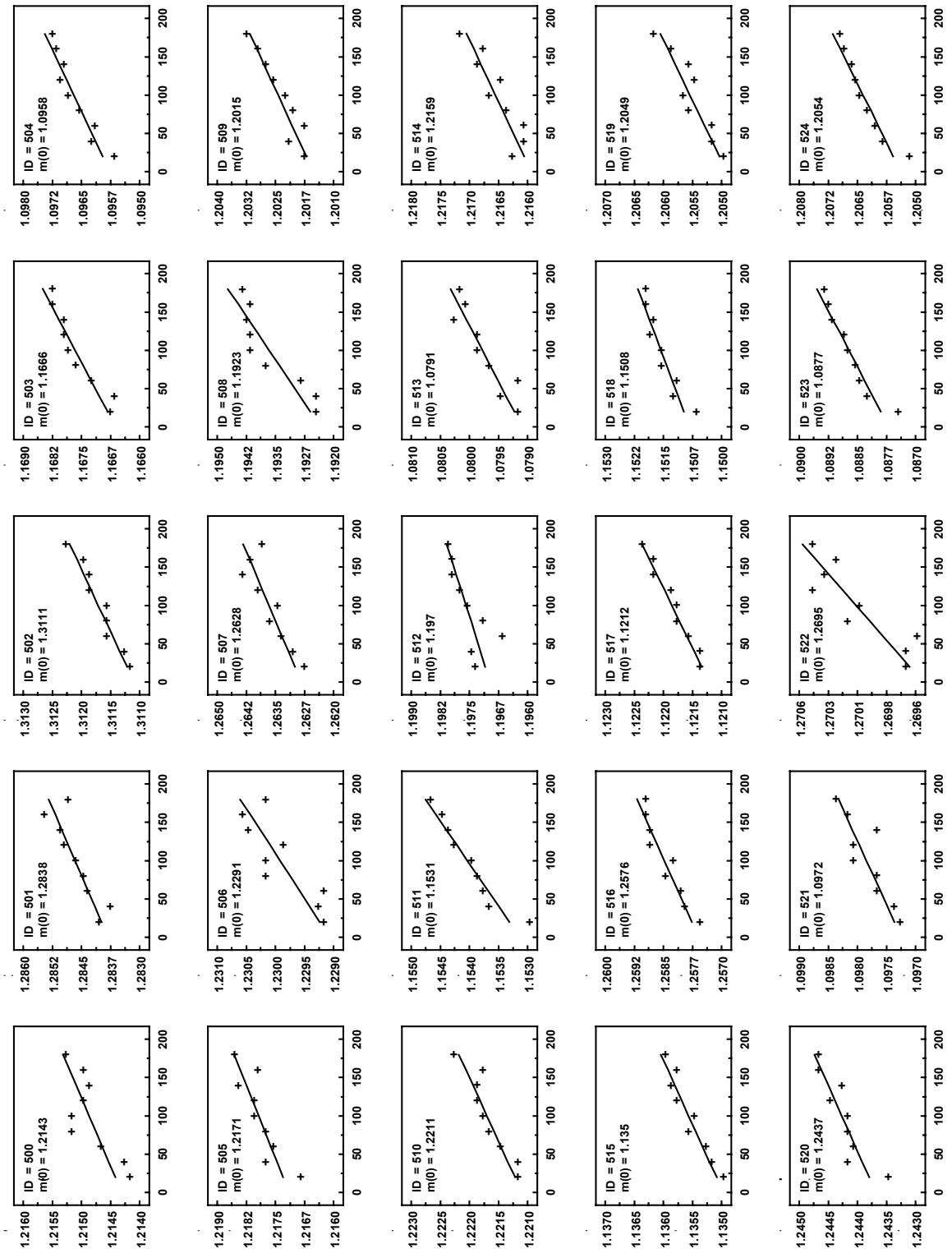

Fig. 25. Panel ID=500-524: Multiple mass observations (in kilograms) as a function of elapsed time (in seconds) for insulation panels 500 through 524. Linear fit for data (shown as solid line) was back-extrapolated to elapsed time zero (t_0) to determine m_0 for each panel.

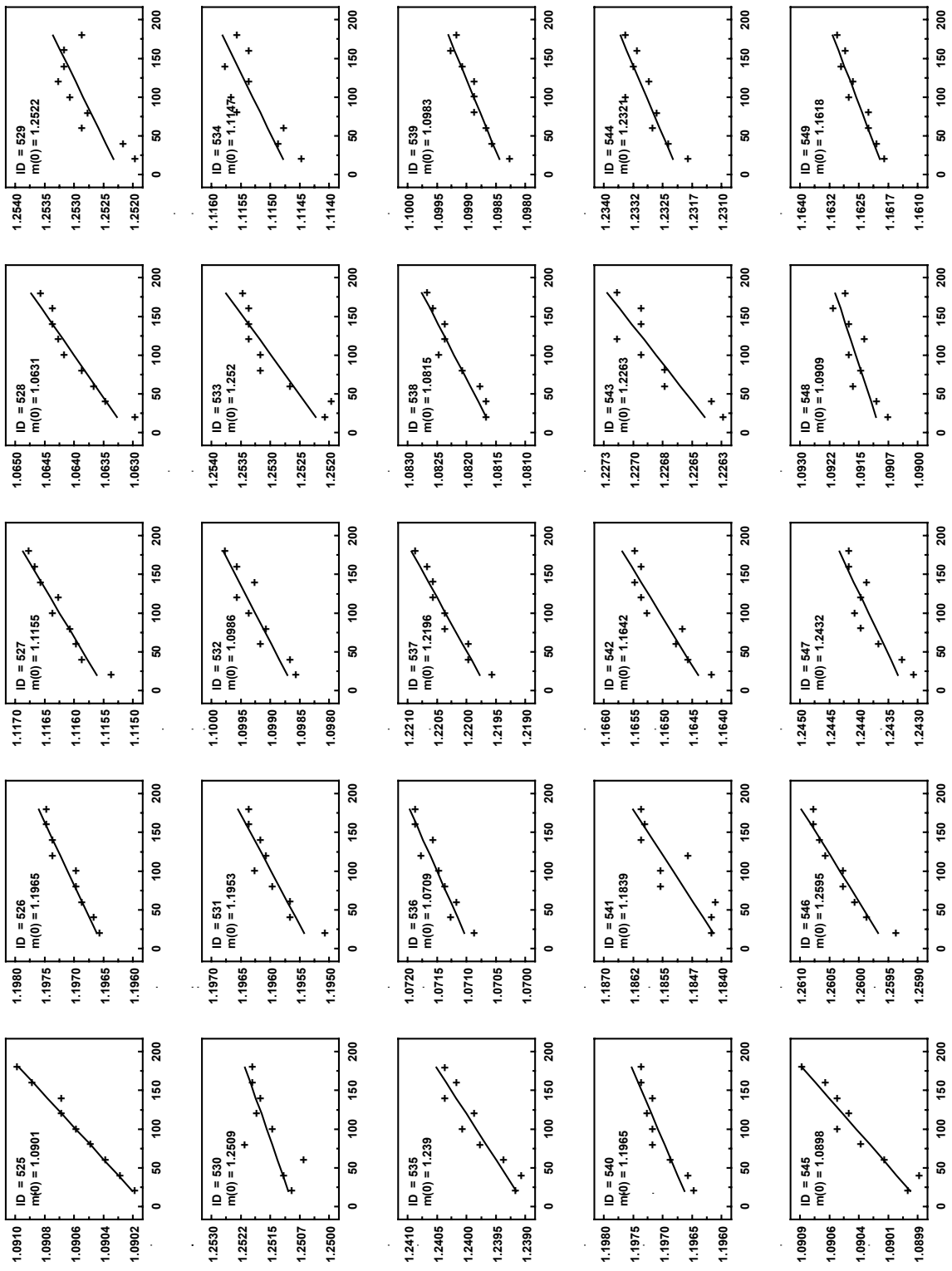

Fig. 26. Panel ID=525-549: Multiple mass observations (in kilograms) as a function of elapsed time (in seconds) for insulation panels 525 through 549. Linear fit for data (shown as solid line) was back-extrapolated to elapsed time zero (t_0) to determine m_0 for each panel.

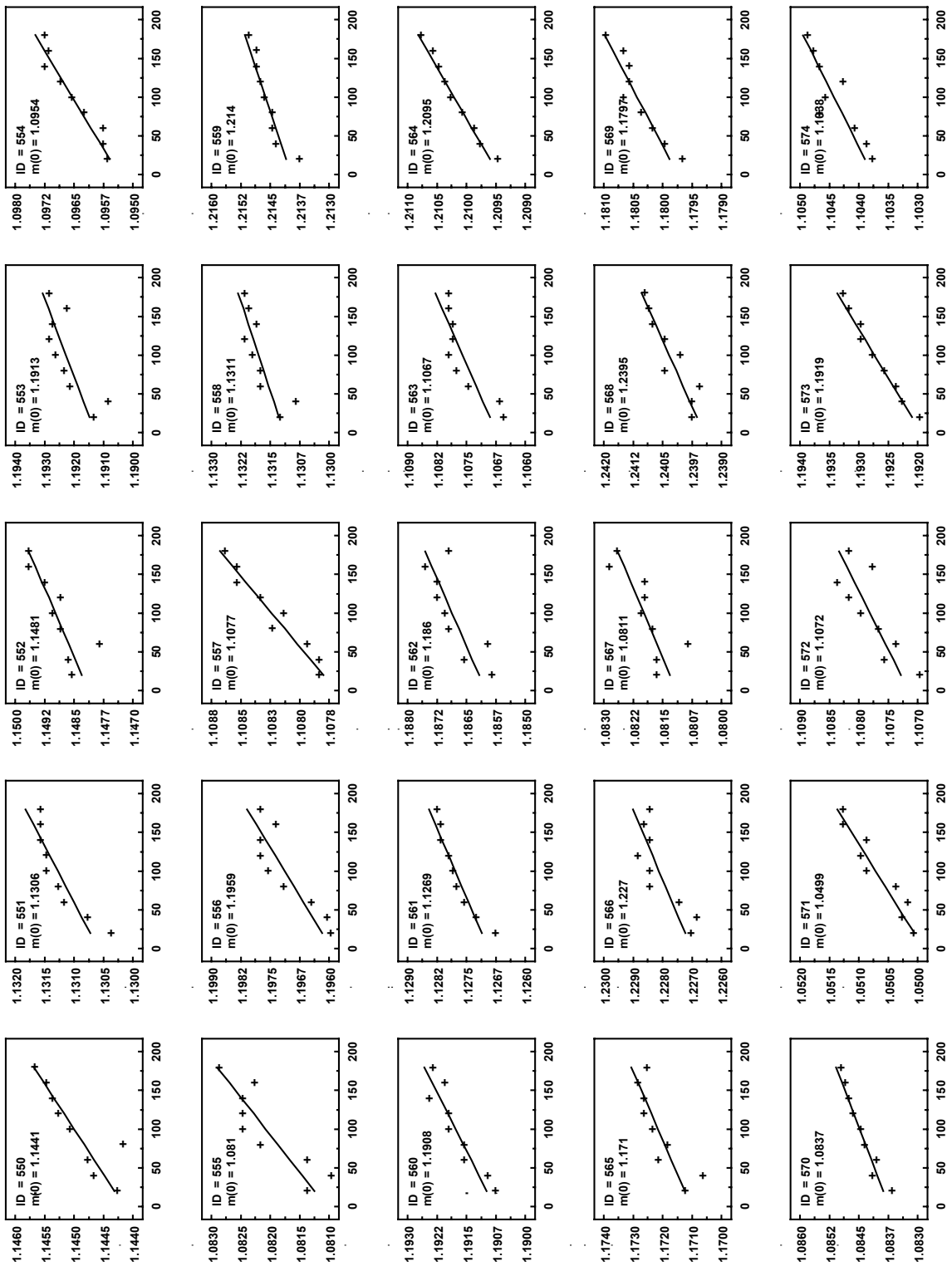

Fig. 27. Panel ID=550-574: Multiple mass observations (in kilograms) as a function of elapsed time (in seconds) for insulation panels 550 through 574. Linear fit for data (shown as solid line) was back-extrapolated to elapsed time zero (t_0) to determine m_0 for each panel.

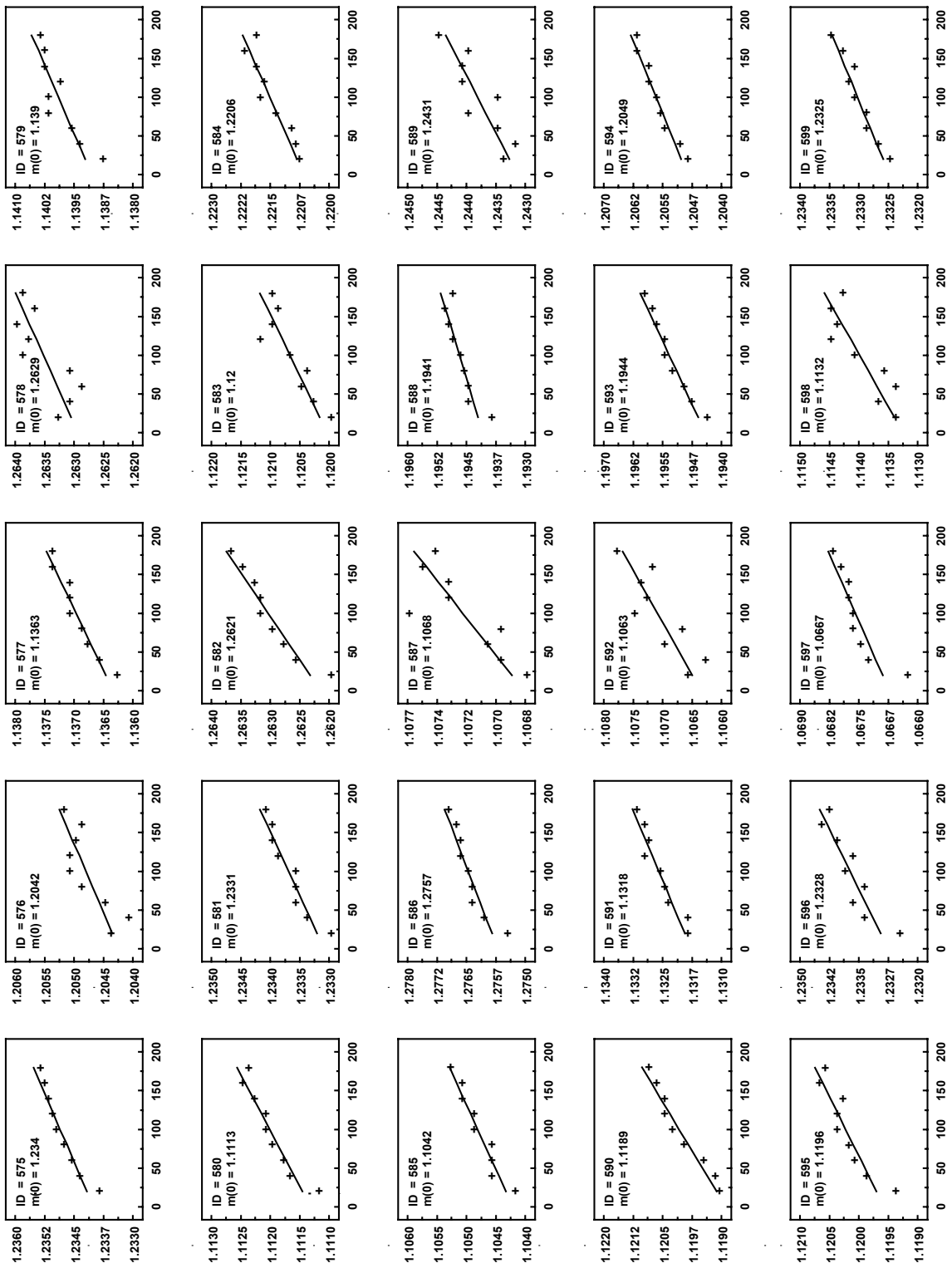

Fig. 28. Panel ID=575-599: Multiple mass observations (in kilograms) as a function of elapsed time (in seconds) for insulation panels 575 through 599. Linear fit for data (shown as solid line) was back-extrapolated to elapsed time zero (t_0) to determine m_0 for each panel.

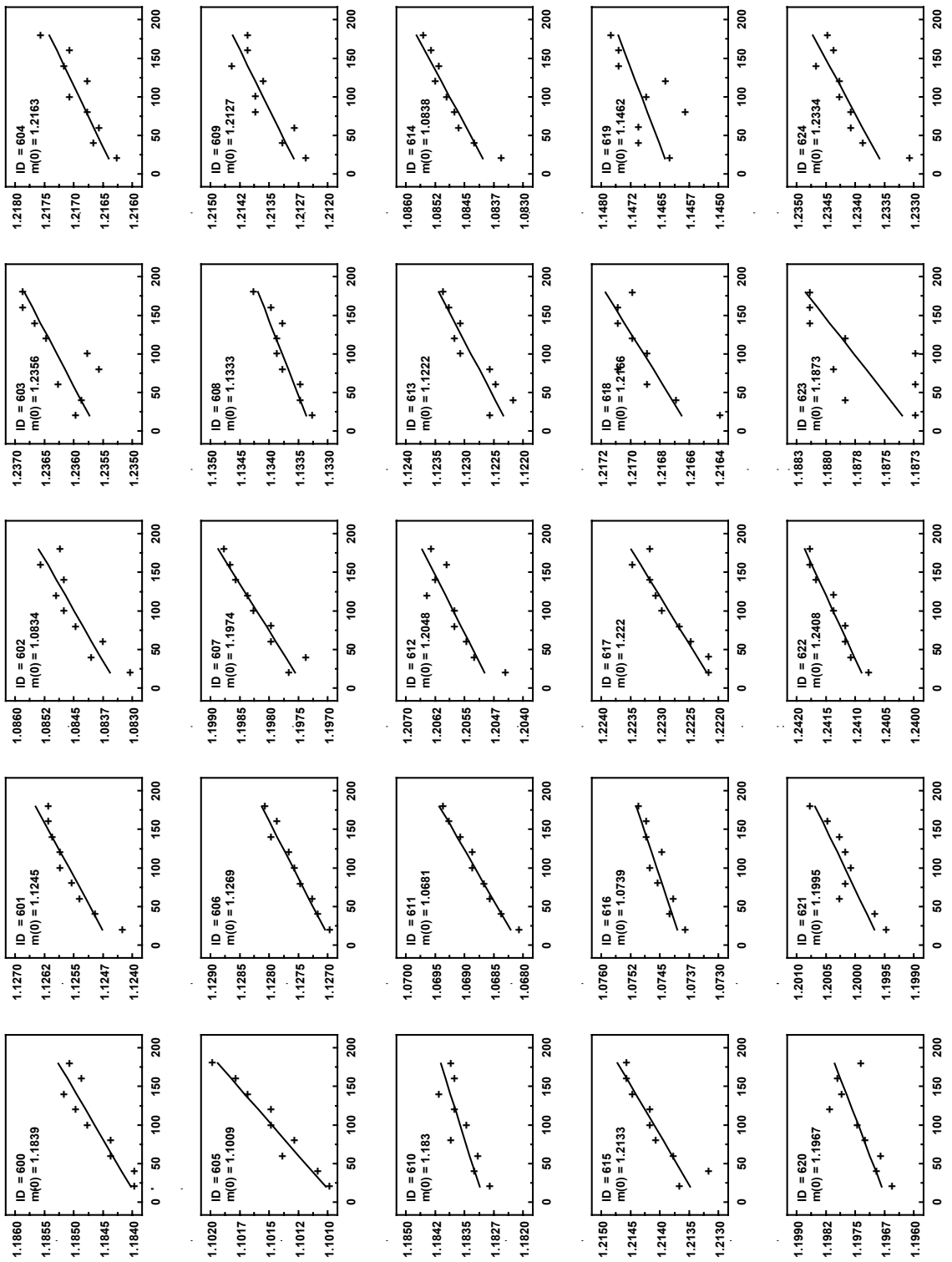

Fig. 29. Panel ID=600-624: Multiple mass observations (in kilograms) as a function of elapsed time (in seconds) for insulation panels 600 through 624. Linear fit for data (shown as solid line) was back-extrapolated to elapsed time zero (t_0) to determine m_0 for each panel.

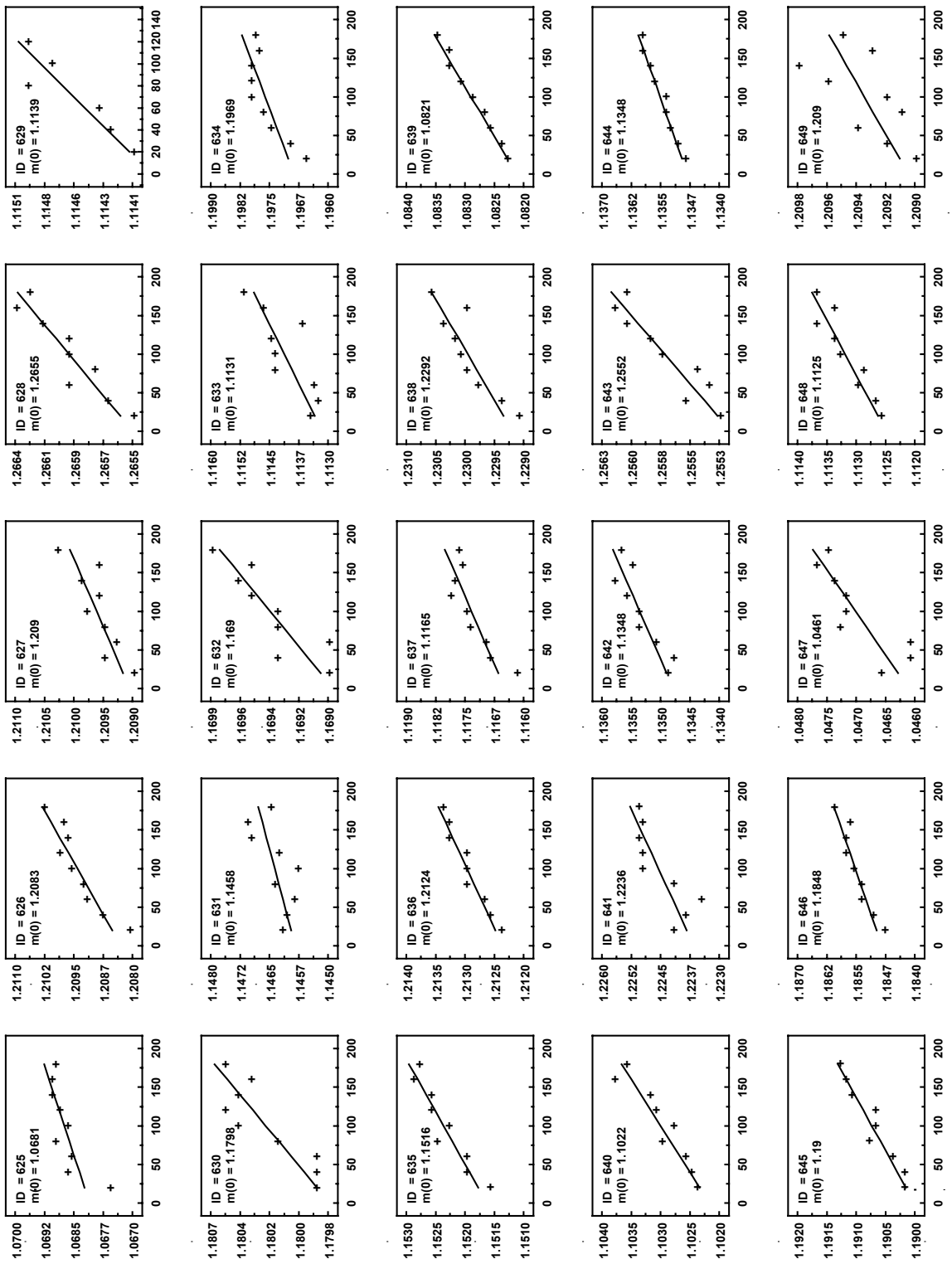

Fig. 30. Panel ID=625-649: Multiple mass observations (in kilograms) as a function of elapsed time (in seconds) for insulation panels 625 through 649. Linear fit for data (shown as solid line) was back-extrapolated to elapsed time zero (t_0) to determine m_0 for each panel. Note that only 6 observations are included for panel 629 due to an interruption in the measurement process.

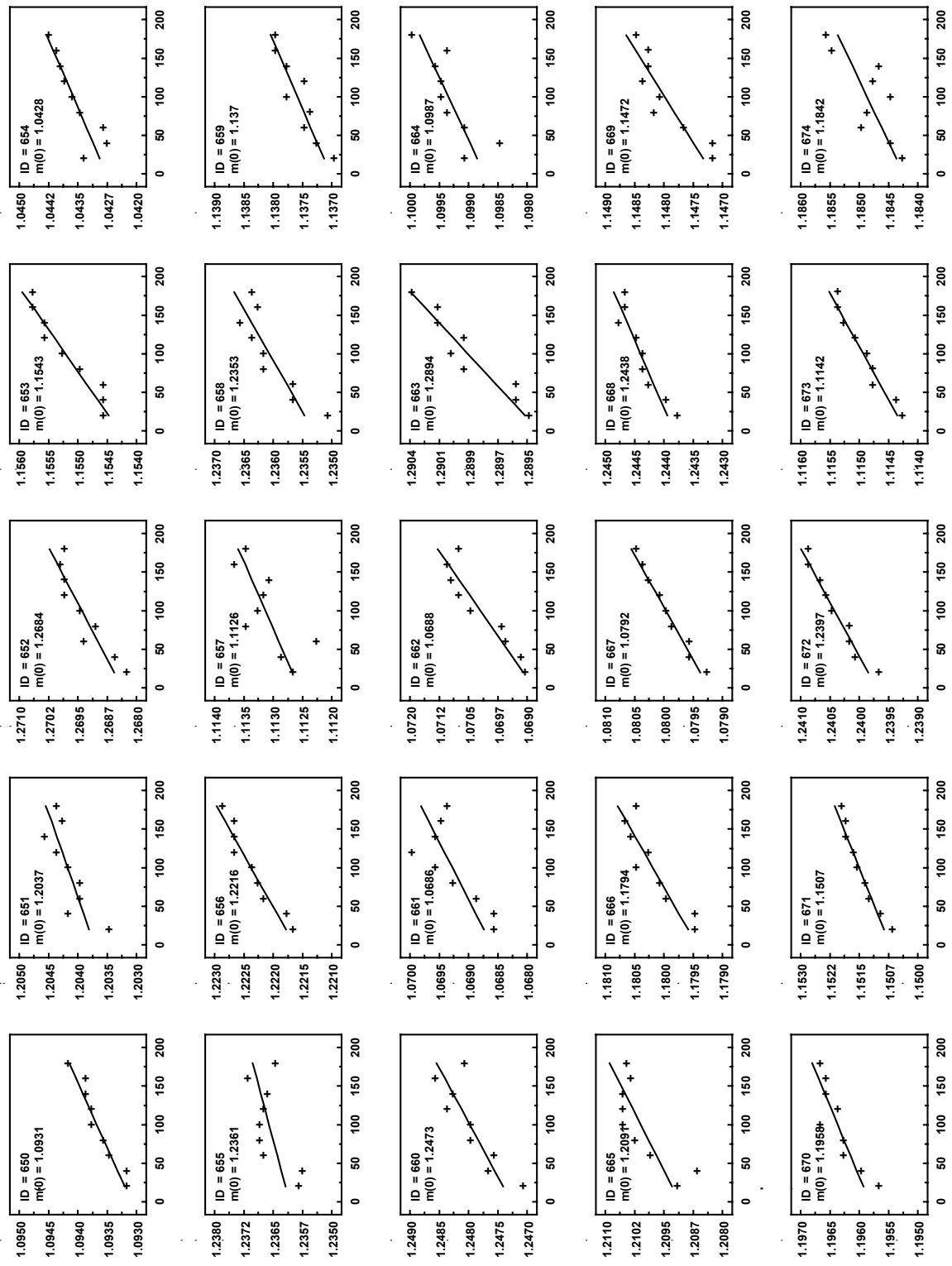

Fig. 31. Panel ID=650-674: Multiple mass observations (in kilograms) as a function of elapsed time (in seconds) for insulation panels 650 through 674. Linear fit for data (shown as solid line) was back-extrapolated to elapsed time zero (t_0) to determine m_0 for each panel.

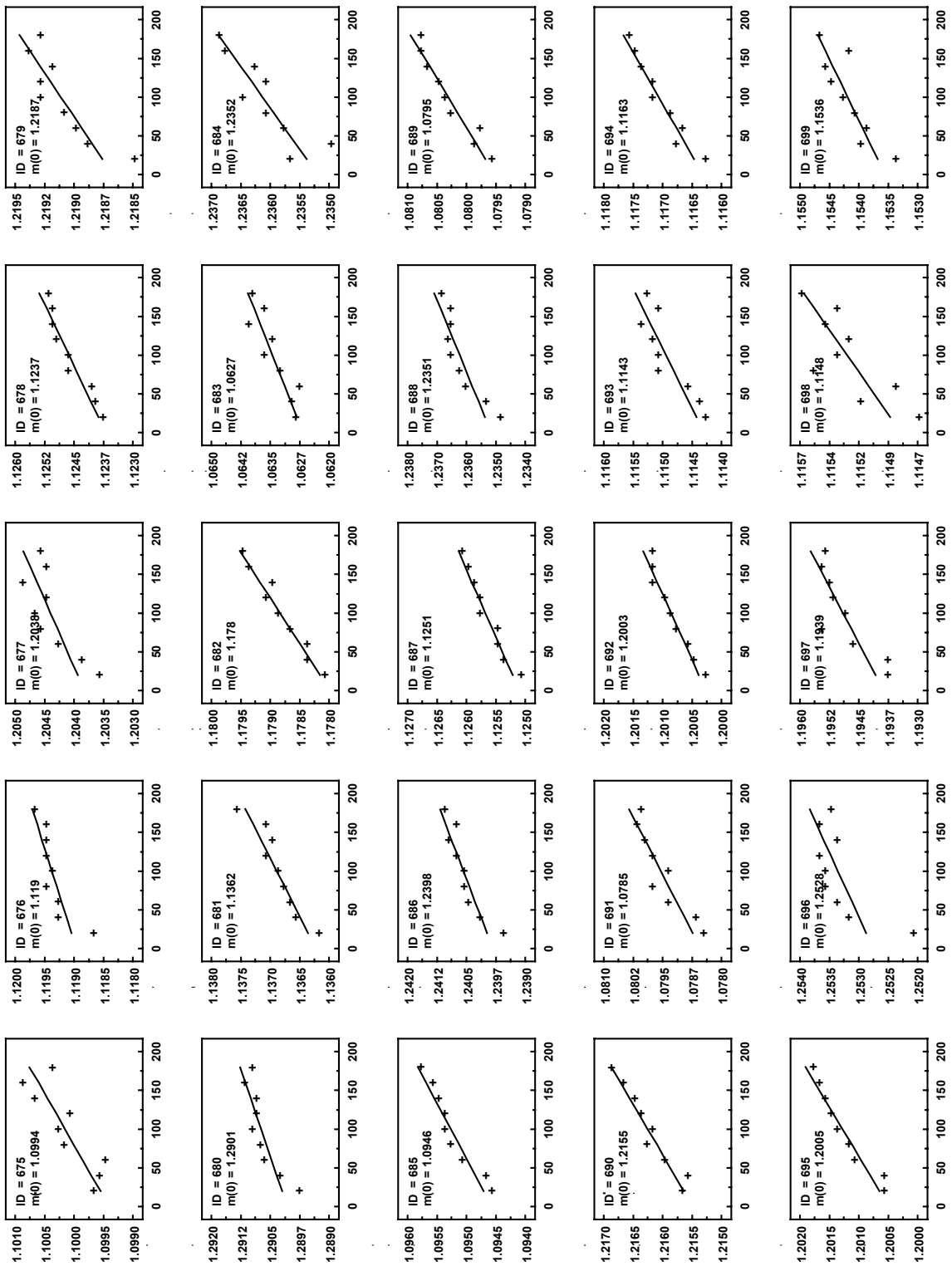

Fig. 32. Panel ID=675-699: Multiple mass observations (in kilograms) as a function of elapsed time (in seconds) for insulation panels 675 through 699. Linear fit for data (shown as solid line) was back-extrapolated to elapsed time zero (t_0) to determine m_0 for each panel.

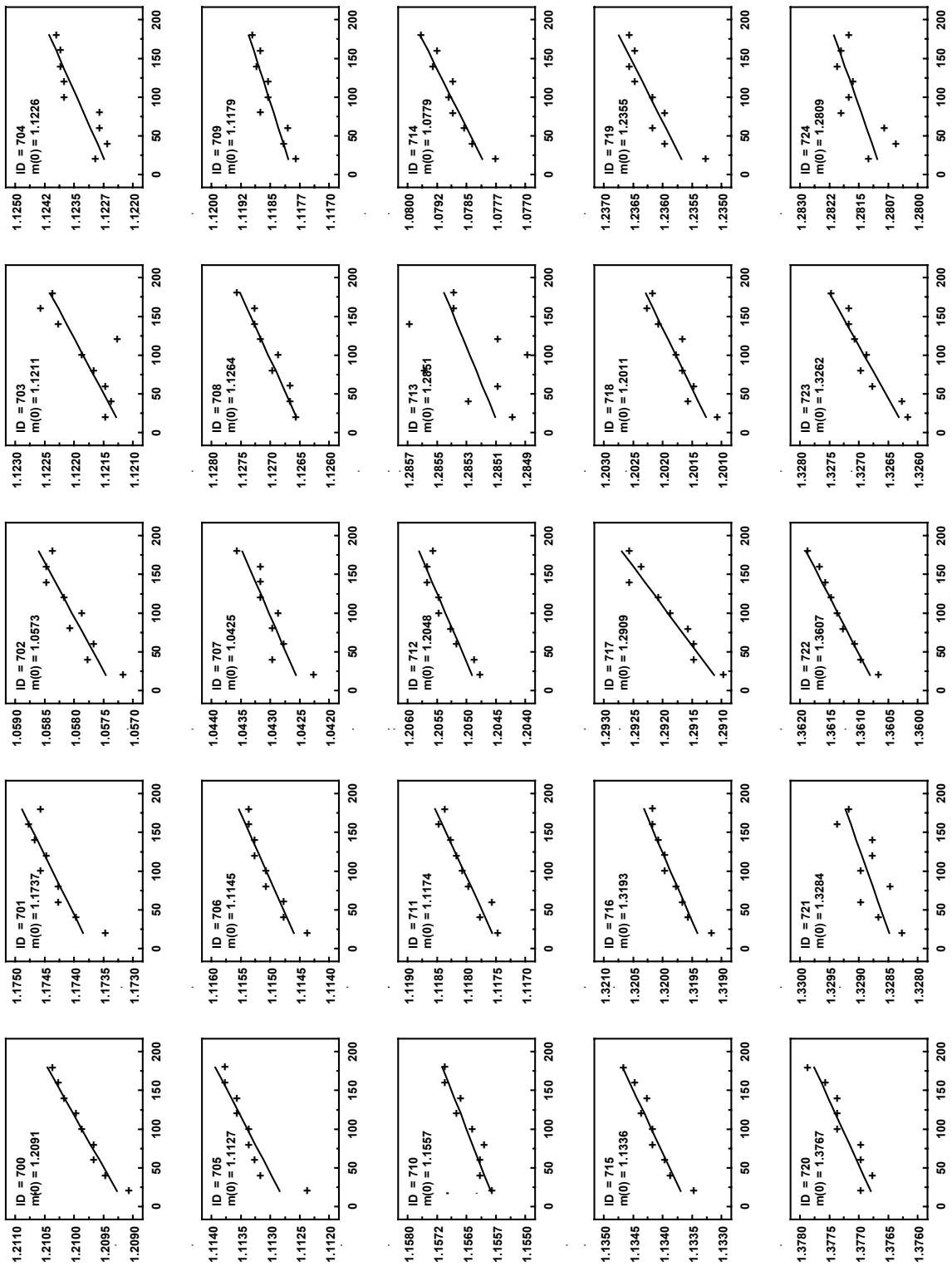

Fig. 33. Panel ID=700-724: Multiple mass observations (in kilograms) as a function of elapsed time (in seconds) for insulation panels 700 through 724. Linear fit for data (shown as solid line) was back-extrapolated to elapsed time zero (t_0) to determine m_0 for each panel.

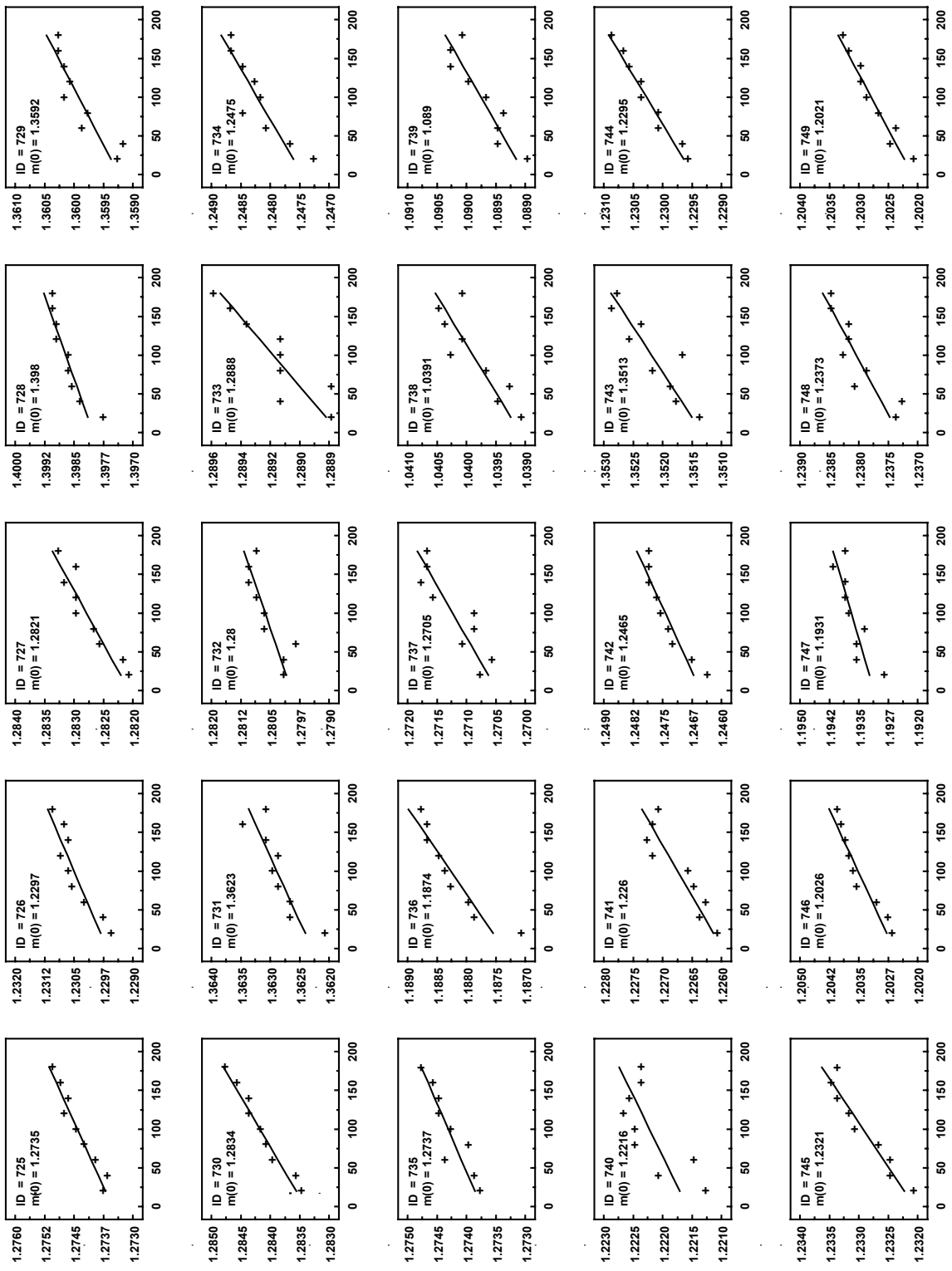

Fig. 34. Panel ID=725-749: Multiple mass observations (in kilograms) as a function of elapsed time (in seconds) for insulation panels 725 through 749. Linear fit for data (shown as solid line) was back-extrapolated to elapsed time zero (t_0) to determine m_0 for each panel.

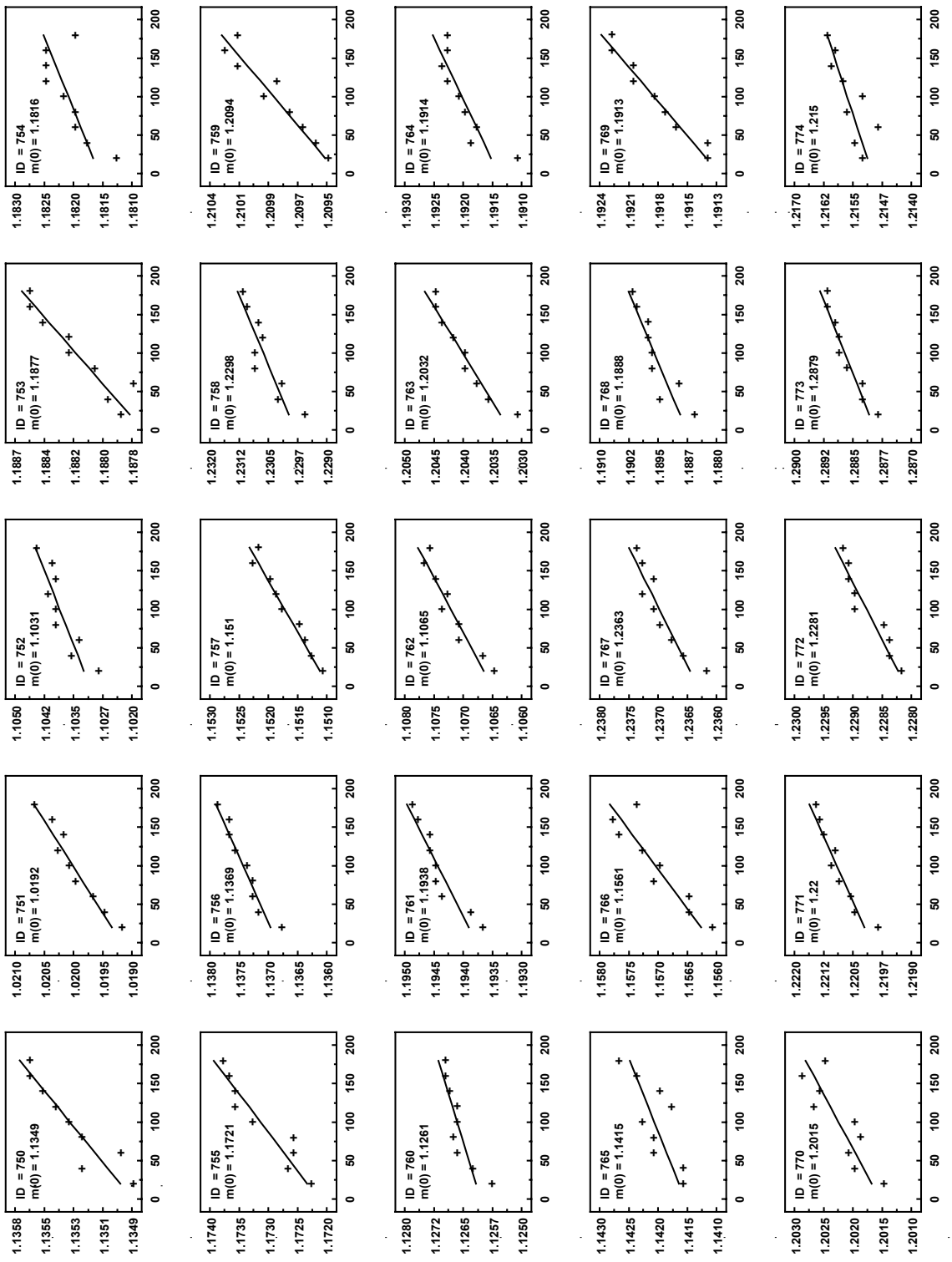

Fig. 35. Panel ID=750-774: Multiple mass observations (in kilograms) as a function of elapsed time (in seconds) for insulation panels 750 through 774. Linear fit for data (shown as solid line) was back-extrapolated to elapsed time zero (t_0) to determine m_0 for each panel.

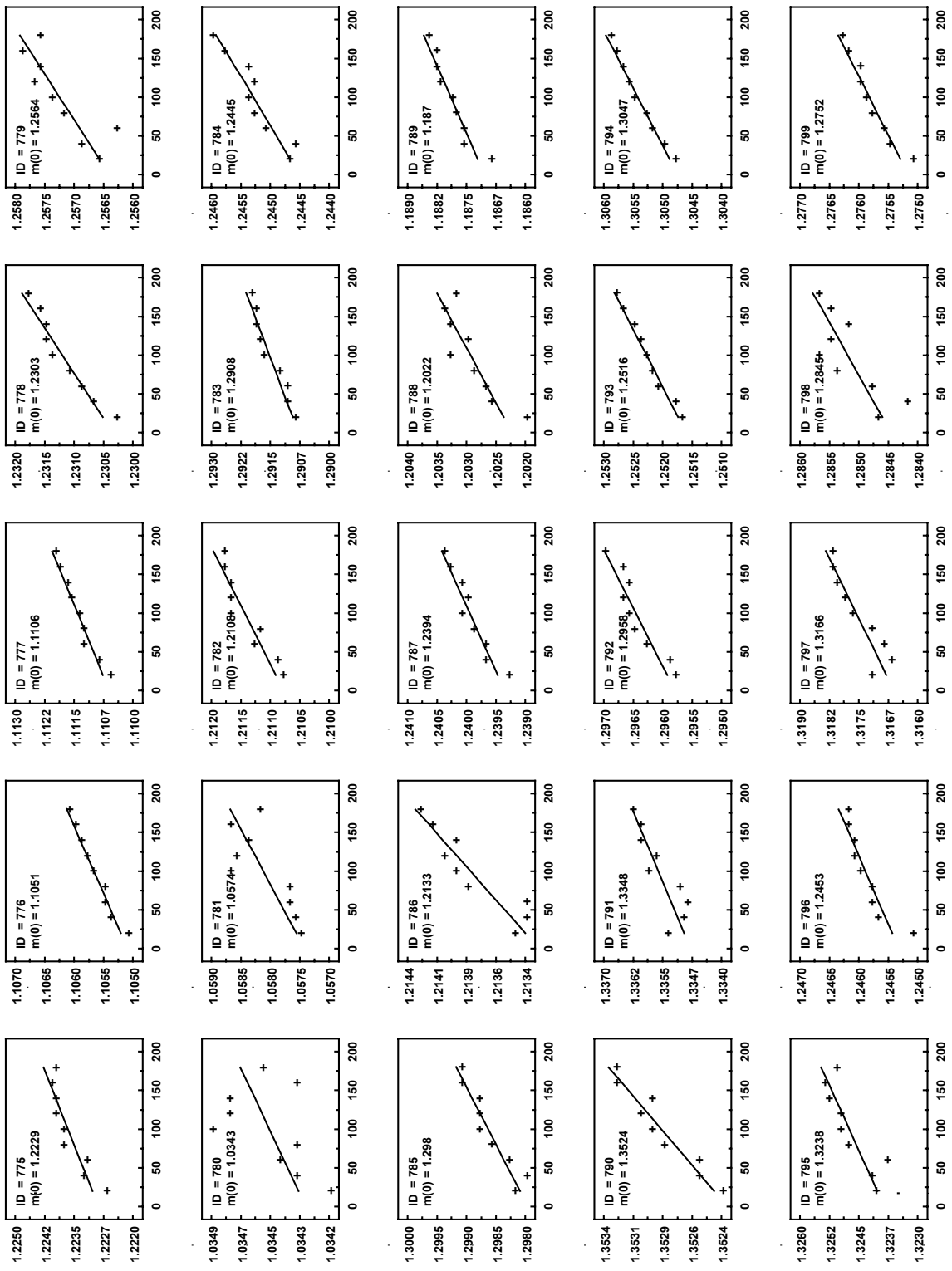

Fig. 36. Panel ID=775-799: Multiple mass observations (in kilograms) as a function of elapsed time (in seconds) for insulation panels 775 through 799. Linear fit for data (shown as solid line) was back-extrapolated to elapsed time zero (t_0) to determine m_0 for each panel.

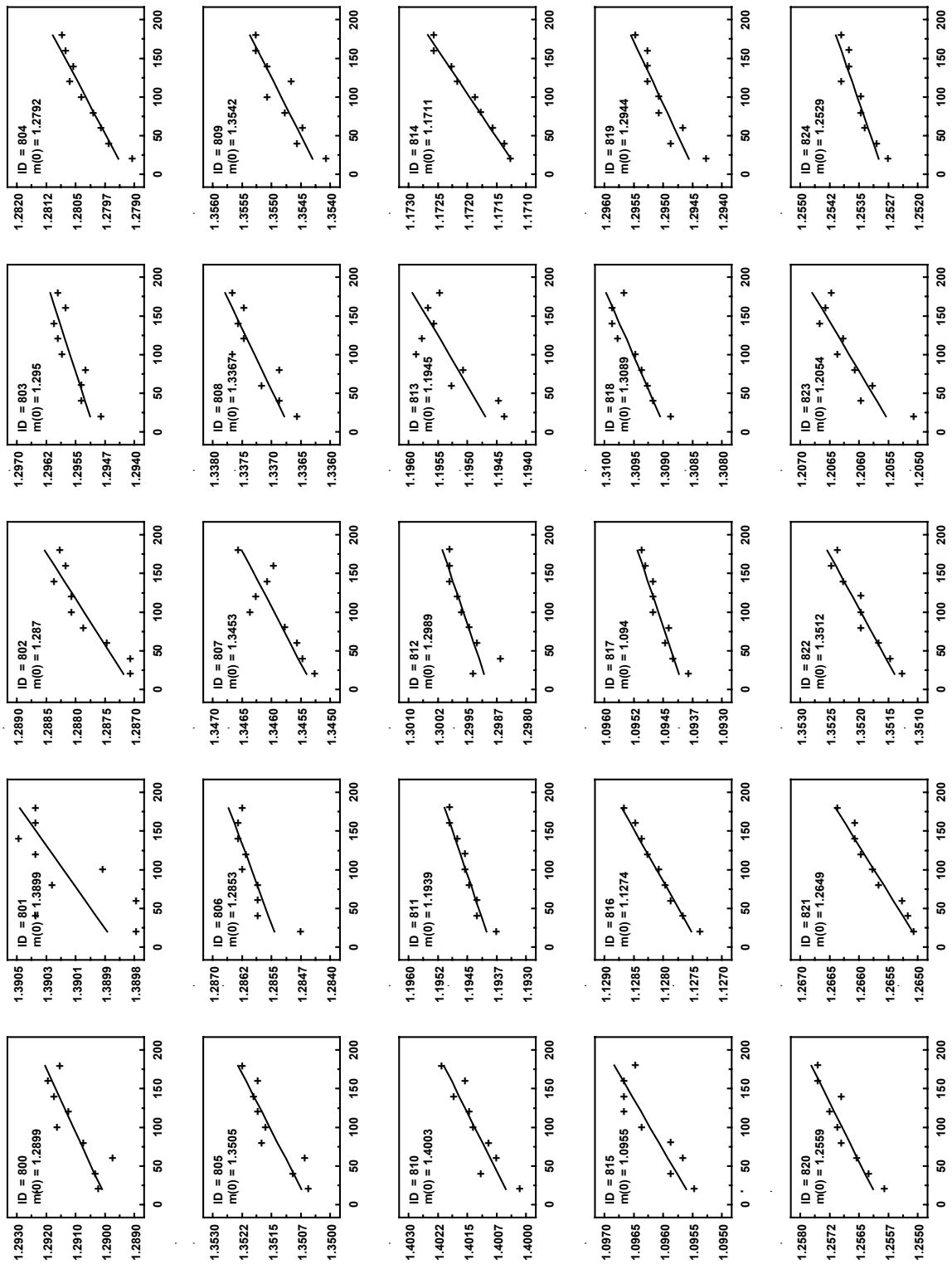

Fig. 37. Panel ID=800-824: Multiple mass observations (in kilograms) as a function of elapsed time (in seconds) for insulation panels 800 through 824. Linear fit for data (shown as solid line) was back-extrapolated to elapsed time zero (t_0) to determine m_0 for each panel.

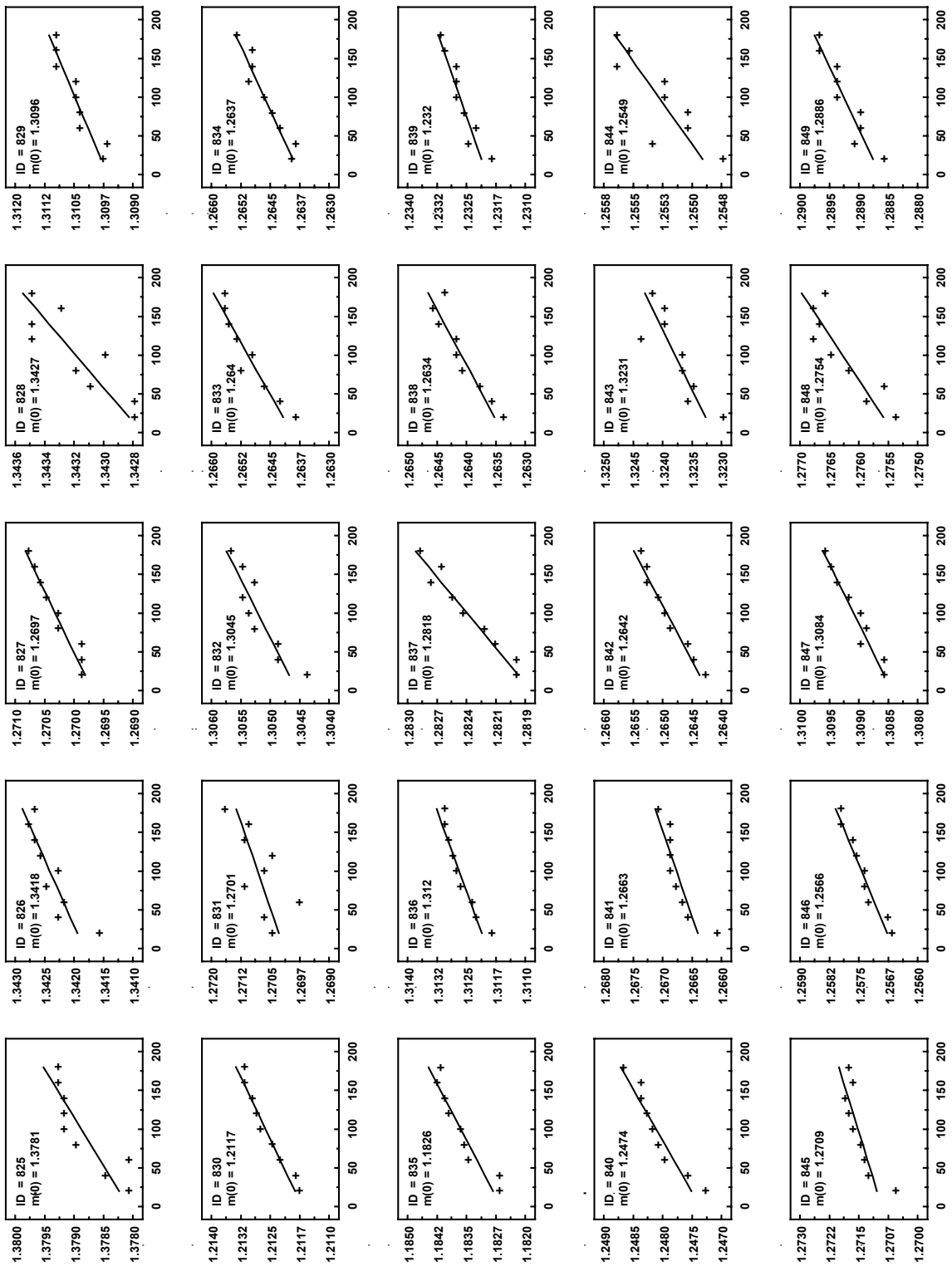

Fig. 38. Panel ID=825-849: Multiple mass observations (in kilograms) as a function of elapsed time (in seconds) for insulation panels 825 through 849. Linear fit for data (shown as solid line) was back-extrapolated to elapsed time zero (t_0) to determine m_0 for each panel.

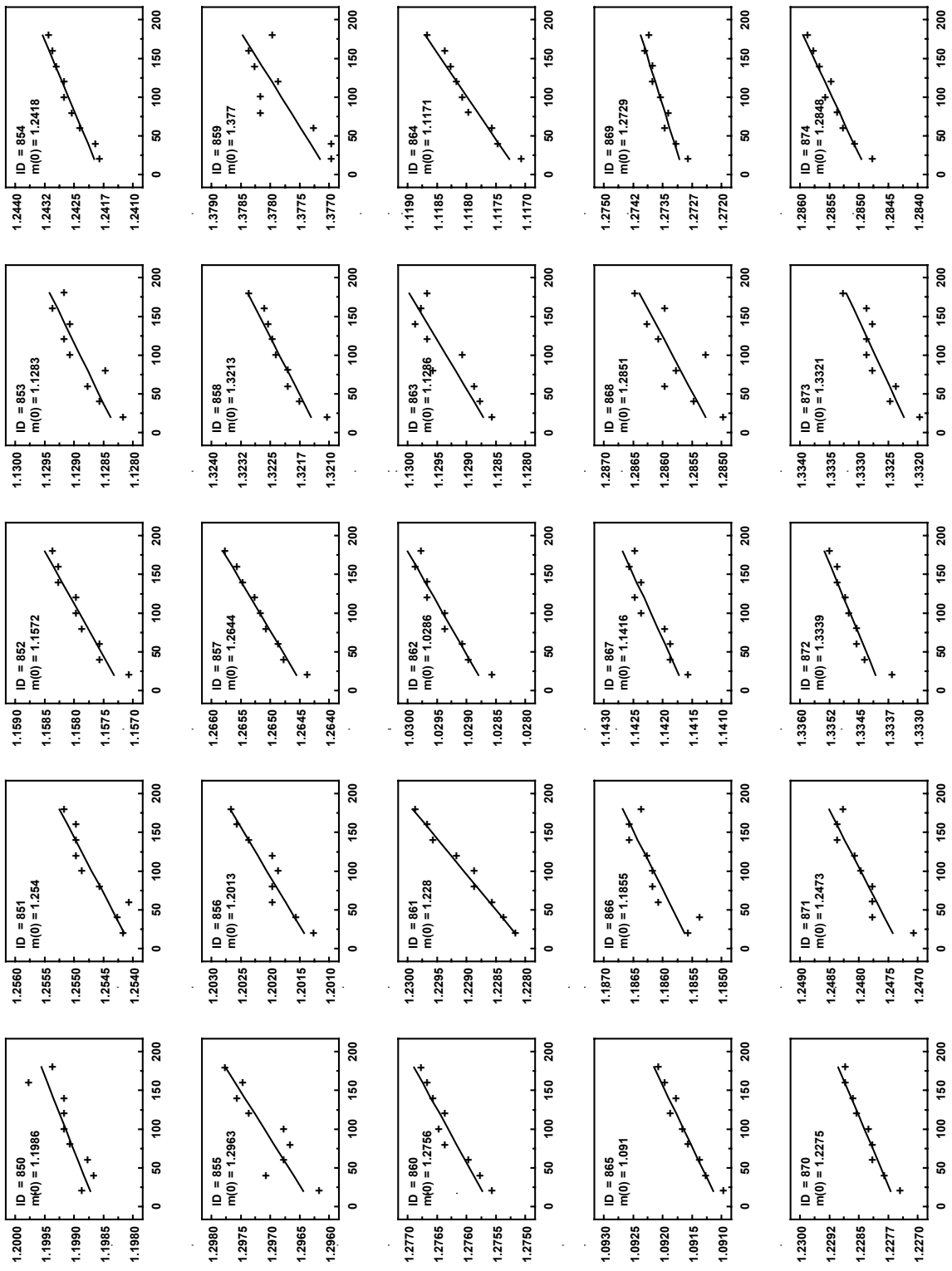

Fig. 39. Panel ID=850-874: Multiple mass observations (in kilograms) as a function of elapsed time (in seconds) for insulation panels 850 through 874. Linear fit for data (shown as solid line) was back-extrapolated to elapsed time zero (t_0) to determine m_0 for each panel.

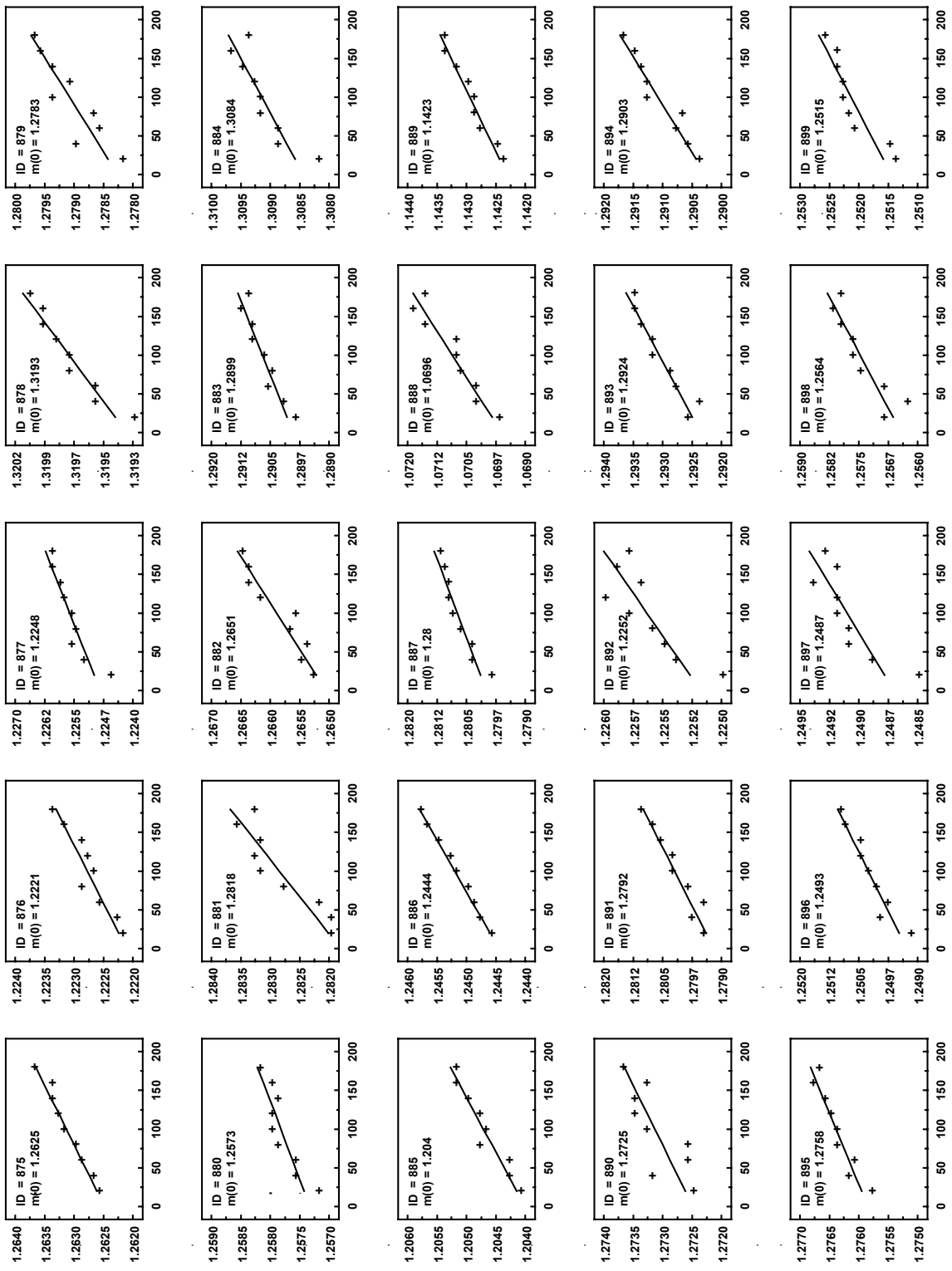

Fig. 40. Panel ID=875-899: Multiple mass observations (in kilograms) as a function of elapsed time (in seconds) for insulation panels 875 through 899. Linear fit for data (shown as solid line) was back-extrapolated to elapsed time zero (t_0) to determine m_0 for each panel.

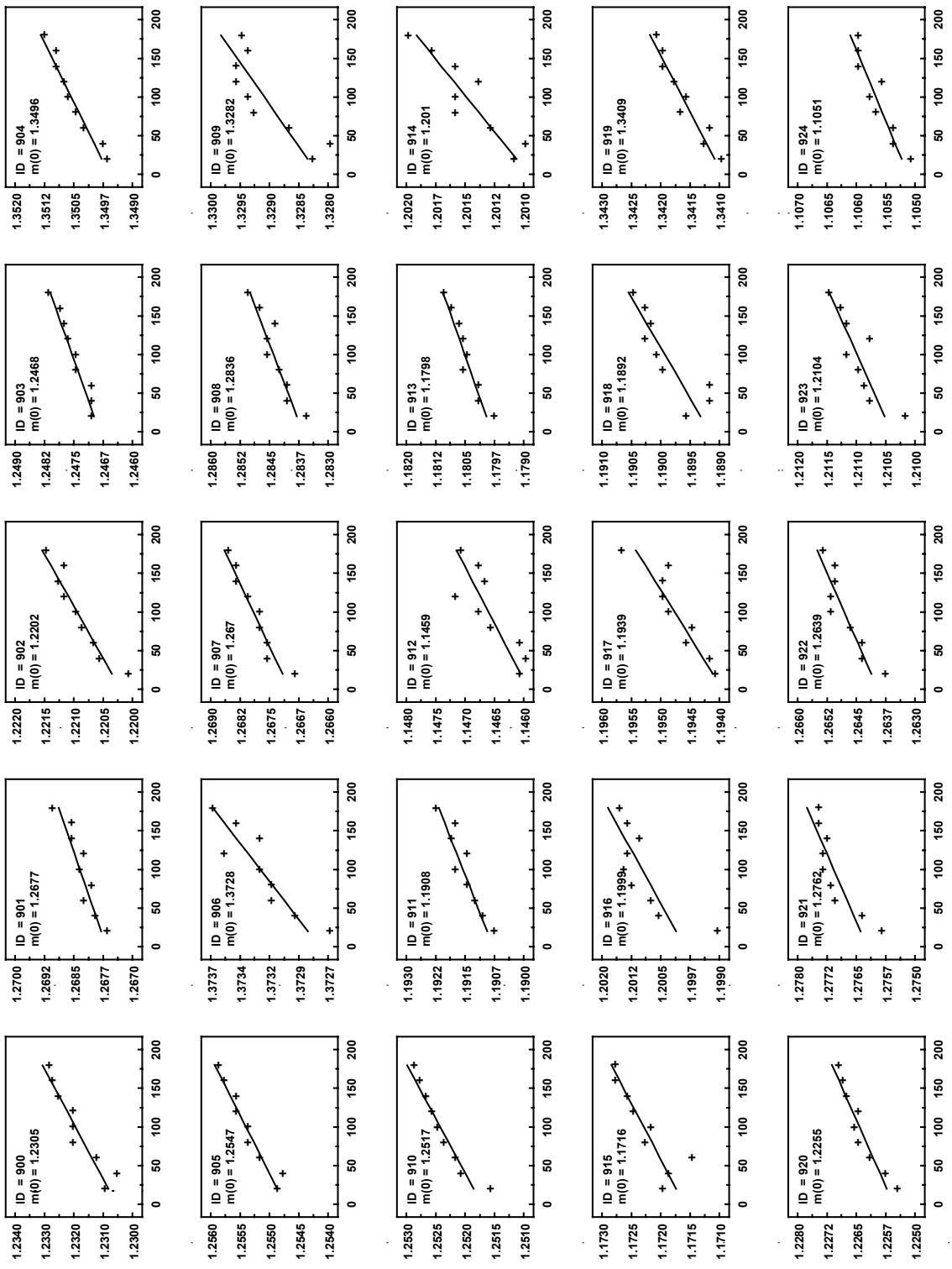

Fig. 41. Panel ID=900-924: Multiple mass observations (in kilograms) as a function of elapsed time (in seconds) for insulation panels 900 through 924. Linear fit for data (shown as solid line) was back-extrapolated to elapsed time zero (t_0) to determine m_0 for each panel.

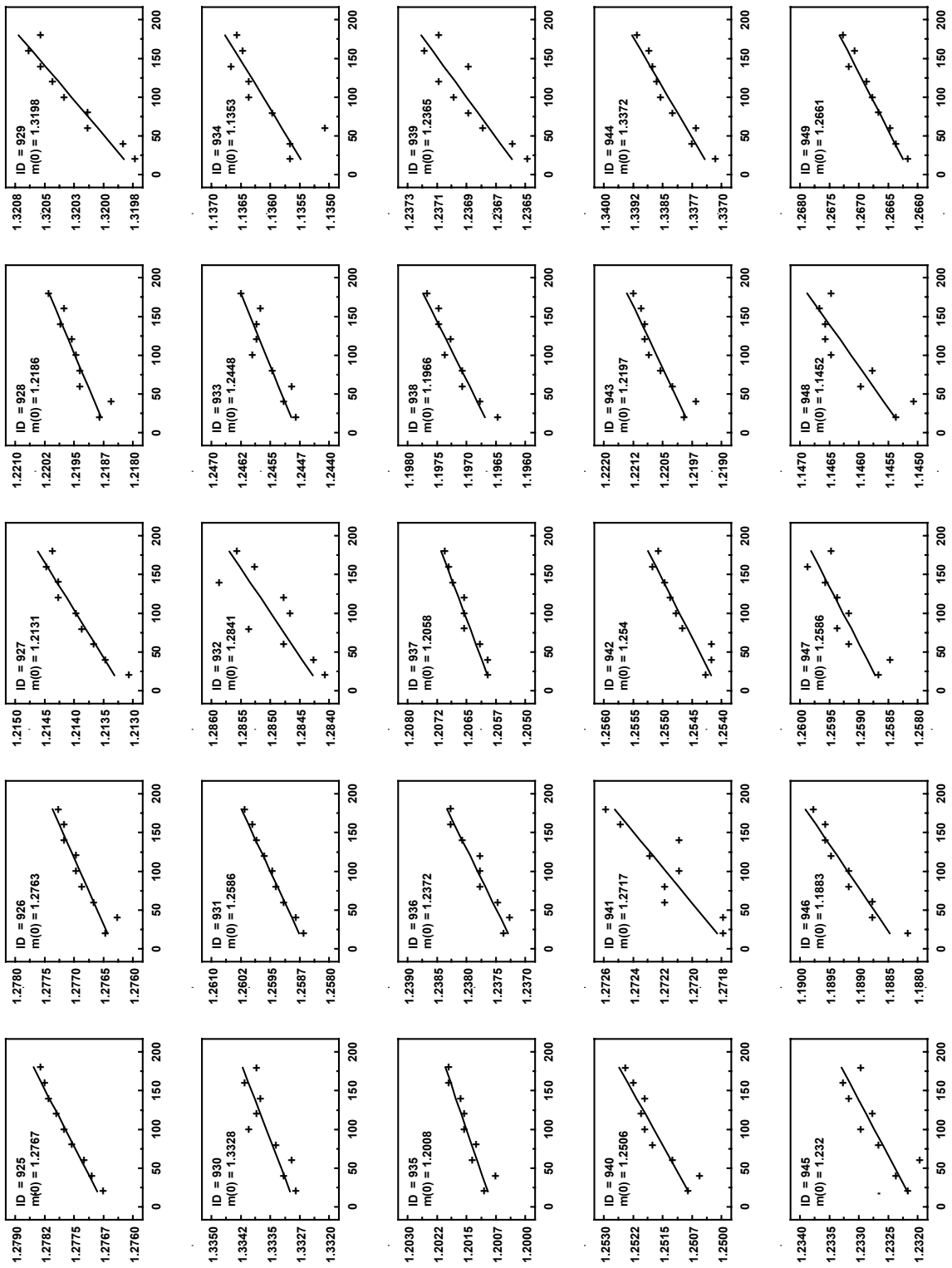

Fig. 42. Panel ID=925-949: Multiple mass observations (in kilograms) as a function of elapsed time (in seconds) for insulation panels 925 through 949. Linear fit for data (shown as solid line) was back-extrapolated to elapsed time zero (t_0) to determine m_0 for each panel.

Appendix C: Thickness Plots (Panel ID: 500 through 949)

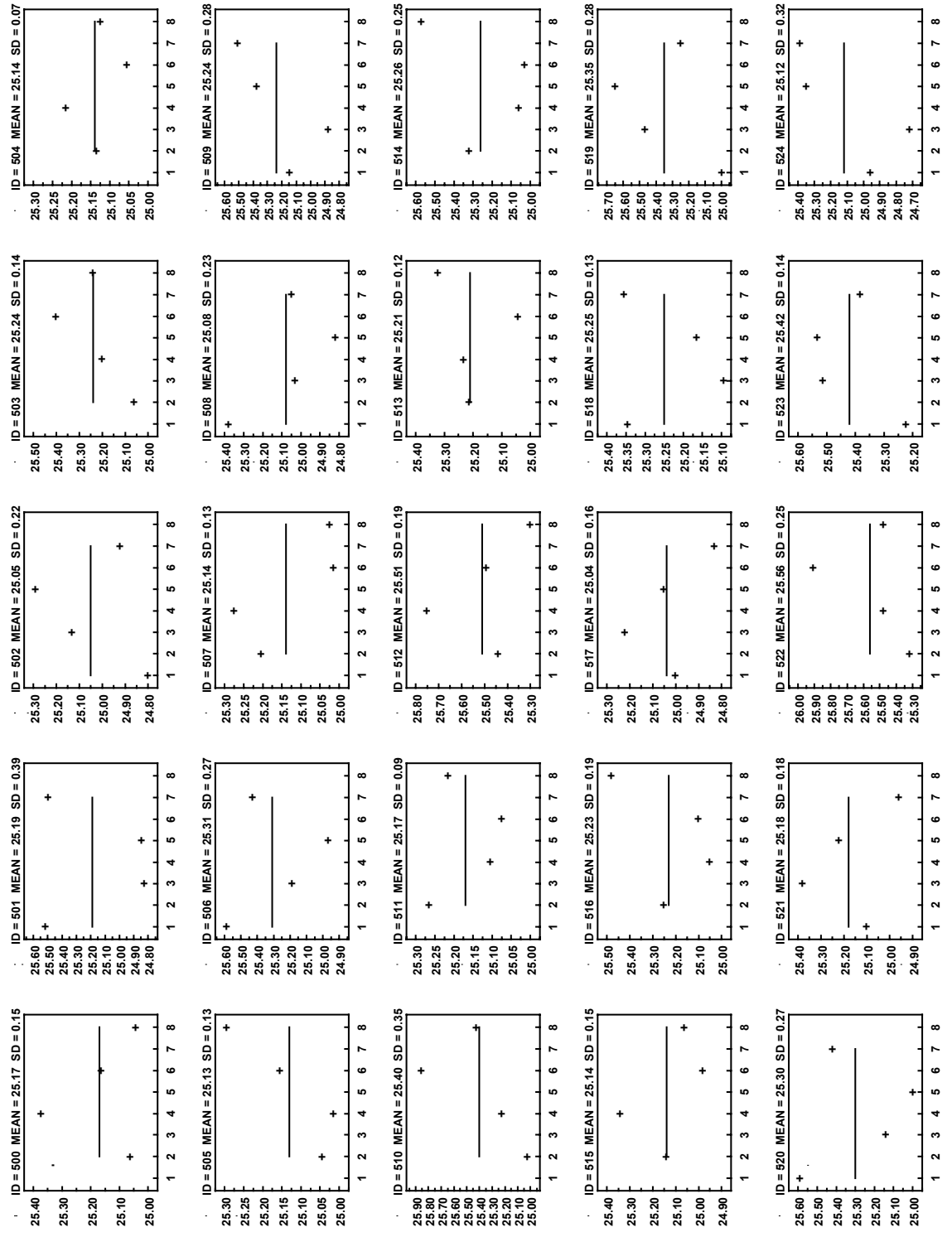

Fig. 43. Panel ID=500-524: Thickness measurements (in millimeters) at locations 1 through 8 (Fig. 3) for insulation panels 500 through 524. Mean is shown as solid line (with numerical values for mean and standard deviation (SD) in the title of each frame).

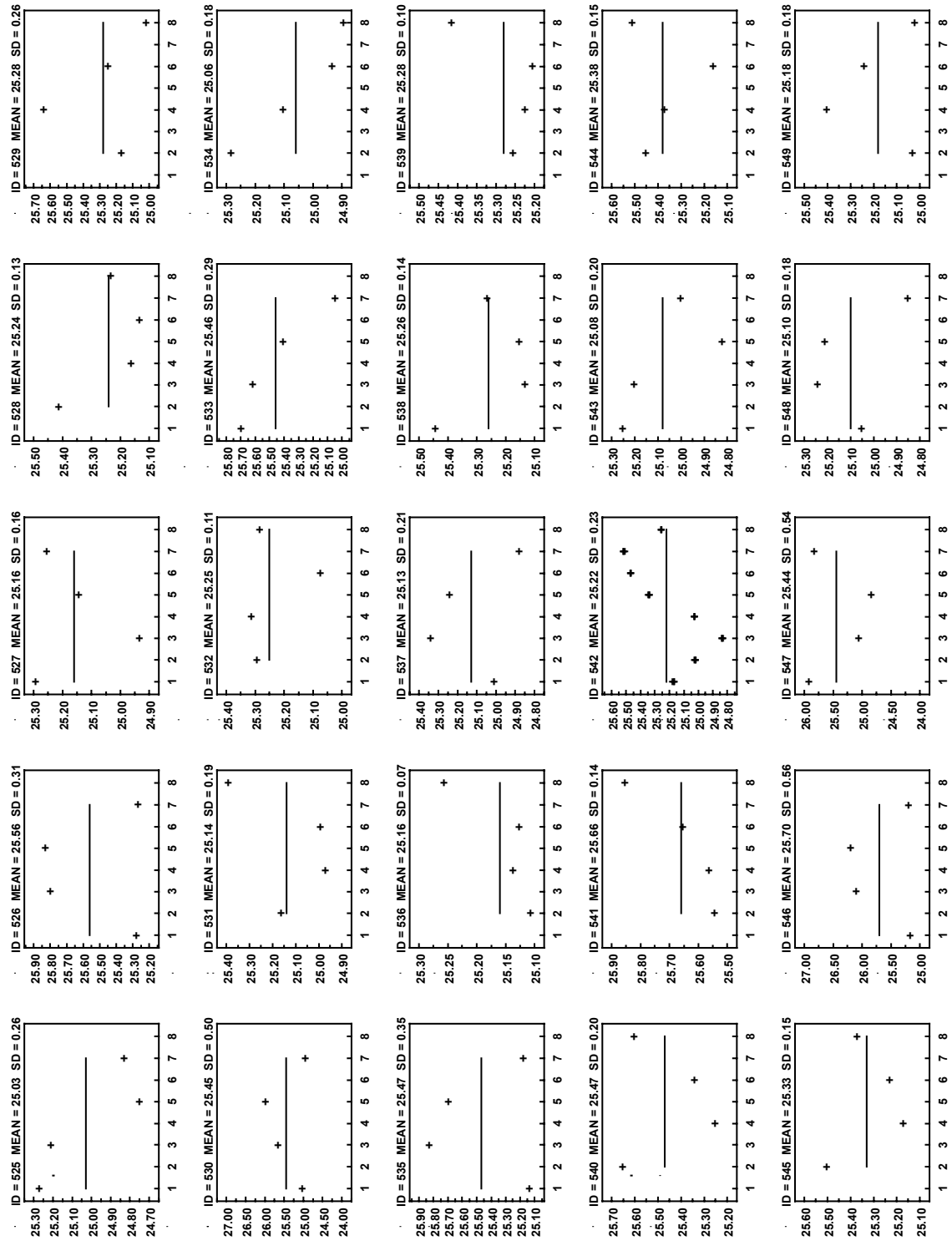

Fig. 44. Panel ID=525-549: Thickness measurements (in millimeters) at locations 1 through 8 (Fig. 3) for insulation panels 525 through 549. Mean is shown as solid line (with numerical values for mean and standard deviation (SD) in the title of each frame).

Appendix C

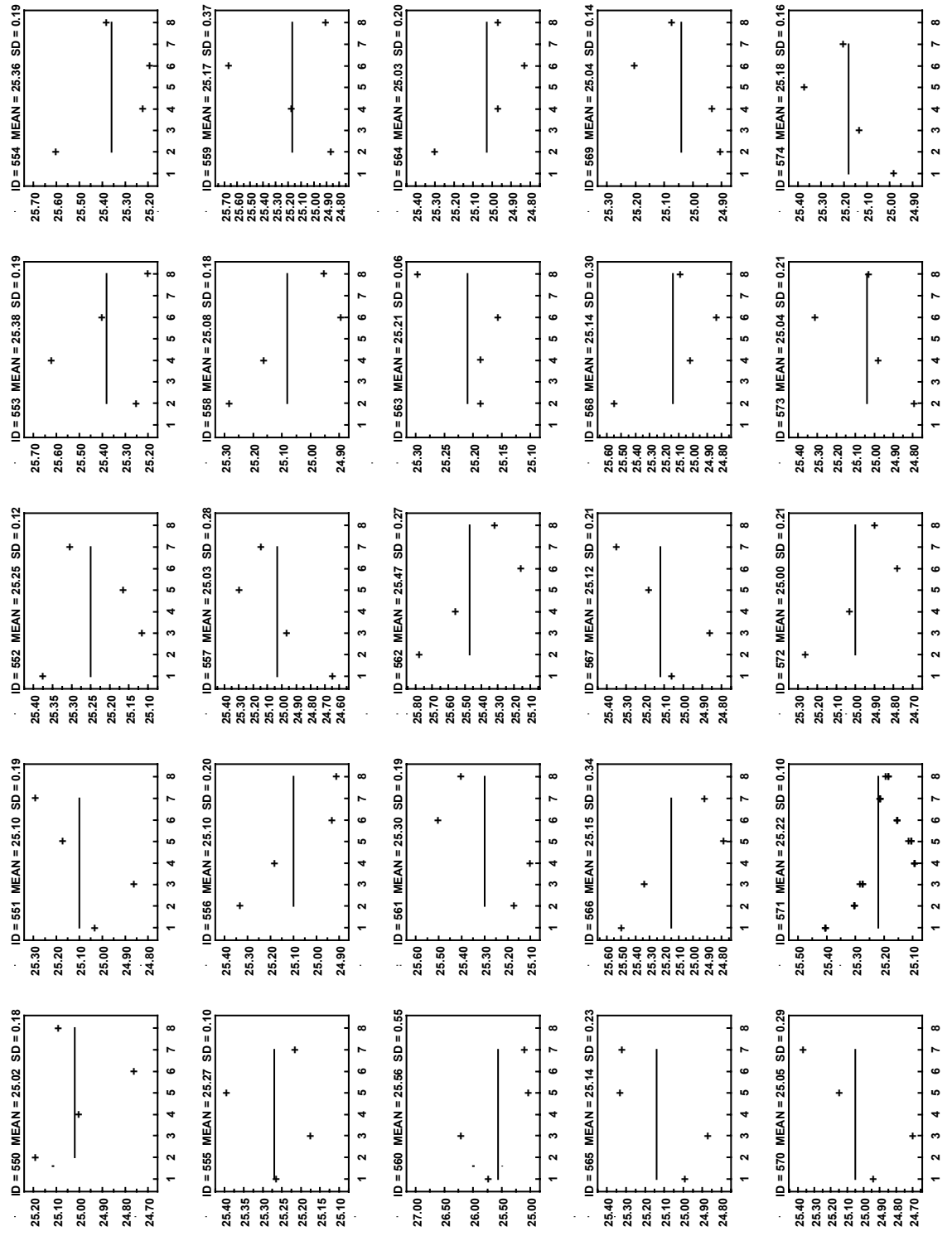

Fig. 45. Panel ID=550-574: Thickness measurements (in millimeters) at locations 1 through 8 (Fig. 3) for insulation panels 550 through 574. Mean is shown as solid line (with numerical values for mean and standard deviation (SD) in the title of each frame).

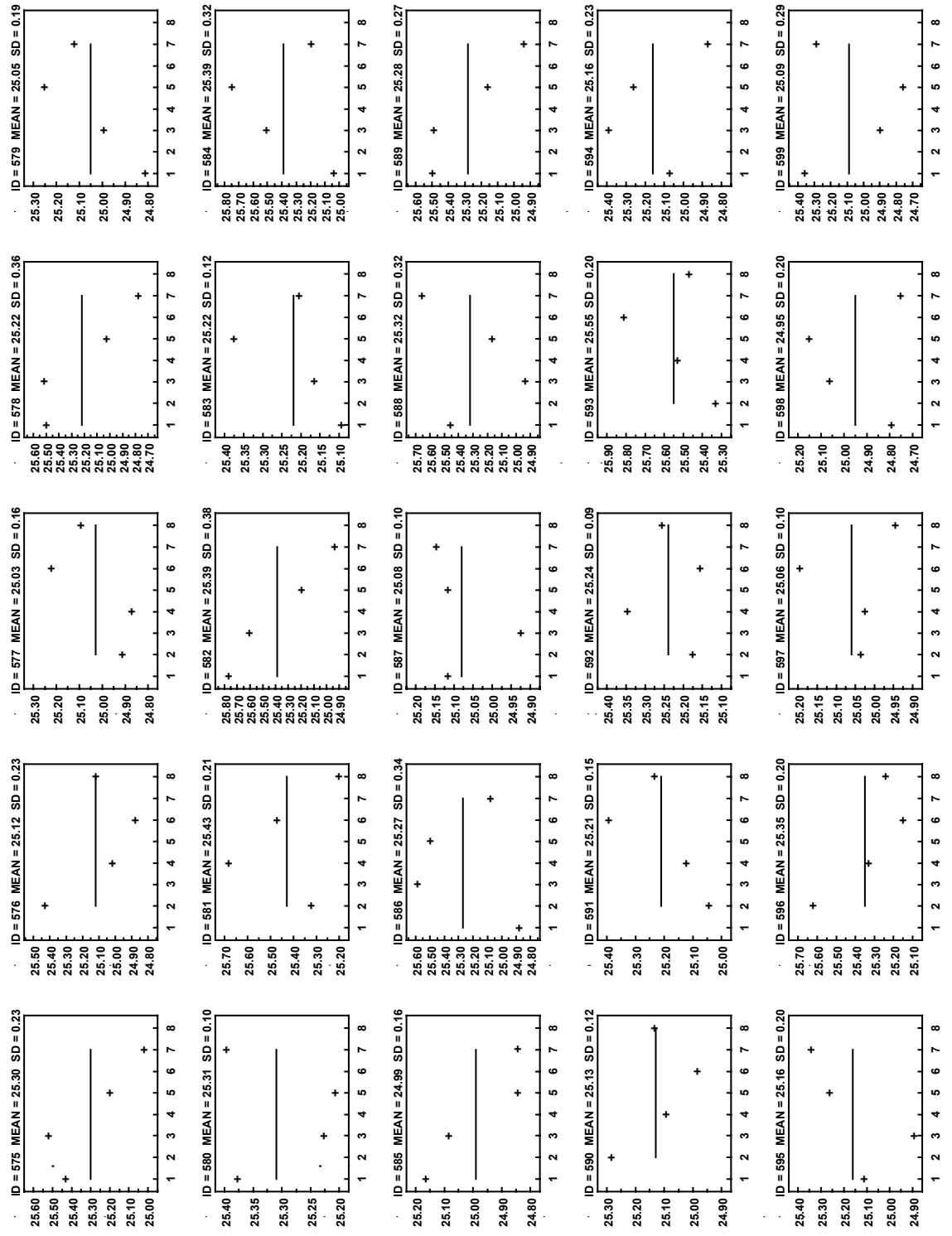

Fig. 46. Panel ID=575-599: Thickness measurements (in millimeters) at locations 1 through 8 (Fig. 3) for insulation panels 575 through 599. Mean is shown as solid line (with numerical values for mean and standard deviation (SD) in the title of each frame).

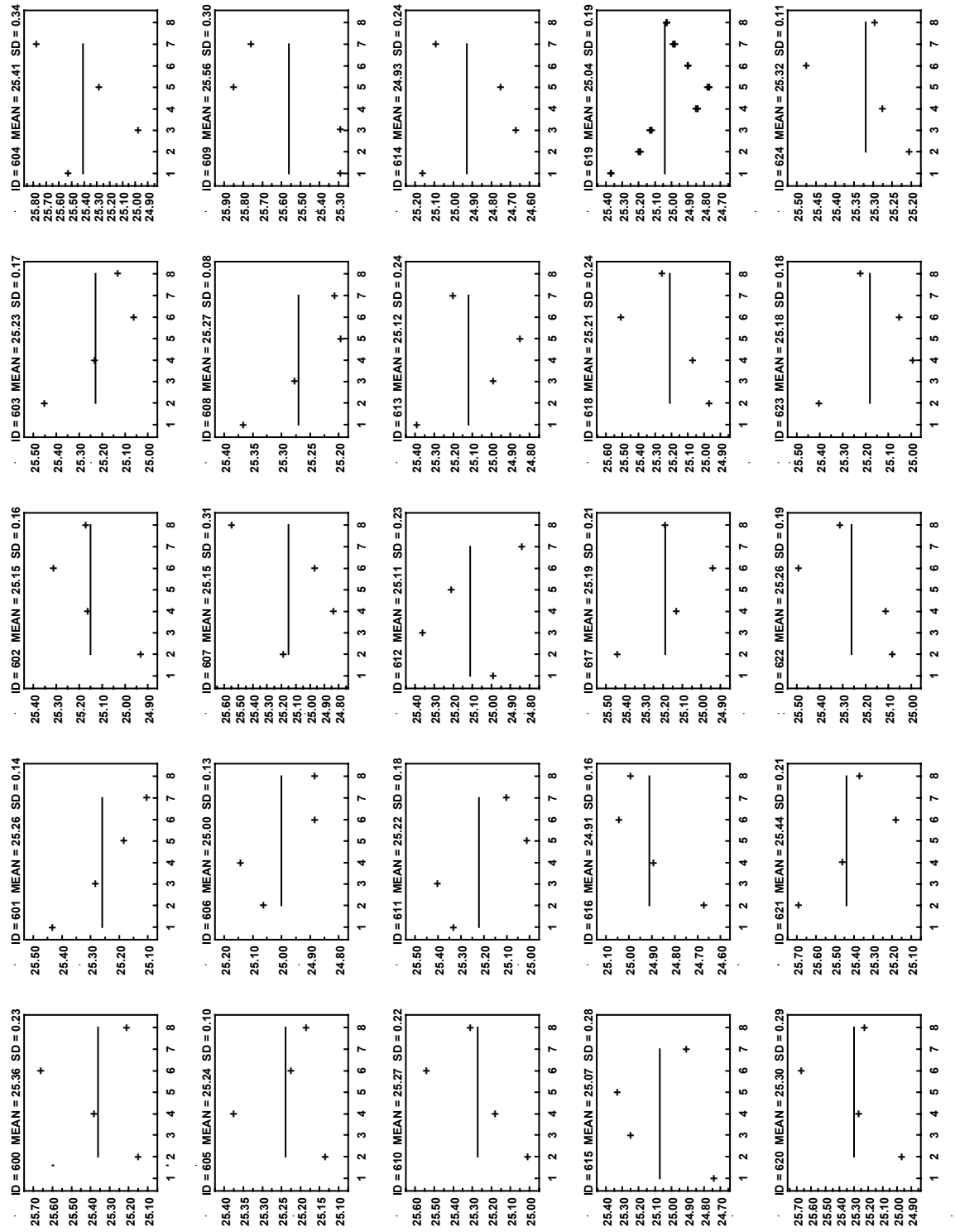

Fig. 47. Panel ID=600-624: Thickness measurements (in millimeters) at locations 1 through 8 (Fig. 3) for insulation panels 600 through 624. Mean is shown as solid line (with numerical values for mean and standard deviation (SD) in the title of each frame).

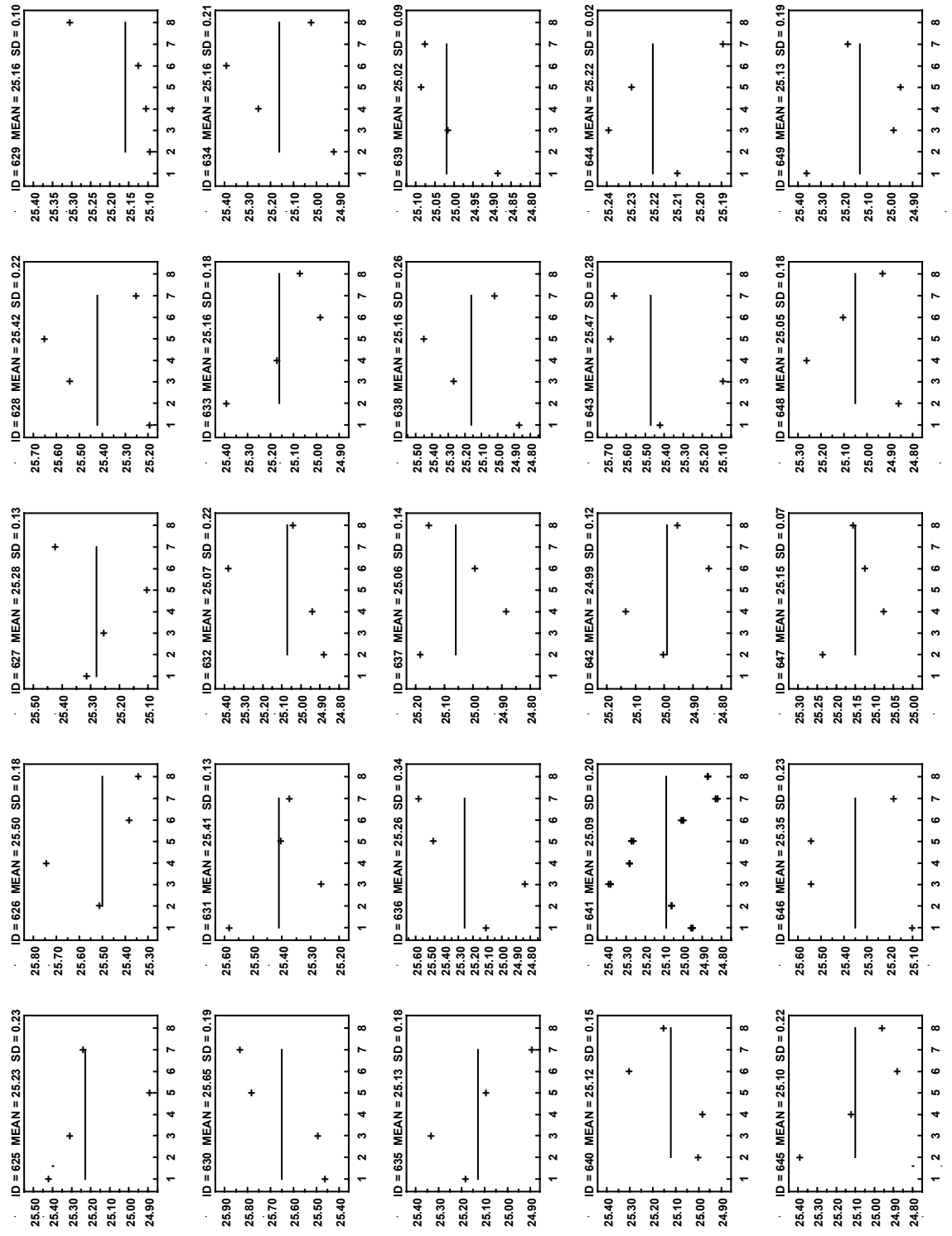

Fig. 48. Panel ID=625-649: Thickness measurements (in millimeters) at locations 1 through 8 (Fig. 3) for insulation panels 625 through 649. Mean is shown as solid line (with numerical values for mean and standard deviation (SD) in the title of each frame).

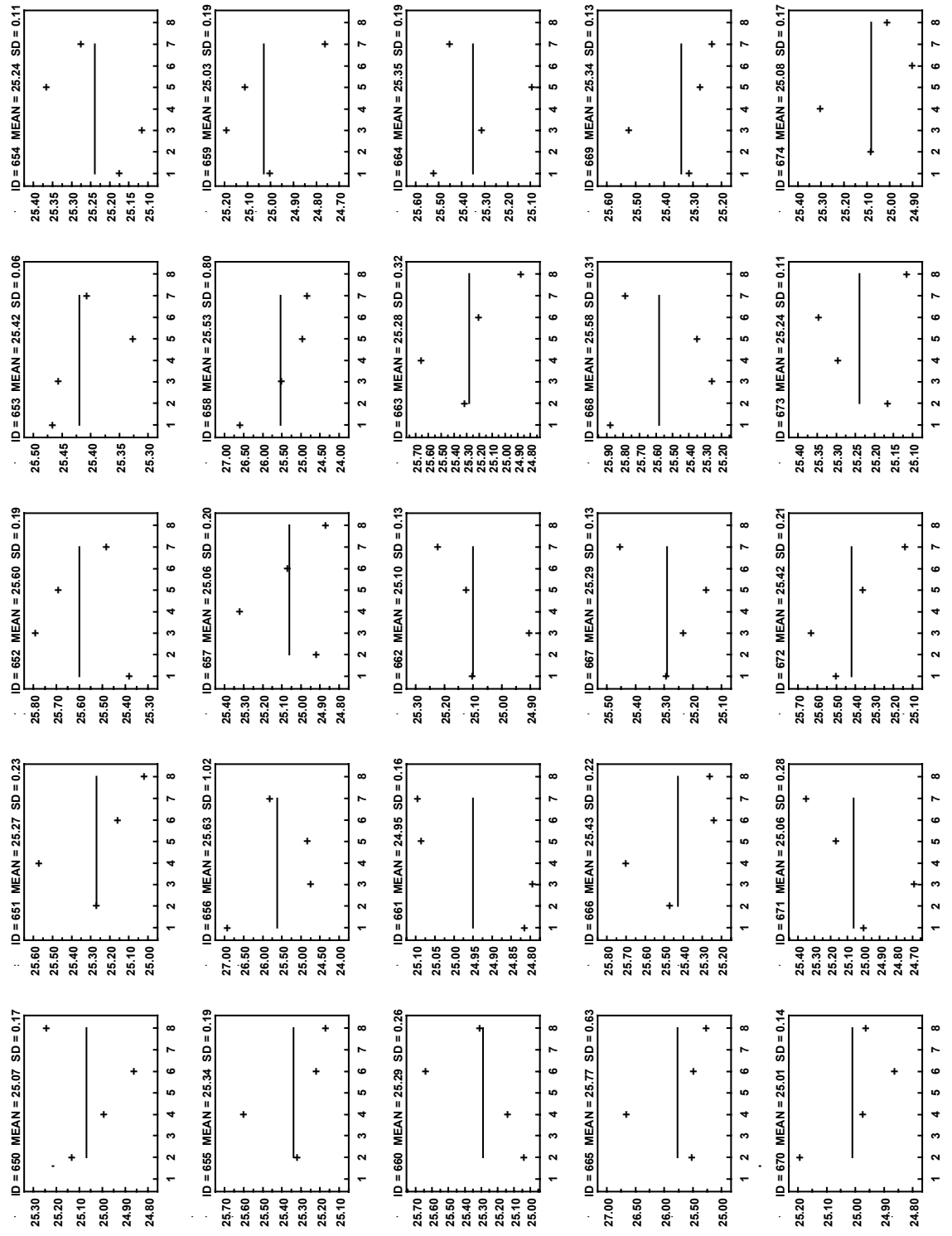

Fig. 49. Panel ID=650-674: Thickness measurements (in millimeters) at locations 1 through 8 (Fig. 3) for insulation panels 650 through 674. Mean is shown as solid line (with numerical values for mean and standard deviation (SD) in the title of each frame).

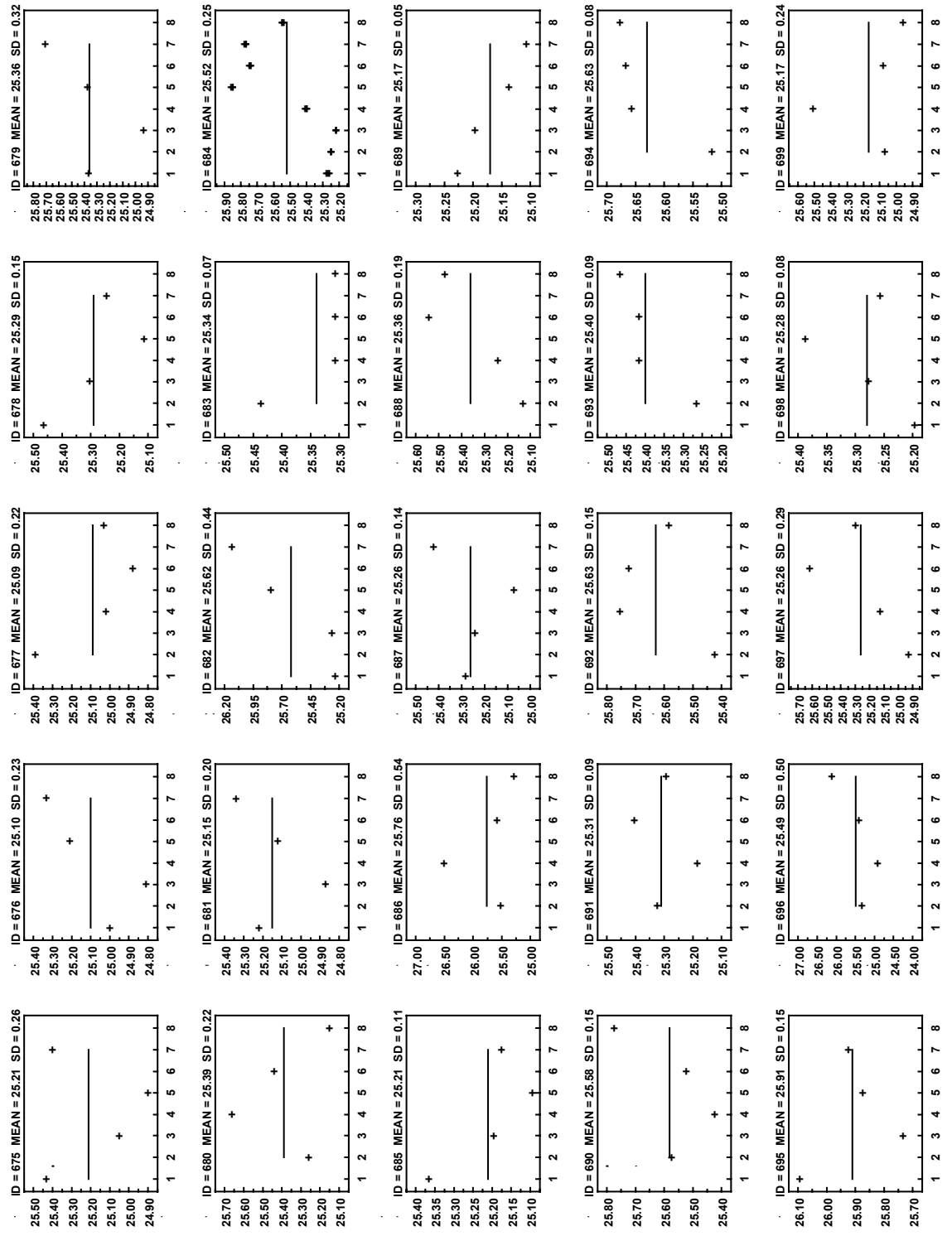

Fig. 50. Panel ID=675-699: Thickness measurements (in millimeters) at locations 1 through 8 (Fig. 3) for insulation panels 675 through 699. Mean is shown as solid line (with numerical values for mean and standard deviation (SD) in the title of each frame).

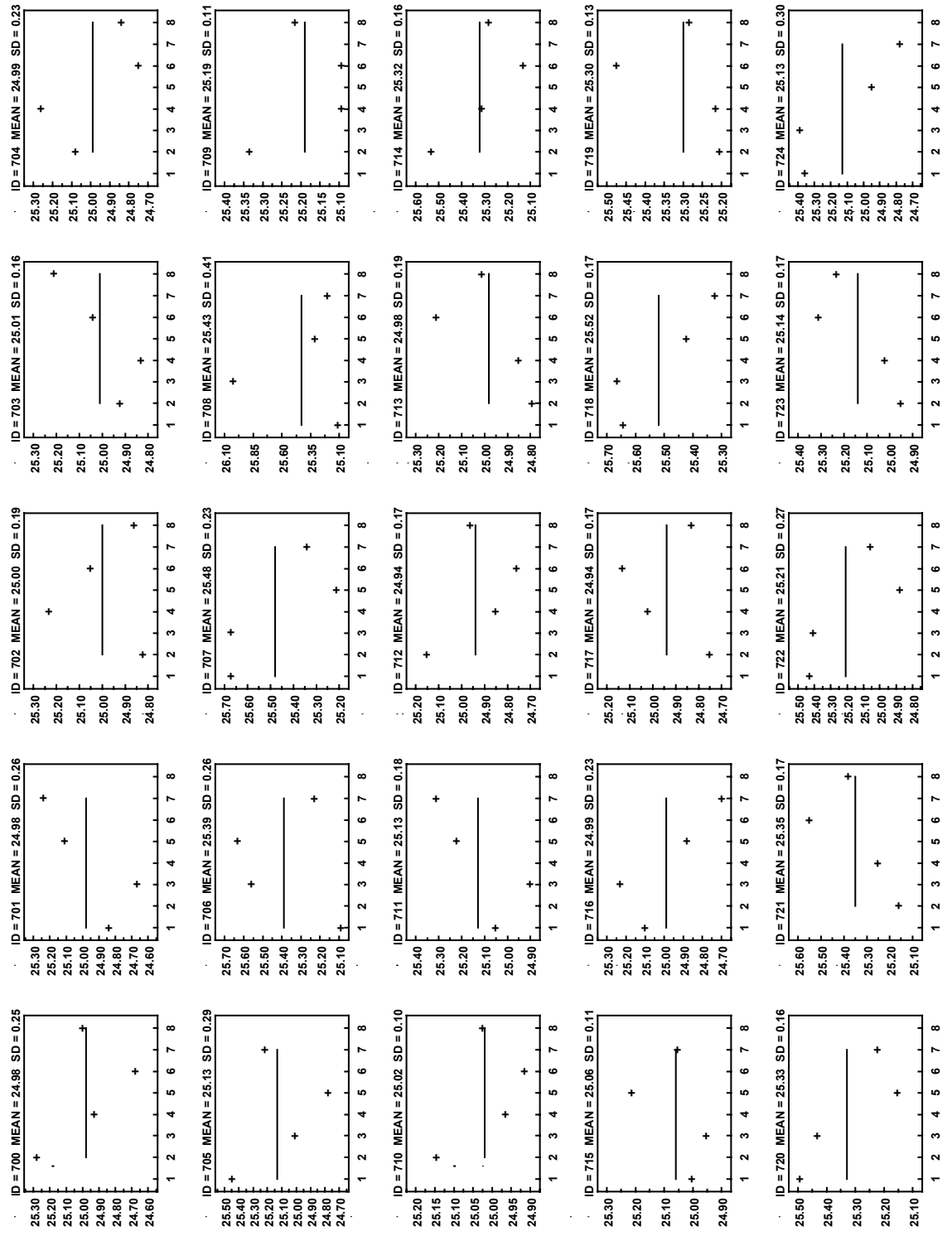

Fig. 51. Panel ID=700-724: Thickness measurements (in millimeters) at locations 1 through 8 (Fig. 3) for insulation panels 700 through 724. Mean is shown as solid line (with numerical values for mean and standard deviation (SD) in the title of each frame).

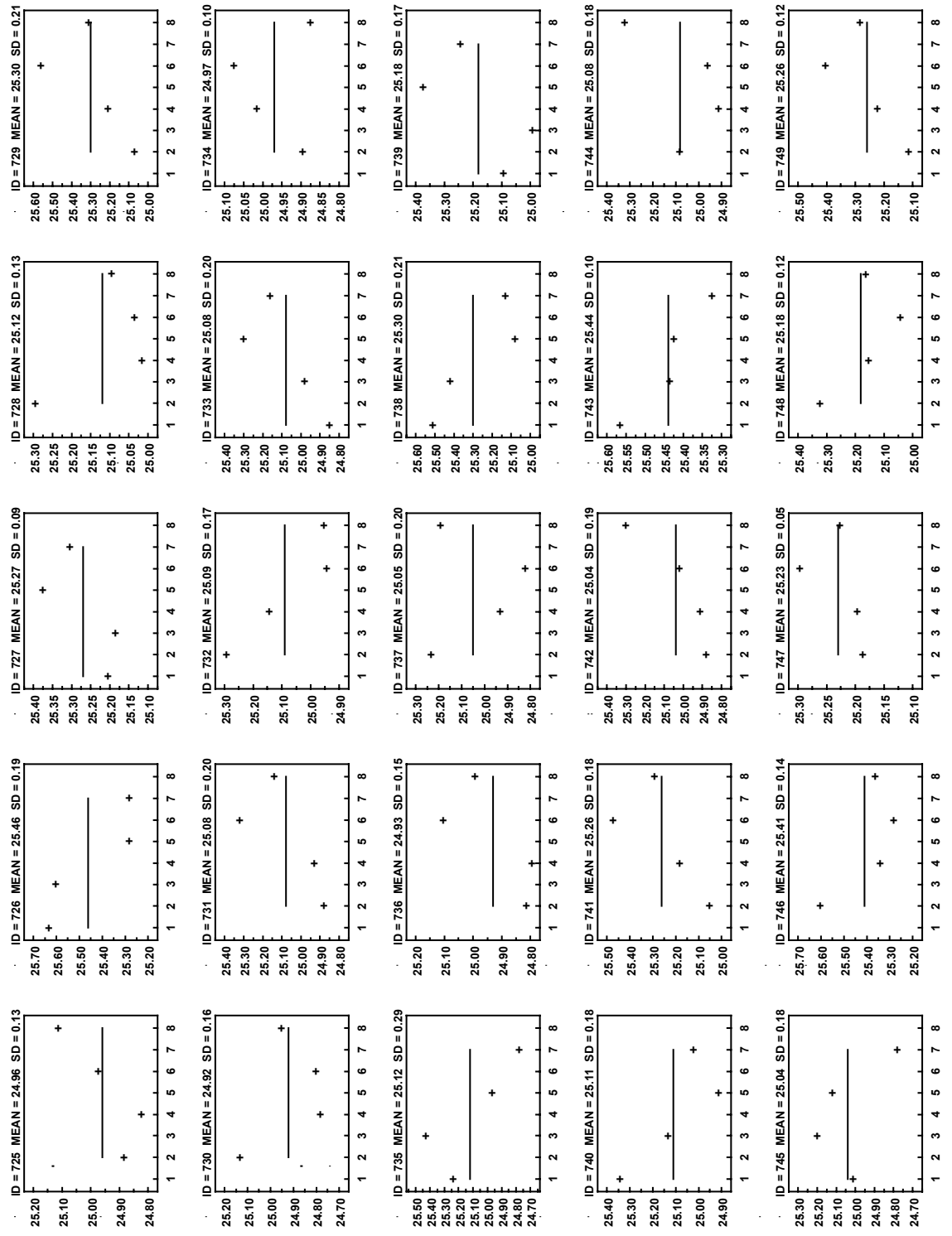

Fig. 52. Panel ID=725-749: Thickness measurements (in millimeters) at locations 1 through 8 (Fig. 3) for insulation panels 725 through 749. Mean is shown as solid line (with numerical values for mean and standard deviation (SD) in the title of each frame).

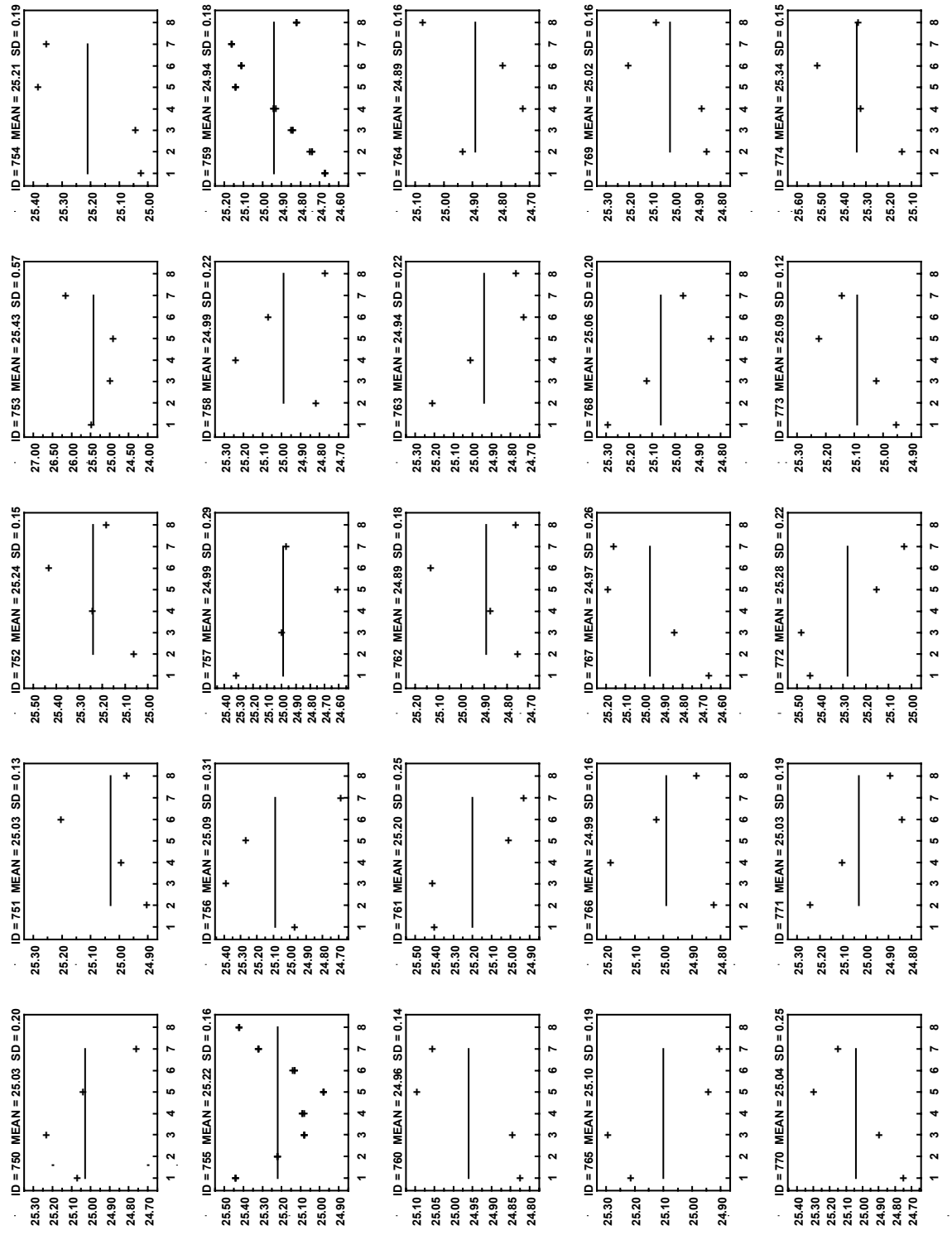

Fig. 53. Panel ID=750-774: Thickness measurements (in millimeters) at locations 1 through 8 (Fig. 3) for insulation panels 750 through 774. Mean is shown as solid line (with numerical values for mean and standard deviation (SD) in the title of each frame).

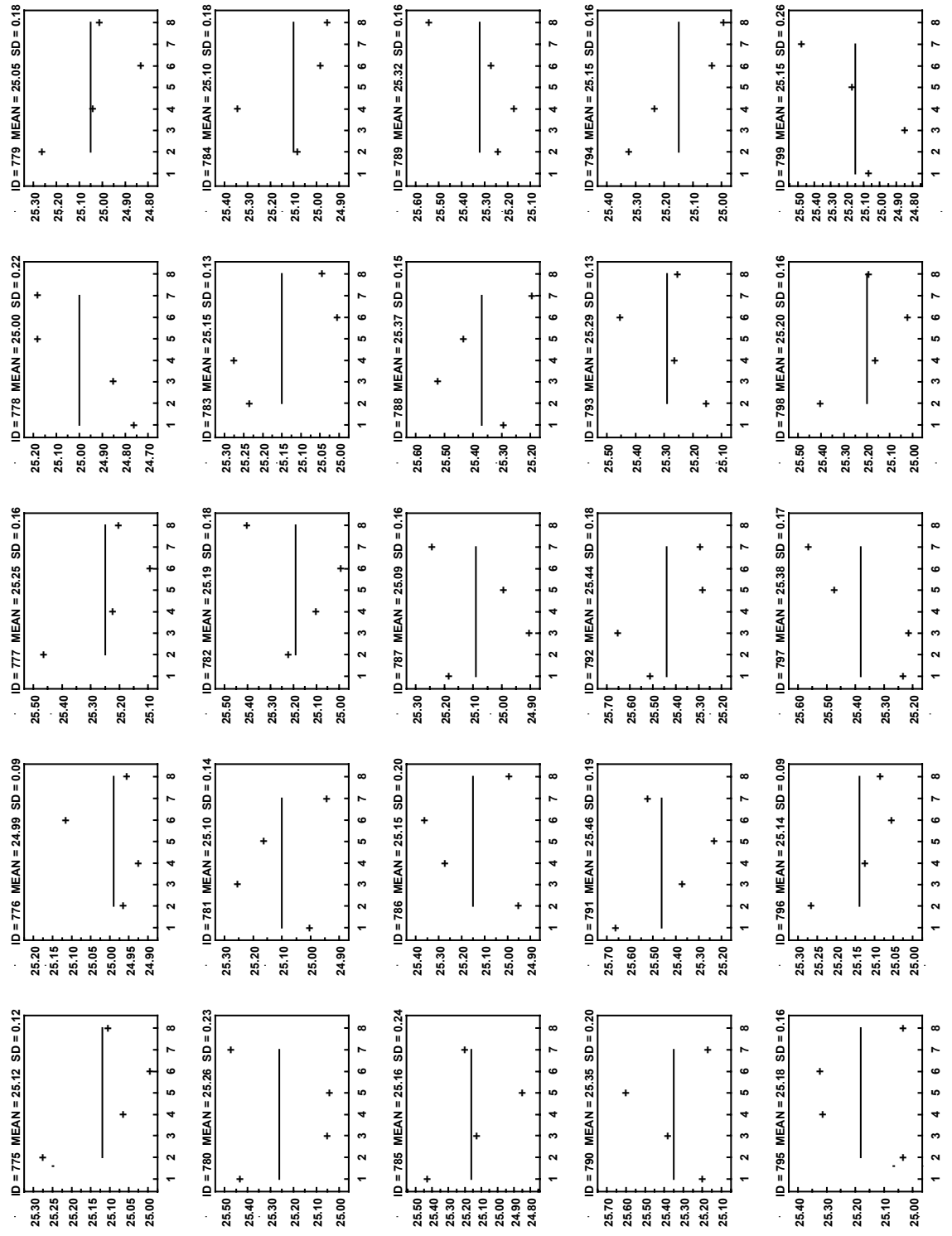

Fig. 54. Panel ID=775-799: Thickness measurements (in millimeters) at locations 1 through 8 (Fig. 3) for insulation panels 775 through 799. Mean is shown as solid line (with numerical values for mean and standard deviation (SD) in the title of each frame).

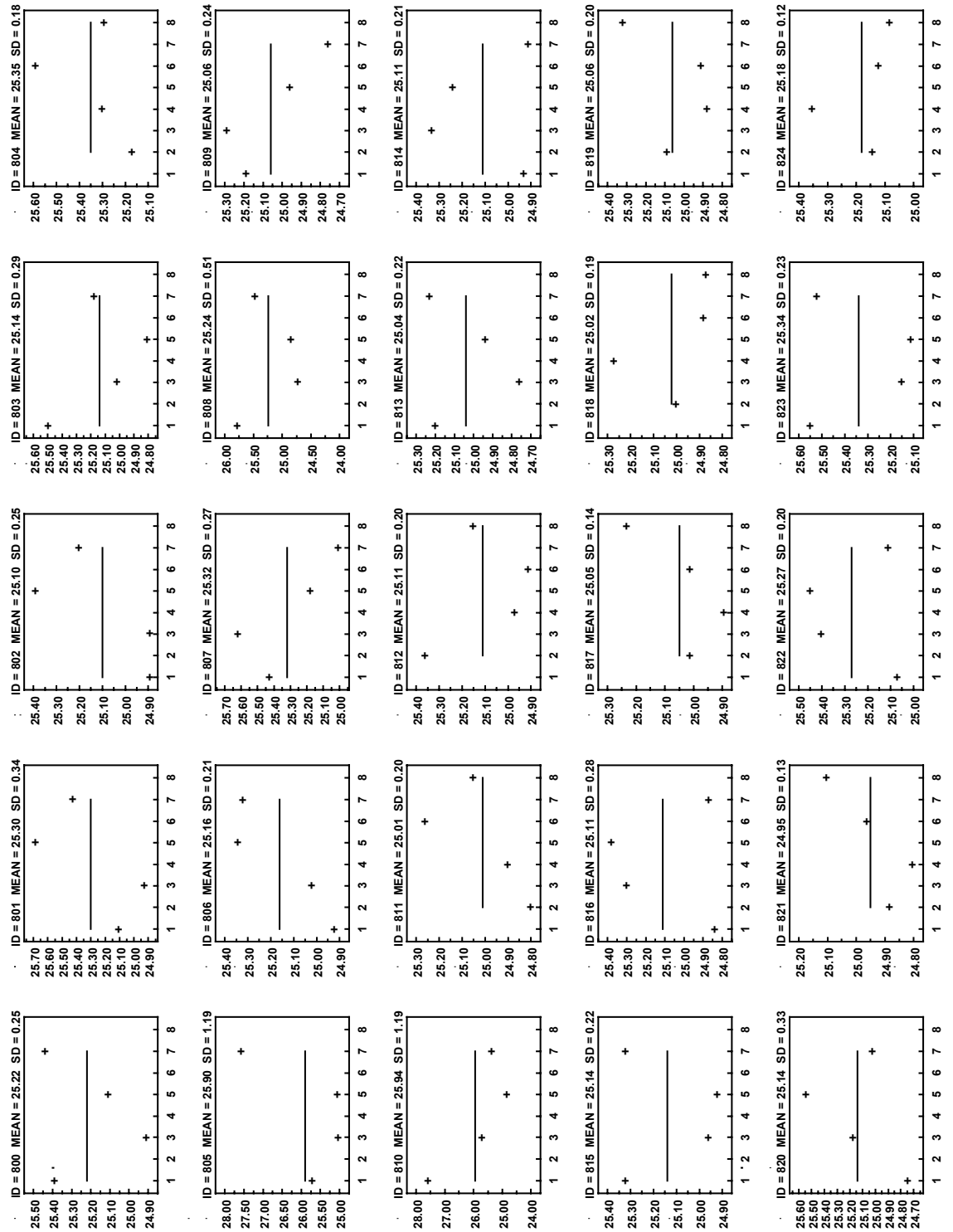

Fig. 55. Panel ID=800-824: Thickness measurements (in millimeters) at locations 1 through 8 (Fig. 3) for insulation panels 800 through 824. Mean is shown as solid line (with numerical values for mean and standard deviation (SD) in the title of each frame).

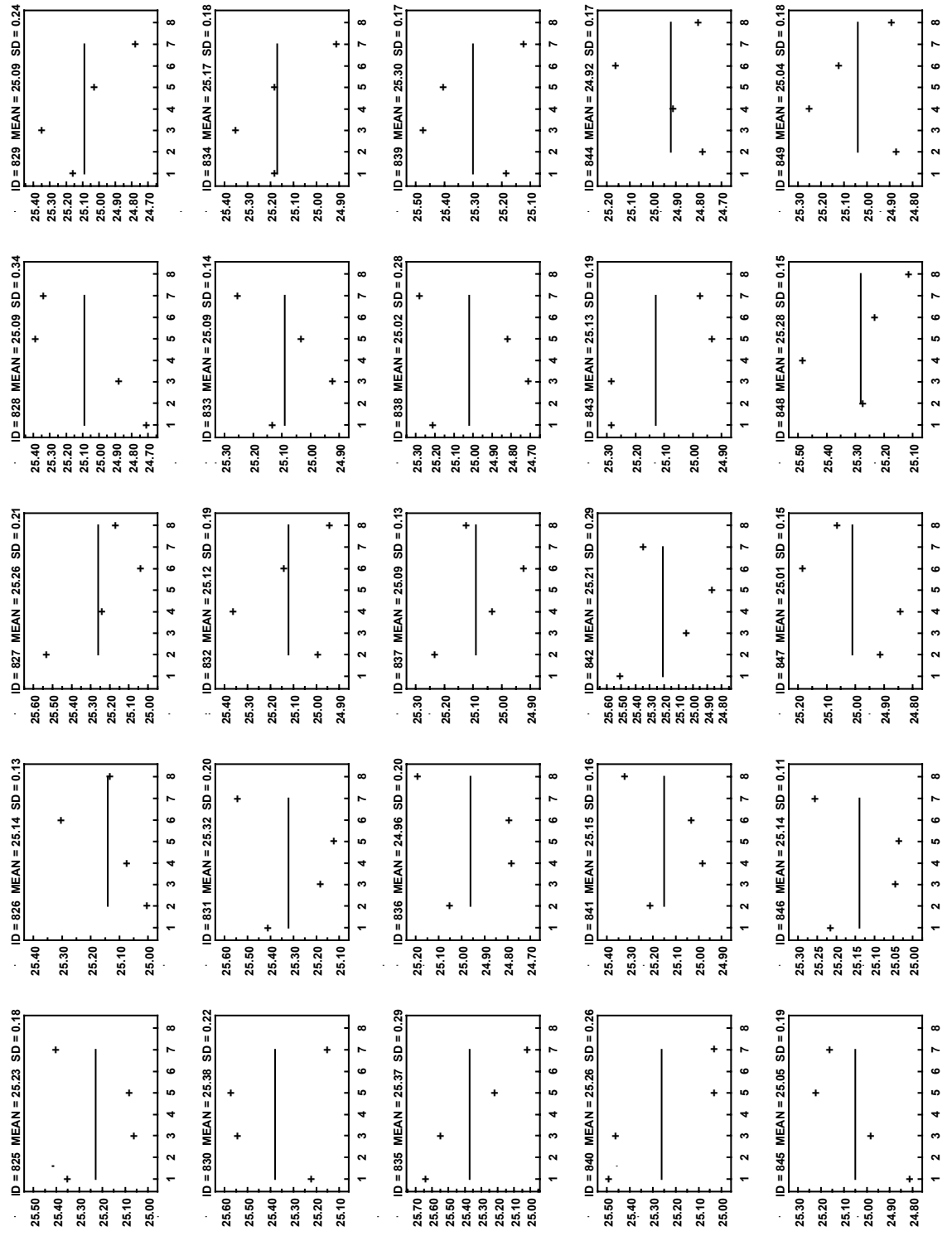

Fig. 56. Panel ID=825-849: Thickness measurements (in millimeters) at locations 1 through 8 (Fig. 3) for insulation panels 825 through 849. Mean is shown as solid line (with numerical values for mean and standard deviation (SD) in the title of each frame).

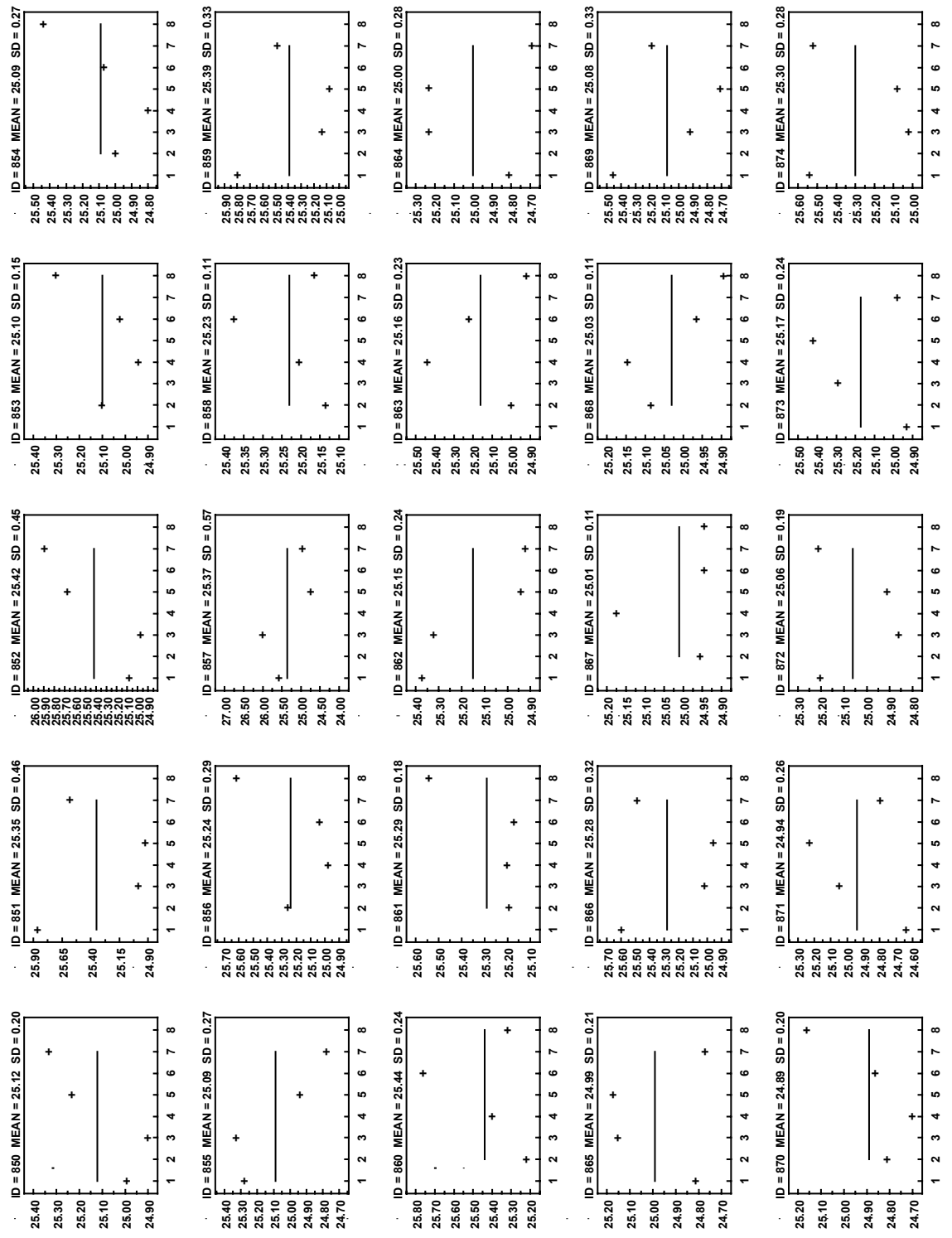

Fig. 57. Panel ID=850-874: Thickness measurements (in millimeters) at locations 1 through 8 (Fig. 3) for insulation panels 850 through 874. Mean is shown as solid line (with numerical values for mean and standard deviation (SD) in the title of each frame).

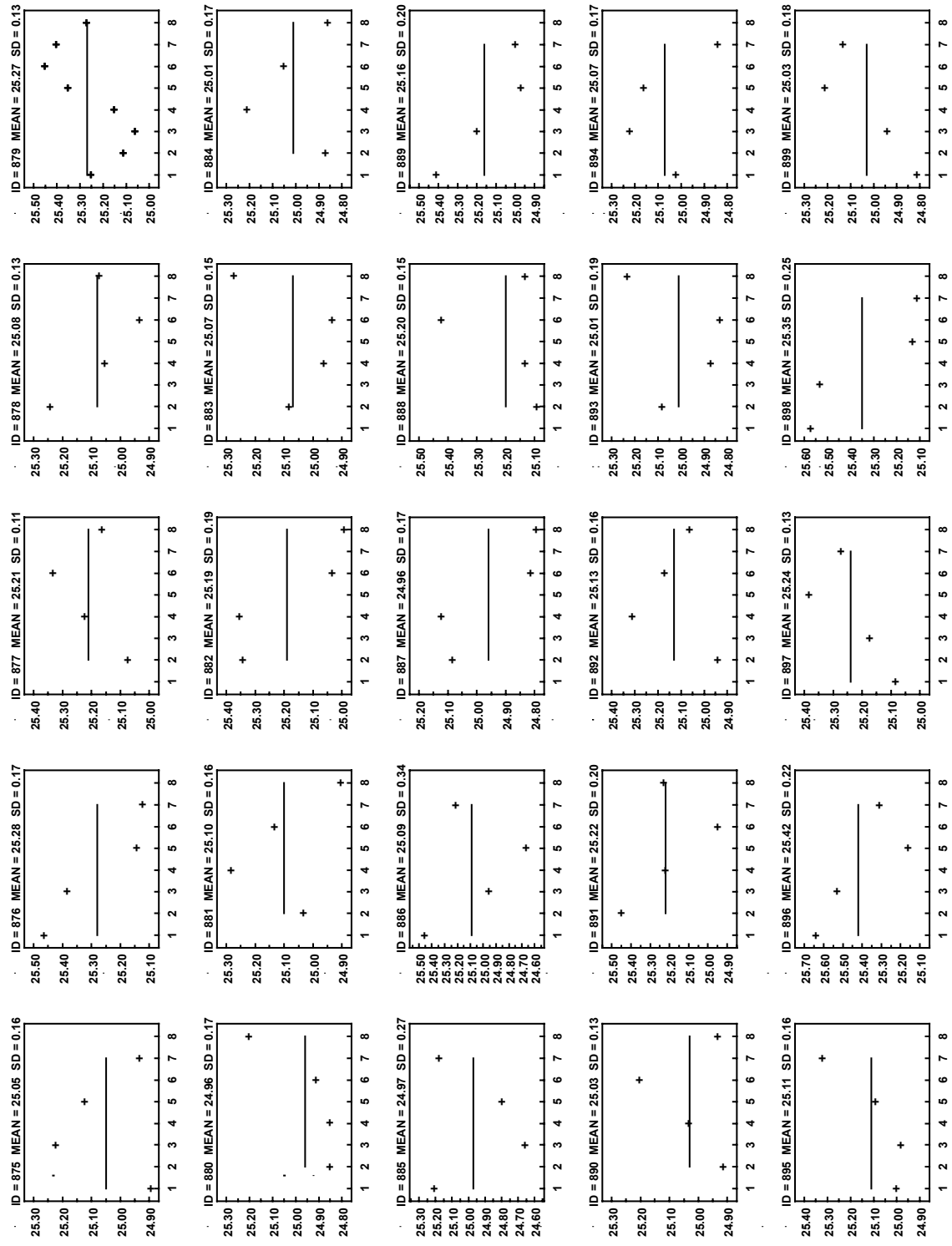

Fig. 58. Panel ID=875-899: Thickness measurements (in millimeters) at locations 1 through 8 (Fig. 3) for insulation panels 875 through 899. Mean is shown as solid line (with numerical values for mean and standard deviation (SD) in the title of each frame).

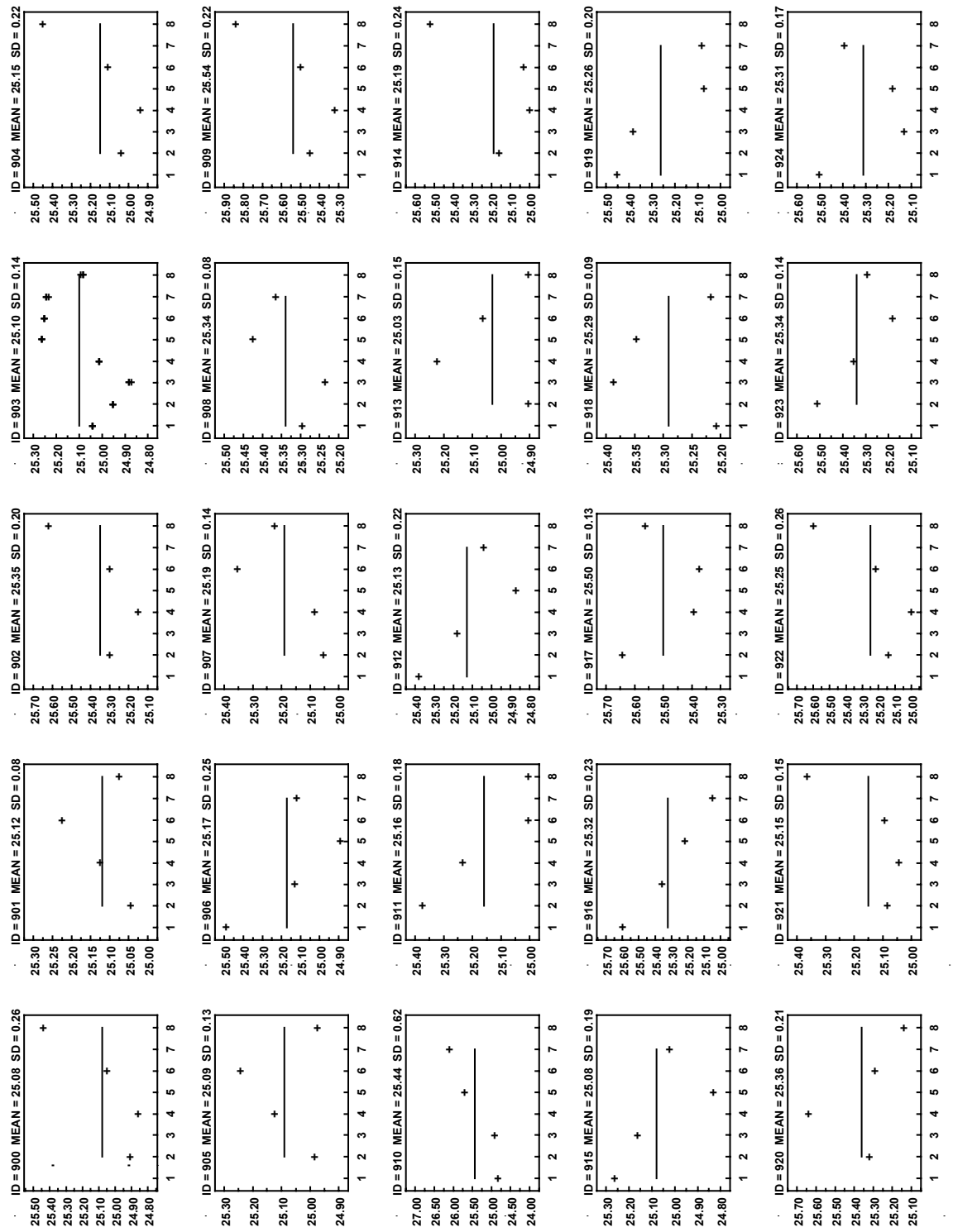

Fig. 59. Panel ID=900-924: Thickness measurements (in millimeters) at locations 1 through 8 (Fig. 3) for insulation panels 900 through 924. Mean is shown as solid line (with numerical values for mean and standard deviation (SD) in the title of each frame).

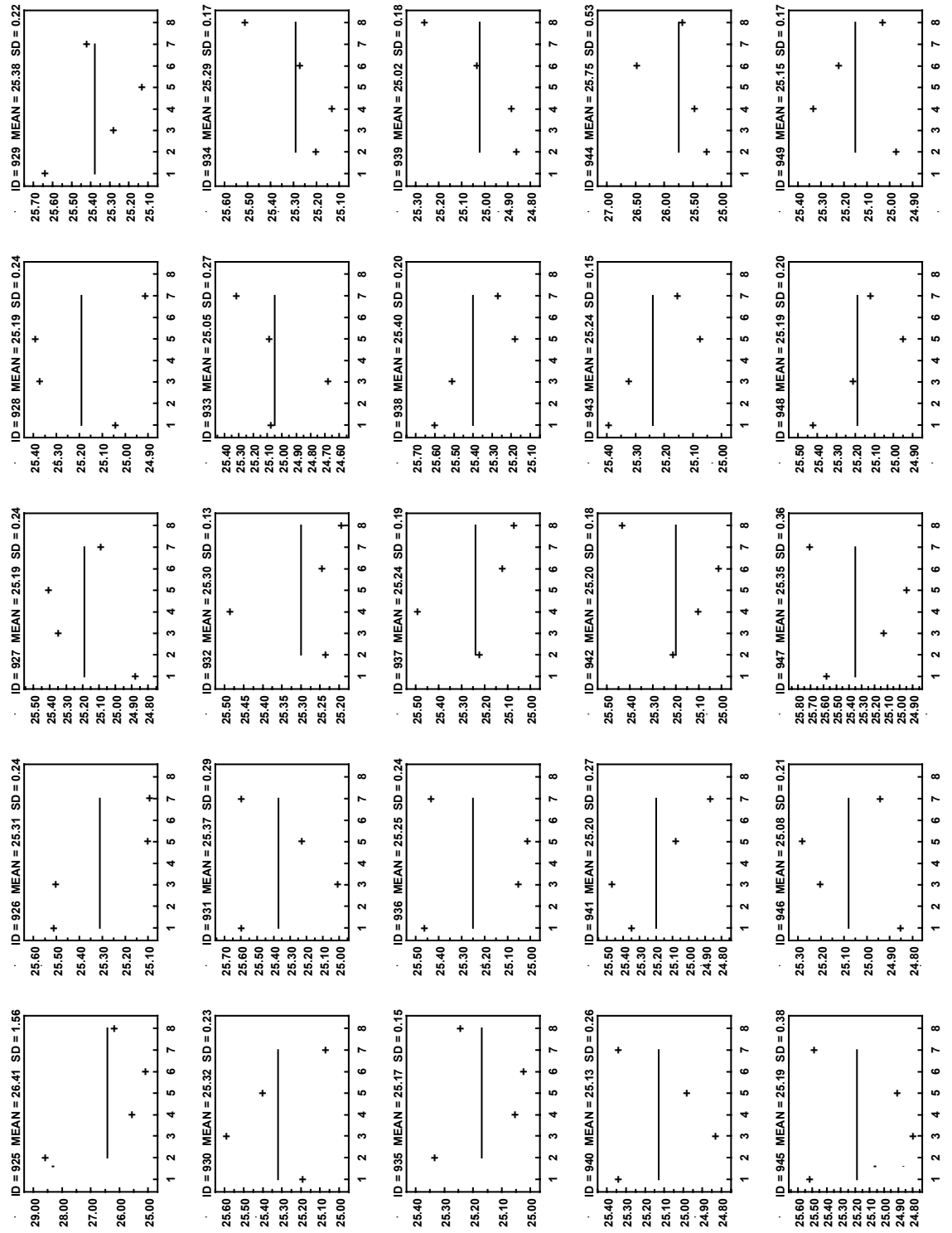

Fig. 60. Panel ID=925-949: Thickness measurements (in millimeters) at locations 1 through 8 (Fig. 3) for insulation panels 925 through 949. Mean is shown as solid line (with numerical values for mean and standard deviation (SD) in the title of each frame).

Appendix D – Bulk Density Uncertainty, Extensive Details

D1.1 Mass (m_0) Uncertainty

The measurement uncertainty of the digital weighing balance was evaluated following NIST recommended guidelines [27] for determining and reporting uncertainties for balances. For a laboratory balance in a controlled environment, the combined standard uncertainty ($k = 1$), $u_{c,\,\mathrm{bal}}$, is calculated using Eq. (D-1)

$$u_{c,\,\mathrm{bal}} = 2\sqrt{u_s^2 + s_p^2} \tag{D-1}$$

where u_s is the standard uncertainty for the standard mass artifact; and, s_p is the process standard deviation. For the 1 kg and 500 g mass standard artifacts used to check the balance (Sec. 5.1), the standard uncertainties (u_s) were obtained from the 2017 Troemner Calibration Certificate 967451-1 to be 0.000 000 25 kg and 0.000 000 125 kg, respectively. Assuming a uniform distribution, the process standard deviation (s_p) was determined from Eq. (D-2) [27]

$$s_p = \frac{b}{\sqrt{3}} \tag{D-2}$$

where b is equal to one display unit (i.e., the resolution) of the balance. For b equal to 0.0001 kg, s_p is equal to 0.000 058 kg.

The combined standard uncertainty for the panel mass, $u_c\,(m)$, was determined from Eq. (D-3)

$$u_{\mathrm{c}}\left(m\right) = 2\sqrt{u^2\left(m_0\right)_{\mathrm{A}} + u_{\mathrm{c,bal}}^2} = 0.0004 \text{ kg} \tag{D-3}$$

where $u\,(m_0)_{\mathrm{A}}$ is evaluated as a Type A standard uncertainty by computing the standard deviations for the 450 fitted intercepts in Eq. (4). The maximum standard deviation across all the slopes, 0.000 397 kg, was taken as a conservative estimate for $u(m_0)_{\mathrm{A}}$. This value was the largest uncertainty in the mass uncertainty model.

D1.2 Height Gage Uncertainty Assessment

The combined standard uncertainties of the electronic height gages, $u_{c,\mathrm{gage}}$, were determined from Eq. (D-4)

$$u_{\mathrm{c,\,gage}} = 2\sqrt{u_s^2 + s_p^2 + u_1^2 + u_2^2 + u_3^2} \tag{D-4}$$

where:

u_s = standard uncertainty for the gage block (standard artifact);
s_p = standard uncertainty of the process (i.e., instrument uncertainty);
u_1 = standard uncertainty of reference datum (i.e., granite surface plate);
u_2 = standard uncertainty due to thermal expansion
u_3 = standard uncertainty due to elastic deformation of the insulation material

Table 17 summarizes the uncertainty budgets for the dimensional measurements performed with the Mitutoyo Digimatic Height Gages (Series 192 with SPC data output). The standard

uncertainties, in millimeters, for the length (l_2), width (l_5), and thickness measurements (L) are presented in the last two columns.

Table 17. Uncertainty budgets for dimensional measurements.

Identifier	Description	Standard uncertainty, k =1 (mm)	
		Length (l_2), width (l_5)	Thickness (L)
u_s	1 inch gage block (EBW1)	---	0.000 014
u_s	12 inch gage blocks (L4M041 and L4M042 wrung together)	0.000 116	---
s_p	Height gage #1 (300 mm)	---	0.0127
s_p	Height gage #2 (610 mm)	0.019 05	---
u_1	Datum surface (granite plate)	0.017 78	0
u_2	Thermal expansion (23.3 °C)	-0.021 12	-0.001 01
u_3	Elastic deformation of insulation	neglected	0.038
$u_{c,\,gage}$	Combined standard uncertainty (k = 1)	0.028	0.044

Detailed description of the standard uncertainties in Table 17 are presented below.

- u_s: The gage blocks were calibrated in 2018 by the NIST Dimensional Metrology Group (NIST Test No. 683/290351-18). The expanded uncertainties (k = 2) for EBW1, L4M041, and L4M042 were 28 nm, 116 nm, and 116 nm, respectively. The calibration uncertainties (u_s) of the gage blocks are negligible in comparison to the other uncertainties in Table 17.
- s_p: The instrument uncertainties for the height gages were obtained from the manufacturer specification. The expanded uncertainties (k = 2) for the 300 mm and 610 mm height gages were ±0.025 mm (±0.001 in.) and ±0.038 mm (±0.0015 in.), respectively.
- u_1: The black granite surface plate was assessed by LTI Metrology on 10/31/2017 (Calibration Certificate NIST001-17-10-41425-1). The overall flatness of the surface plate (48W by 72L by 8H) was determined to be less than or equal to 0.036 mm (0.0014 in.), designated as a Grade B surface plate. For the thickness measurement (L), u_1 was assumed to be zero because the height gage was not moved from its tare position.
- u_2: The effect of thermal expansion on the gage blocks [28] was determined by Eq. (D-5) at a maximum surface plate temperature of 23.3 °C. For gage blocks of hardened steel less than 100 mm or greater than 500 mm, Ref. [28] recommends α equal 12×10^{-6} °C^{-1} or 10.5×10^{-6} °C^{-1}, respectively.

$$\Delta L_{gb} = \alpha\left(20\ ^{\circ}\mathrm{C} - t\right) L_{gb} \tag{D-5}$$

- u_3: The effects due to elastic deformation of the material were determined from the loading of the workpiece/touch probe (Figs. 2 and 3) and the previous compression assessment of SRM 1450d [11]. The applied loading from the workpiece (36 g) and the measuring force of the touch probe were 0.35 N and 0.4 N, respectively. For the 32 mm diameter workpiece, the contact pressure was 936 Pa resulting in an estimated deformation (for transverse loading of the fibers) of

1.5 % (0.038 mm). Deformation in the lateral dimensions (i.e., in the axial fiber dimension) was neglected.

D1.3 Panel Uncertainty Assessment (Type A Evaluation)

The standard uncertainties due to variations in the specimen dimensions (squareness, thickness variation etc.) were computed from the square root of the pooled variances of the multiple measurements for the nine panels on which a complete set of measurements were taken (IDs: 542, 571, 619, 641, 684, 755, 759, 879, and 903)

$$s_{\text{pool}} = \sqrt{\frac{\sum_{i=1}^{n} s_i^2}{n}} \tag{D-6}$$

where n is equal to 18 or 9 for lateral or thickness dimensional measurements, respectively.

Table 18 summarizes the lateral dimensions (l_1, l_2, l_3, l_4, l_5, and l_6), average lengths and widths, and variances for the nine panels. The pooled variance for the lateral dimensional measurements is 0.098 153 mm and the standard uncertainty (s_{pool}) is equal to 0.313 29 mm.

Table 18. Length, width dimensional data for nine panels (multiple measurements).

	Panel (mm)								
	542	**571**	**619**	**641**	**684**	**755**	**759**	**879**	**903**
l_1	609.69	609.98	609.65	610.63	610.02	612.31	611.17	611.82	610.16
l_1	609.69	609.98	609.65	610.63	610.00	612.31	611.16	611.82	610.16
l_1	609.70	609.98	609.65	610.63	610.01	612.31	611.16	611.81	610.15
l_2	609.50	609.96	609.62	610.05	609.97	612.24	610.85	610.85	610.09
l_2	609.49	609.96	609.61	610.05	609.96	612.24	610.84	610.86	610.09
l_2	609.49	609.96	609.61	610.05	609.96	612.24	610.83	610.85	610.09
l_3	609.46	609.90	609.48	609.14	610.01	612.21	610.70	610.36	610.03
l_3	609.46	609.89	609.48	609.13	610.00	612.21	610.69	610.41	610.03
l_3	609.46	609.89	609.48	609.13	610.00	612.21	610.69	610.41	610.03
l_4	610.88	609.24	610.35	609.56	609.78	610.64	612.33	612.46	609.24
l_4	610.88	609.24	610.35	609.56	609.77	610.63	612.33	612.45	609.24
l_4	610.88	609.24	610.35	609.56	609.77	610.64	612.32	612.45	609.24
l_5	610.62	609.19	610.86	609.68	609.25	610.33	612.47	612.69	608.85
l_5	610.61	609.19	610.86	609.68	609.24	610.33	612.46	612.69	608.84
l_5	610.61	609.19	610.86	609.67	609.24	610.32	612.46	612.70	608.84
l_6	610.29	609.74	611.36	609.71	608.66	610.05	612.85	613.03	608.41
l_6	610.29	609.74	611.35	609.71	608.66	610.04	612.85	613.03	608.41
l_6	610.29	609.74	611.36	609.71	608.66	610.05	612.84	613.03	608.40
$\text{Avg.}_{1,2,3}$	609.56	609.95	609.59	610.04	609.99	612.26	610.93	611.10	610.10
$s^2_{1,2,3}$	0.0120	0.0016	0.0060	0.4271	0.0005	0.0020	0.0434	0.3959	0.0030
$\text{Avg.}_{4,5,6}$	610.59	609.39	610.86	609.65	609.23	610.34	612.55	612.73	608.83
$s^2_{4,5,6}$	0.0655	0.0694	0.1900	0.0047	0.2326	0.0654	0.0545	0.0630	0.1303

Table 19 summarizes the thickness dimensions (L_1, L_2, L_3, L_4, L_5, L_6, L_7, and L_8), averages and variances for the nine panels. The pooled variance for the thickness measurements is 0.032 51 mm and the standard uncertainty (s_{pool}) is equal to 0.180 29 mm.

Table 19. Thickness dimensional data for multiple measurements of nine panels.

	Panel (mm)								
	542	**571**	**619**	**641**	**684**	**755**	**759**	**879**	**903**
L_1	25.18	25.41	25.38	24.97	25.27	25.45	24.68	25.26	25.05
L_1	25.19	25.41	25.38	24.96	25.29	25.45	24.68	25.26	25.05
L_1	25.18	25.41	25.38	24.96	25.28	25.45	24.68	25.26	25.05
L_2	25.04	25.31	25.20	25.07	25.26	25.23	24.76	25.12	24.96
L_2	25.03	25.31	25.21	25.07	25.26	25.23	24.75	25.12	24.96
L_2	25.03	25.31	25.20	25.07	25.26	25.23	24.75	25.12	24.96
L_3	24.85	25.29	25.13	25.40	25.23	25.09	24.85	25.07	24.89
L_3	24.85	25.28	25.14	25.39	25.23	25.09	24.85	25.07	24.89
L_3	24.84	25.28	25.14	25.39	25.23	25.09	24.86	25.07	24.88
L_4	25.04	25.10	24.85	25.29	25.41	25.10	24.95	25.16	25.02
L_4	25.04	25.10	24.85	25.29	25.41	25.10	24.94	25.16	25.02
L_4	25.04	25.10	24.86	25.29	25.42	25.09	24.95	25.16	25.02
L_5	25.36	25.11	24.78	25.28	25.86	24.99	25.15	25.36	25.27
L_5	25.35	25.11	24.78	25.28	25.86	24.99	25.15	25.36	25.27
L_5	25.35	25.12	24.79	25.27	25.87	24.99	25.15	25.36	25.27
L_6	25.48	25.16	24.91	25.01	25.75	25.14	25.12	25.46	25.26
L_6	25.48	25.16	24.91	25.02	25.76	25.15	25.12	25.46	25.26
L_6	25.48	25.16	24.91	25.01	25.75	25.14	25.12	25.46	25.26
L_7	25.53	25.22	25.00	24.83	25.79	25.33	25.17	25.41	25.24
L_7	25.53	25.22	24.99	24.83	25.78	25.33	25.17	25.41	25.25
L_7	25.52	25.22	24.99	24.84	25.78	25.33	25.17	25.41	25.25
L_8	25.27	25.20	25.04	24.88	25.56	25.43	24.83	25.28	25.09
L_8	25.27	25.19	25.04	24.88	25.56	25.43	24.83	25.28	25.09
L_8	25.27	25.19	25.04	24.88	25.55	25.43	24.83	25.28	25.10
Avg.	25.22	25.22	25.04	25.09	25.52	25.22	24.94	25.27	25.10
s^2	0.0509	0.0102	0.0354	0.0390	0.0605	0.0261	0.0328	0.0181	0.0196

D1.4 Dimensional (l_2, l_5, and L) Uncertainties

The combined standard uncertainties (k = 1) for l_2, l_5, and L were determined from Eq. (D-7). In both cases, the standard uncertainties due to variations in the panel dimensions (squareness or thickness variation) dominated the standard uncertainties associated with the measurement process.

$$u_c(l_2) = u_c(l_5) = \sqrt{u^2_{c,gage\#1} + u^2(l)_A} = \sqrt{0.028^2 + 0.313\,29^2} = 0.315 \text{ mm}$$
$$u_c(L_p) = \sqrt{u^2_{c,gage\#2} + u^2(L_p)_A} = \sqrt{0.044^2 + 0.180\,29^2} = 0.186 \text{ mm} \quad \text{(D-7)}$$

Appendix E – Thermal Conductivity Uncertainty, Extensive Details

The uncertainty assessment for the thermal conductivity measurements follows the mandatory requirements covered in ASTM Test Method C 177 [1]. The approach considers the following four contributory uncertainties shown before in Eq. (22) .

- specimen heat flow (Q);
- temperature difference (ΔT);
- (in-situ) thickness (L); and,
- meter area (A)

Appendix E consists of four main sections for each input quantity – Q, ΔT, L, and A . Each section presents the governing equation for the quantity and examines all known (but not exhaustive) subordinate causal standard uncertainties. The final relative standard uncertainty for each input quantity (Q, ΔT, L, and A) is summarized in Table 15 in the main text.

E1.1 Specimen Heat Flow *(Q)*

The specimen heat flow Q is essentially determined by measuring the direct current and voltage provided to the meter-plate heater (Q_m). The measurement approach for Q_m is shown schematically in Fig. 61. A direct-current (DC) power supply provides current (I) to the circuit which is determined by the measurement V_s across the four-terminal 0.1 Ω standard resistor placed in an oil bath at 25.00 °C. The voltage across the meter-plate heater (V_m) is measured with voltage taps soldered to the heater leads in the center of the guard gap. The meter plate power (Q_m) is the product of I and V_m.

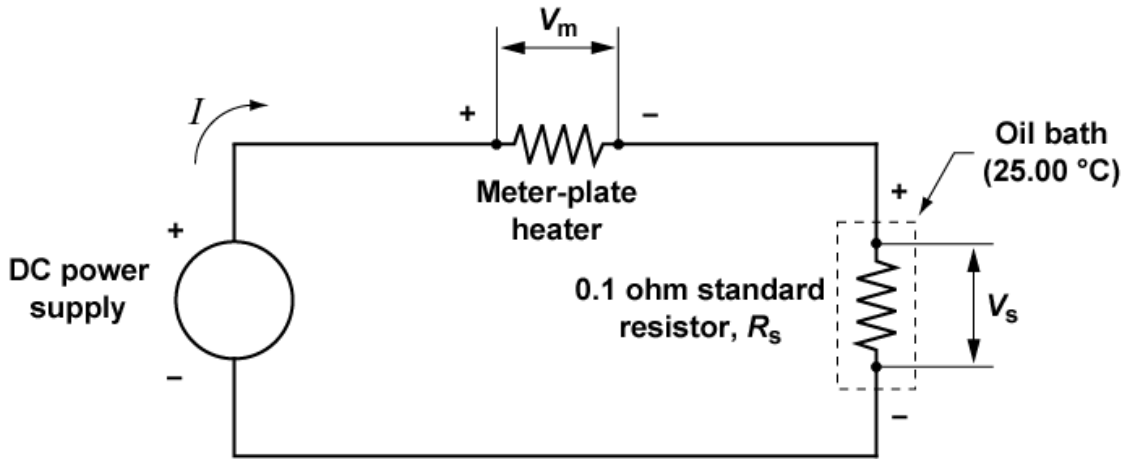

Fig. 61. Electrical schematic for the meter-plate power measurement.

Equation (E-1) defines Q_m, the power input to the meter-plate heater. Under ideal guarding, Q_m is equal to the specimen heat flow Q in Eq. (18).

$$Q_m = I V_m = \frac{V_s}{R_s} V_m \tag{E-1}$$

where I is the current determined from the voltage drop (V_s) across the standard resistor (R_s); and, V_m is the voltage drop across the meter-plate heater measured with voltage taps located at the midpoint of the guard gap.

The contributory uncertainties for $u(Q_m)$ include: a) standard platinum resistance thermometer (SPRT) resistive heating; b) calibration of the 0.1 Ω standard resistor; c) repeated observations during testing; and, d) voltage measurements for V_s and V_m.

- *SPRT joule heating power*: The long-stem SPRT in the meter-plate was continuously excited by a 1 mA current during each test. The joule heating power for the nominal 25 Ω sensor was 0.000 025 W.
- *Standard resistor*: The standard resistor is an Otto Wolff Model N85-7a7, Serial No. 5350, calibrated on April 28, 2018 by the NIST Quantum Measurement Division (Test Report No. 291216-18). The electrical resistances at 0.316 A and 1.0 A are 0.100 092 10 Ω and 0.100 092 21 Ω, respectively. The expanded uncertainty ($k = 2$) was 0.000 002 Ω (2 ppm) which was used to determine $u(R_s)$ in Eq. (E-2).

$$u(R_s) = \frac{0.000\,002\,\Omega}{2} = 0.000\,001\,\Omega \tag{E-2}$$

- *Repeated observations* $u(\bar{Q}_m)_A$: For each test, 4 h of data ($n = 240$ observations) were acquired and averaged. The standard uncertainty of the mean ($\bar{Q}$) was computed from the variance of the mean (Eq. (E-3)) for each level of T_m.

$$u(\bar{Q}_m)_A = \sqrt{s^2(\bar{Q}_m)} = \sqrt{\frac{s^2(Q_m)}{n}} \tag{E-3}$$

- $u(V_s)$ and $u(V_m)$: The input voltages V_s and V_m were measured by an Agilent 3458A digital multimeter that was calibrated on April 10, 2018 by Keysight Technologies. The contributory uncertainties for V_s and V_m were estimated from the 2-year manufacturer specification for the 100 mV and 10 V ranges, respectively. A uniform rectangular distribution was assumed for the accuracy specification and characteristic standard uncertainties were computed from Eq. (E-4).

$$\begin{aligned} u(V_s) &= \left[0.000\,014 \times 0.100 + 0.000\,003 \times 0.100 + 0.000\,002\right] \mu V / \sqrt{3} = 2.14\,\mu V \\ u(V_m) &= \left[0.000\,014 \times 10 + 0.000\,0005 \times 10 + 0.000\,002\right] \mu V / \sqrt{3} = 84.9\,\mu V \end{aligned} \tag{E-4}$$

E1.1.1 Combined Standard Uncertainty for Meter-Plate Power Input (Q_m)

Propagating the contributory uncertainties in Eq. (E-1) based on a Taylor series approximation yields Eq. (E-5)

$$u_c(Q_m)_B = \sqrt{c_{V_s}^2\, u^2(V_s)^2 + c_{R_s}^2\, u^2(R_s)^2 + c_{V_m}^2\, u^2(V_m)^2} \tag{E-5}$$

where the sensitivity coefficients (c_i) are equal to the partial derivative of an input quantity ($\partial f / \partial X_i$) evaluated for the input quantity equal to an input estimate ($X_i = x_i$)

$$c_{V_s} = \frac{\partial Q_m}{\partial V_s} = \frac{V_m}{R_s}$$

$$c_{R_s} = \frac{\partial Q_m}{\partial R_s} = -\frac{V_s V_m}{R_s^2}$$

$$c_{V_m} = \frac{\partial Q_m}{\partial V_m} = \frac{V_s}{R_s} = I$$

The combined standard uncertainty for the meter plate power input is given by Eq. (E-6).

$$u_c(Q_m) = \sqrt{u^2(Q_{SPRT})_B + u^2(\bar{Q}_m)_A + u^2(Q_m)_B} \quad \text{(E-6)}$$

Table 20 summarizes the standard uncertainties as a function of T_m for the SPRT, repeated observations, and for the propagation of contributory uncertainties, $u(Q_m)$. Input values for $\bar{Q}$, V_m and V_s are also included. The input value for the standard resistor was taken to be 0.100 092 21 Ω. The Type B evaluations in Table 20 are about two times greater than the Type A evaluations. As evident in Table 20, the Type A and Type B evaluations increase with T_m. The last column expresses the relative combined standard uncertainty, $u_{c,r}(Q_m)$, as a percent of the power input ($\bar{Q}$). For all levels of T_m, the relative combined standard uncertainties are small, approximately 0.003 %.

Table 20. Combined standard uncertainties for meter-plate power input.

T_m (K)	$u(Q_{SPRT})_B$ (W)	$\bar{Q}$ (W)	$u(\bar{Q}_m)_A$ (W)	V_m (V)	V_s (V)	$u(Q_m)_B$ (W)	$u_{c,r}(Q_m)_B$ (%)
280	0.000 025	2.000 3	0.000 020	2.353 150	0.085 084	0.000 054	0.0032
300	0.000 025	2.068 0	0.000 022	2.494 420	0.082 979	0.000 057	0.0032
320	0.000 025	2.221 3	0.000 033	2.691 470	0.082 605	0.000 061	0.0033
340	0.000 025	2.355 9	0.000 035	2.882 350	0.081 809	0.000 065	0.0033
360	0.000 025	2.524 6	0.000 028	3.099 470	0.081 525	0.000 070	0.0031

E1.1.2 Imbalanced Guard Heat Flows (ΔQ)

A detrimental heat flow, occurring as either a gain or loss, arises when the temperature of a thermal guard is imbalanced causing a deviation (ΔQ) in the one-dimensional heat flow Q. Under steady-state conditions, the primary guard heat flows were controlled to be less than 0.001 W. The lateral heat flows associated with the primary guard gap (Q_g) and two secondary guards – the edge guard (Q_e) and SPRT connection guard (Q_{HPCG}) – can cause, under imbalanced conditions, significant uncertainties in the measurement of Q.

As part of a previous sensitivity study [25], an imbalance model was developed for a pair of similar 25 mm thick, fibrous-glass specimens at a nominal temperature of 310 K. The measurement system for this material was well described by the empirical model in Eq. (E-7) where x_j are coded as –1 or +1.

$$\lambda_{pred} = \beta_0 + 1/2\left[\beta_2 x_2 + \beta_{12} x_1 x_2 + \beta_3 x_3 + \beta_1 x_1\right] \quad \text{(E-7)}$$

where

$$\begin{aligned}\beta_0 &= 0.033\,587\\ \beta_2 &= -0.004\,791\\ \beta_{12} &= 0.000\,931\\ \beta_3 &= -0.000\,034\\ \beta_1 &= -0.000\,022.\end{aligned}$$

The terms x_1, x_2, and x_3 represent coded values (of ±1) for the temperature differences across the specimen (ΔT), guard gap (ΔT_{gap}), and the hot plate connection guard (ΔT_{HPCG}), respectively. The empirically-derived model in Eq. (E-7) does not include a term for the edge guard imbalance because the term was determined to be statistically insignificant [25].

For the uncertainty analysis, the upper and lower limits for ΔT, ΔT_{gap}, and ΔT_{HPCG} were based on conservative engineering assessments and estimated to be ±0.01 K, ±0.005 K, and ±0.1 K, respectively. A uniform rectangular distribution was assumed for each interval. Using the coded limits in Ref. [25], Eq. (E-8) calculates the standard uncertainties for each quantity and the subsequent coded values for x_1, x_2, x_3.

$$\begin{aligned} x_1 &= \frac{u(\Delta T)}{5\ \mathrm{K}} = \frac{\left(0.01\ \mathrm{K}/\sqrt{3}\right)}{5\ \mathrm{K}} = 0.0012\\ x_2 &= \frac{u(\Delta T_{gap})}{0.25\ \mathrm{K}} = \frac{\left(0.005\ \mathrm{K}/\sqrt{3}\right)}{0.25\ \mathrm{K}} = 0.012\\ x_3 &= \frac{u(\Delta T_{HPCG})}{0.5\ \mathrm{K}} = \frac{\left(0.1\ \mathrm{K}/\sqrt{3}\right)}{0.5\ \mathrm{K}} = 0.12 \end{aligned} \qquad \text{(E-8)}$$

Table 21 summarizes computations of λ_{pred} from Eq. (E-7) and relative differences from the baseline case where $x_1 = x_2 = x_3 = 0$ and $\lambda_0 = 0.033587\ \mathrm{W{\cdot}m^{-1}{\cdot}K^{-1}}$ at 310 K. For mean temperatures other than 310 K, an additional level of uncertainty equal to 10 % for every 10 K difference from T_m equal to 310 K was applied. The final uncertainty estimates, $u(\Delta Q)$, presented in the last column dominate the measurement uncertainties (on the order of 0.003 %) calculated in Table 20.

Table 21. Relative standard uncertainties for guard temperature imbalances.

T_m (K)	x_1	x_2	x_3	λ ($\mathrm{W{\cdot}m^{-1}{\cdot}K^{-1}}$)	$(\lambda-\lambda_0)/\lambda_0$ (%)	Uncertainty Level for T_m	$u(\Delta Q)$ (%)
280	0.0012	0.012	0.12	0.033 557	-0.0882	30	-0.115
300	0.0012	0.012	0.12	0.033 557	-0.0882	10	-0.097
320	0.0012	0.012	0.12	0.033 557	-0.0882	10	-0.097
340	0.0012	0.012	0.12	0.033 557	-0.0882	30	-0.115
360	0.0012	0.012	0.12	0.033 557	-0.0882	50	-0.132

E1.1.3 Combined Standard Uncertainty $u(Q)$

The combined standard uncertainty $u(Q)$ was computed from Eq. (E-9).

$$u_{c,r}(Q) = \sqrt{u_{c,r}^2(Q_m) + u^2(\Delta Q)} \tag{E-9}$$

Table 22 summarizes estimates for $u_{c,r}(Q)$ at levels of T_m from 280 K to 360 K. The final column in Table 22 was rounded and reproduced in Table 15 (Sec. 7.4).

Table 22. Combined standard uncertainties ($k = 1$) for Q.

T_m (K)	$u_{c,r}(Q_m)$ (%)	$u(\Delta Q)$ (%)	$u_{c,r}(Q)$ (%)
280	0.0032	-0.115	0.115
300	0.0032	-0.097	0.097
320	0.0033	-0.097	0.097
340	0.0033	-0.115	0.115
360	0.0031	-0.132	0.132

E1.2 Temperature Difference (ΔT)

The term, ΔT, in Eq. (18), is defined as the surface-to-surface temperature difference across the specimen pair where T_h is the temperature of the hot plate surface and T_{c1} and T_{c2} are the temperatures of the inboard and outboard cold plate surfaces, respectively. Under steady-state operating conditions when T_{c1} is nearly the same as T_{c2} (equals T_c), ΔT is defined by Eq. (E-10).

$$\Delta T = T_h - \left(T_{c1} + T_{c2}\right)/2 = T_h - T_c \tag{E-10}$$

The primary temperature sensor, located in the geometric center of each plate, is a long-stem, metal-sheath, standard platinum resistance thermometer (SPRT), Model 162CE from Rosemont Aerospace, Inc. The SPRT sensors have a 4-wire sensing element within the sensitive portion (50 mm) of the sheath tip. The SPRT was placed in a well that was brazed at the midplane of the plate so that the sensing region resides at the geometric center of the plate (Fig. 62). To check the temperature uniformity of a plate, six Type N metal sheathed thermocouples, 1.6 mm in diameter, were brazed in the surface of each plate at the locations shown in Fig. 62 for the hot plate.

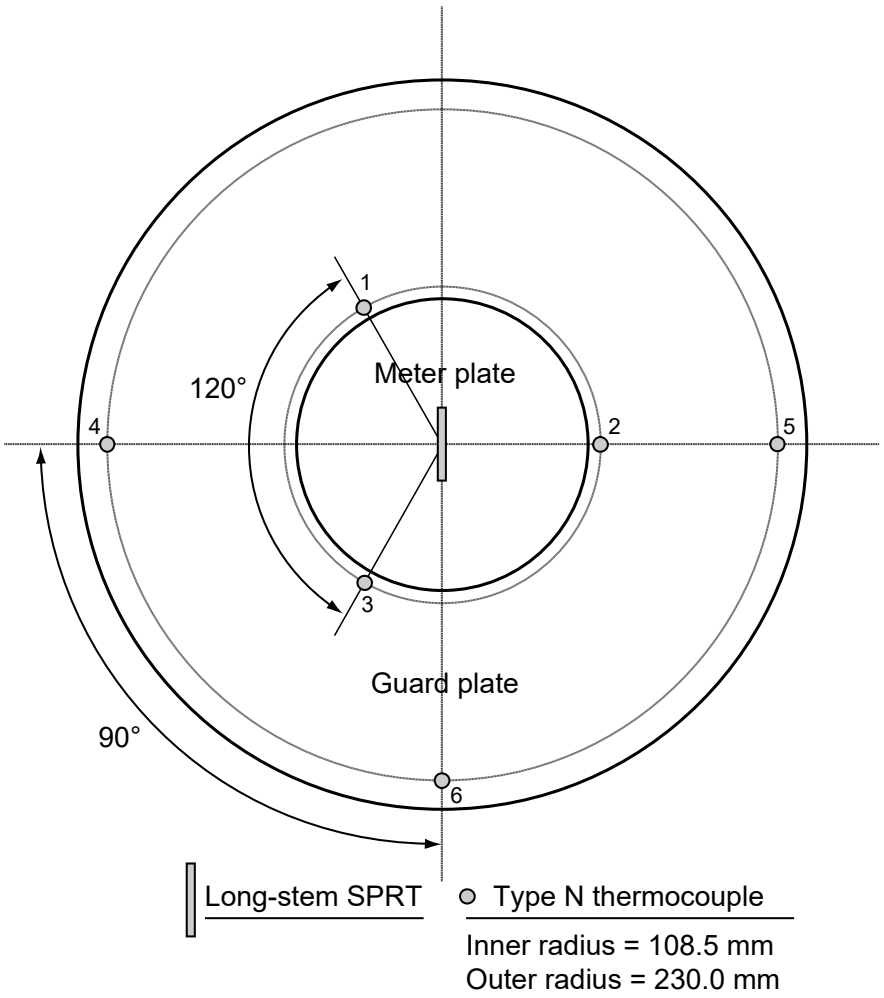

Fig. 62. Temperature sensor locations for NIST 500 mm diameter plates.

E1.2.1 Repeated Observations, $u(\Delta\overline{T})_A$

The standard uncertainty for the mean temperature difference was determined using the same process as was done for $u(\overline{Q}_m)_A$ in Sec. E1.1. The standard uncertainties for repeated observations at levels of $\Delta\overline{T}$ (in millikelvin) from 280 K to 360 K are summarized in Table 23.

Table 23. Standard uncertainties for repeated observations of $\Delta\overline{T}$.

T_m (K)	ΔT (K)	$u(\Delta\overline{T})_A$ (mK)
280	25.0030	0.088
300	25.0065	0.091
320	25.0027	0.157
340	25.0029	0.132
360	24.9997	0.083

E1.2.2 Contributory Temperature Uncertainties

The contributory uncertainties for the temperature measurements include: a) calibration of the SPRTs; b) uncertainty of the DC resistance ratio bridge; c) calibration of the external reference resistor for the DC bridge; d) contact resistance; e) plate temperature uniformity; and, f) mid-plane temperature correction.

- *SPRT calibration*: The long-stem SPRTs were calibrated on March 1, 2000 by the NIST Process Measurements Division (Test Report 262640-00). A conservative estimate of 0.64 mK for the expanded uncertainty ($k = 2$) was selected from the calibration data. The standard uncertainty for the calibration is given by Eq. (E-11).

$$u_1(T) = \frac{0.64\,\text{mK}}{2} = 0.32\ \text{mK} \tag{E-11}$$

- *DC resistance ratio bridge* : The resistances of the SPRTs were measured by an Isotech microK precision thermometer bridge with a microsKanner channel expander. The resistances were referenced against an external standard resistor providing a resistance ratio, W, for each SPRT. The manufacturer specification is 0.8 mK over the full range of the instrument. A uniform rectangular distribution was assumed for the accuracy specification.

$$u_2(T) = \frac{0.8\,\text{mK}}{\sqrt{3}} = 0.46\,\text{mK} \tag{E-12}$$

- *Reference resistor*: The standard resistor is a Tinsley Model 5685-A (Wilkens type), Serial No. 274591, calibrated on April 11, 2018 by the NIST Quantum Measurement Division (Test Report No. 291216-18). The standard resistor was calibrated in its thermal enclosure at 35.95 °C. The electrical resistances at 0.01 A is 25.000 458 6 Ω. The expanded uncertainty ($k = 2$) was 0.2 μΩ/(Ω·ppm) which was neglected in further analysis.

- *SPRT joule heating temperature rise*: , The joule heating power for the 25 Ω SPRT was calculated to be 0.000 025 W (Sec. E1.1). The thermal conductance of the metal-to-air-to-metal interface between the sensor and the thermometer well was estimated to be 0.058 $\text{W}\cdot\text{K}^{-1}$. The standard uncertainty due to the temperature rise due to joule heating was estimated by Eq. (E-13).

$$u_3(T) = \frac{0.000\,025\ \text{W}}{0.000\,058\ \text{W}\cdot\text{mK}^{-1}} = 0.43\ \text{mK} \tag{E-13}$$

- *Plate temperature uniformity (lateral variation)*: The spatial temperature variation of the hot plate, δT_s, was computed for each run from the standard deviation of the measured temperatures of the inner three thermocouples (#1, #2, and #3 indicated in Fig. 62). The standard deviations were subsequently pooled (see formula in Eq. D-6 where n is equal to 9) across the nine runs (3 levels of ρ × 3 levels of p) conducted at each T_m. The standard uncertainty, $u_4(\delta\overline{T}_s)$ was computed at each T_m from Eq. (E-14).

$$u_4\left(\delta\overline{T}_s\right)_A = \sqrt{\frac{\left[s^2_{\text{pool}}\left(\delta\overline{T}_s\right)\right]_{T_m}}{3}} \tag{E-14}$$

The standard uncertainties for δT_s are summarized in Table 24 at levels of T_m from 280 K to 360 K. The standard uncertainties increased (considerably at 360 K) as T_m departs from ambient conditions near 293 K.

Table 24. Standard uncertainties for spatial temperature variation, $\delta\overline{T}_s$.

T_m (K)	ΔT (K)	$u_4(\delta\overline{T}_s)$ (mK)
280	25.0030	34.1
300	25.0065	12.1
320	25.0027	46.3
340	25.0029	43.3
360	24.9997	71.8

- *Mid-plane temperature correction*: The term ΔT is defined as the surface-to-surface temperature difference across the specimen pair (Sec. E1.2). Each SPRT, however, measured the temperature at the centroid of the plate (Fig. 62). The correction ($\delta T_{\text{corr.}}$) due to the temperature change across the thickness of the nickel plate was calculated by Eq. (E-15) for the hot and cold plates.

$$\begin{aligned} \delta T_h &= q\,\lambda_{\text{Ni}}\left(T_h\right) f_{\text{mp}} \\ \delta T_c &= q\,\lambda_{\text{Ni}}\left(T_c\right)\frac{m_{\text{c}}}{2} \end{aligned} \tag{E-15}$$

where

q is the heat flux determined from the specimen heat flow divided by the metering area (Q/A);
λ_{Ni} is the thermal conductivity of the nickel thermometry plate;
f_{mp} is a geometrical factor for the meter plate equal to 0.00479 m [29]; and,
m_c is the thickness of the thermometry cold plate (near 293 K).

The standard uncertainty due to the small temperature changes across the thickness of the nickel plates from the surface to the center midplane of the SPRT was calculated from Eq. (E-16).

$$u_5\left(\delta T_{\text{corr.}}\right) = \sqrt{\left(\delta T_h\right)^2 + \left(\delta T_c\right)^2} \tag{E-16}$$

The standard uncertainties are summarized in Table 25 at levels of T_m from 280 K to 360 K.

Table 25. Standard uncertainties due to the midplane-to-surface temperature correction.

T_m (K)	ΔT (K)	$u_5(\delta T_{\text{corr.}})$ (mK)
280	25.0030	2.9
300	25.0065	3.2
320	25.0027	3.5
340	25.0029	3.8
360	24.9997	4.1

E1.2.3 Combined Standard Uncertainty for T and ΔT

Equation (E-17) computes the combined standard uncertainty (k = 1) for the temperature measurement of the meter plate in millikelvin.

$$u_c(T) = \sqrt{u_1^2(T) + u_2^2(T) + u_3^2(T) + u_4^2\left(\delta\overline{T}_s\right) + u_5^2\left(\delta T_{corr.}\right)} \quad \text{(E-17)}$$

Table 26 summarizes values for contributory uncertainties and $u_c(T)$ in millikelvin as a function of T_m.

Table 26. Combined standard uncertainties for the temperature measurement.

T_m (K)	ΔT (K)	$u_1(T)$ (mK)	$u_2(T)$ (mK)	$u_3(T)$ (mK)	$u_4(\delta\overline{T}_s)$ (mK)	$u_5(\delta T_{corr.})$ (mK)	$u_c(T)$ (mK)
280	25.0030	0.32	0.46	0.43	34.1	2.9	34.2
300	25.0065	0.32	0.46	0.43	12.1	3.2	12.5
320	25.0027	0.32	0.46	0.43	46.3	3.5	46.4
340	25.0029	0.32	0.46	0.43	43.3	3.8	43.4
360	24.9997	0.32	0.46	0.43	71.8	4.1	72.0

The combined standard uncertainty for ΔT was computed using Eq. (E-18). The factor of 2 accounts for both the uncertainty of the hot plate and cold plate.

$$u_c(\Delta T) = \sqrt{u^2\left(\Delta\overline{T}\right) + 2 \times u_c^2(T)} \quad \text{(E-18)}$$

Table 27 summarizes the combined standard uncertainties for ΔT in kelvin as a function of mean temperature. The final column in Table 27 was reproduced in Table 15 (Sec. 7.4).

Table 27. Combined standard uncertainties (k = 1) for ΔT.

T_m (K)	ΔT (K)	$u_c(\Delta T)$ (K)	$u_{c,r}(\Delta T)$ (%)
280	25.0030	0.049	0.19
300	25.0065	0.018	0.07
320	25.0027	0.066	0.26
340	25.0029	0.062	0.25
360	24.9997	0.102	0.41

E1.3 Thickness (L)

Figure 63 schematically illustrates the calibration and measurement principles for the in-situ determination of thickness during the guarded-hot-plate tests.

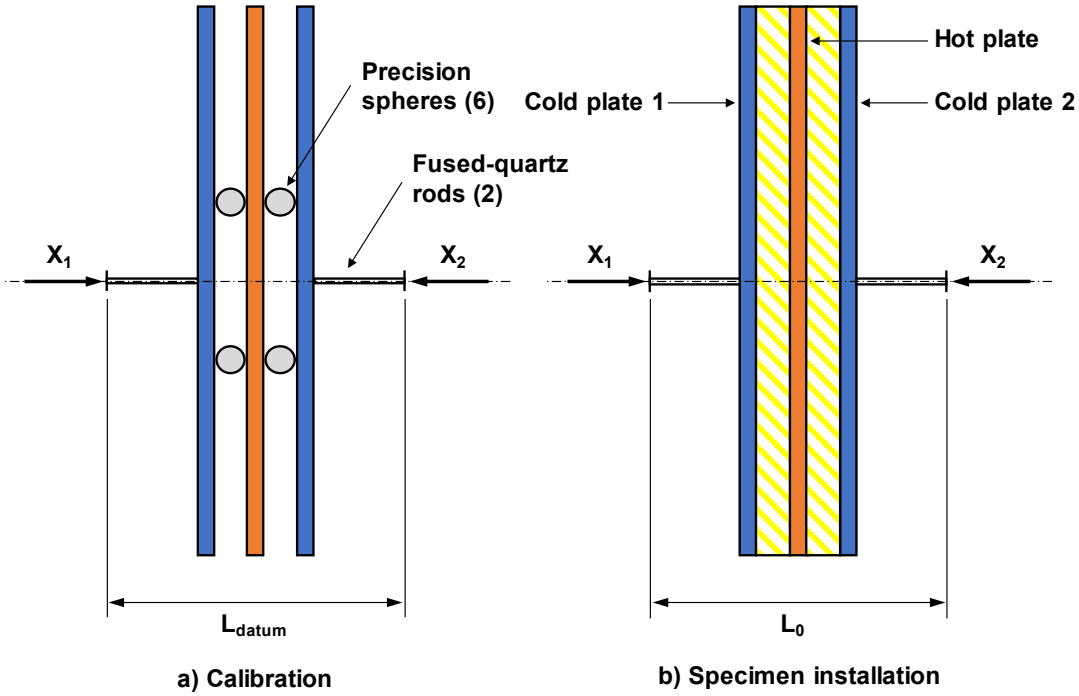

Fig. 63. a) Calibration and b) Measurement principles for in-situ thickness determination.

The dimensional quantities L_{datum} and L_0 indicated in Fig. 63 were measured at ambient conditions with two Heidenhain-Metro MT12 length gages connected in additive sum mode (X_1+X_2) to a Heidenhain ND231B digital display (not shown in Fig. 63). The measurement principle of the length encoders utilized photoelectric scanning of precision graduations etched on glass substrates. The length gages were mounted by a clamping shank so that the gage plunger was orthogonal to the button end of a fused quartz rod located on the axial centerline of the apparatus (Fig. 63). The rounded end of the rod was pressed gently against the center of the rear surface of the circular thermometer plate by a disc spring providing an axial force of 26.7 N (6 lb_f). The length gages were precisely positioned during testing on platforms utilizing kinematic components, i.e., truncated balls and rollers, having three spherical points of contact. The kinematic mount system eliminated the six degrees of motion without using clamping or other excessive constraints.

As summarized in Sec. 6.6.3, L_{datum} was set at laboratory ambient conditions prior to the specimen installation using a dual arrangement of three 25.4 mm (1 in.) diameter precision spheres positioned on either side of the hot plate and spaced evenly around the circumference of a 190 mm-diameter circle. For illustrative purposes, Fig. 63a only shows two spheres on either side of the hot plate. The datum setting (L_{datum}) was defined to be 50.8064 mm for each test, based on the NIST calibration of the spheres' diameters. The following baseline conditions were maintained during the datum setting.

- The coolant baths and heaters (for the plate and guards) were powered down (OFF) 12 h to 24 h prior to setting L_{datum}.
- The water-jacket baths circulating distilled water to the apparatus were operated at a setpoint of 20.0 °C. The laboratory ambient air temperature was controlled from 23 °C to 25 °C.
- During datum entry, the clamping load applied to the plates ranged from 133 N to 178 N (30 lb_f to 40 lb_f). After calibration, the specimen pair was installed at an initial value of L_0 (Fig. 63b) at a clamping load comparable to the calibration loading.

The average (uncorrected) specimen thickness (at T_m) was determined from the combined signals of the encoders X_1 and X_2 (Fig. 63) by the Heidenhain ND231B display from Eq. (E-19).

$$L_{\text{uncorr.}} = \frac{X_1 + X_2}{2} \tag{E-19}$$

E1.3.1 Thickness Correction due Thermal Expansion/Contraction

During a test, the thickness measurement situation was somewhat more complicated since it was necessary to consider the thermal expansion or contraction of the hot plate, two cold plates and two fused-quartz rods [29] shown in Fig. 63. The change in the combined reading of the length gages (δL), relative to the initial reading L_0 taken at room temperature [29], is given by Eq. (E-20).

$$\delta L = 2\,\Delta L\left(T_m\right) + \Delta m_{\text{h}}\left(T_h\right) + \Delta m_{\text{c}_1}\left(T_{c_1}\right) + \Delta m_{\text{c}_2}\left(T_{c_2}\right) + \Delta L_{\text{q}_1}\left(T_{\text{q}_1}\right) + \Delta L_{\text{q}_2}\left(T_{\text{q}_2}\right) \tag{E-20}$$

where

- $\Delta L(T_m)$, which is to be determined, is the change in the average thickness of the specimen pair at T_m;
- $\Delta m_{\text{h}}(T_h)$ is the change in the thickness of the nickel hot plate at T_h;
- $\Delta m_{\text{c}}(T_c)$ is the change in the thickness of the nickel cold plate at T_c; and,
- $\Delta L_{\text{q}}(T_{\text{q}})$ is the change in the length of the fused-quartz rod at T_{q}.

Rearranging Eq. (E-20), the change in average specimen thickness is given by

$$\Delta L\left(T_m\right) = \left[\delta L - \Delta m_{\text{h}}\left(T_h\right) - \Delta m_{\text{c}_1}\left(T_{c_1}\right) - \Delta m_{\text{c}_2}\left(T_{c_2}\right) - \Delta L_{\text{q}_1}\left(T_{\text{q}_1}\right) - \Delta L_{\text{q}_2}\left(T_{\text{q}_2}\right)\right] \Big/ 2 \tag{E-21}$$

The thermal expansion corrections [29] for the plates and fused-quartz rods are computed from Eq. (E-22)

$$\begin{aligned} \Delta m_{\text{h}}\left(T_h\right) &= m_{\text{h}}\left(T_r\right) \times \overline{\alpha}_{\text{Ni}}\left(T_h - T_r\right) \\ \Delta m_{\text{c}}\left(T_c\right) &= m_{\text{c}}\left(T_r\right) \times \overline{\alpha}_{\text{Ni}}\left(T_c - T_r\right) \\ \Delta L_{\text{q}}\left(T_{\text{q}}\right) &= L_{\text{q}}\left(T_r\right) \times \left(\Delta L_{\text{q}} / L_{\text{q293}}\right) \end{aligned} \tag{E-22}$$

where m_{h} and m_{c}, are the thicknesses of the hot and cold thermometry plates, respectively at the reference temperature (T_r) of 293.15 K. The term L_q represents the lengths of the fused-quartz rods at the reference temperature (T_r) of 293 K. The mean thermal expansion coefficient for nickel ($\overline{\alpha}$) was determined from published data by Kollie [30]. The thermal

expansion of fused quartz ($\Delta L_q/L_{q293}$) was determined from data for NIST SRM 739, Fused-Silica Thermal Expansion [31].

Following Eq. (E-21) as a template, Eq. (E-19) was modified so that the corrected thickness at $L(T_m)$ was computed from the average of the combined length gages minus the thermal expansion effects due to the hot plate, cold plates, and fused quartz rods.

$$L(T_m) = \frac{(X_1 + X_2)_{T_m} - L_{\text{corr.}}}{2}$$
$$L(T_m) = \frac{(X_1 + X_2)_{T_m}}{2} - \frac{\Delta m_{\text{h}}(T_h) + \Delta m_{\text{c}_1}(T_{c_1}) + \Delta m_{\text{c}_2}(T_{c_2}) + \Delta L_{\text{q}_1}(T_{\text{q}_1}) + \Delta L_{\text{q}_2}(T_{\text{q}_2})}{2} \quad \text{(E-23)}$$

Table 28 summarizes values for the average corrected thickness L, the corresponding thickness correction, and standard uncertainty at levels of T_m from 280 K to 360 K. As expected, the values of $L_{\text{corr.}}$ increase as T_m departs from ambient conditions near 293 K.

Table 28. Thickness corrections and corresponding standard uncertainties.

T_m (K)	$L(T_m)$ (mm)	$L_{\text{corr.}}$ (mm)	$u(L_{\text{corr.}})$ (mm)	$u(L_{\text{corr.}})$ (%)
280	24.8619	-0.0112	0.000 13	0.0005
300	25.2112	0.0017	0.000 20	0.0008
320	24.9313	0.0148	0.000 18	0.0007
340	25.0282	0.0281	0.000 39	0.0015
360	25.0721	0.0416	0.000 45	0.0018

E1.3.2 Repeated Observations, $u(\bar{L})_A$

The standard uncertainty for the mean in-situ thickness was determined using the same process as was done for $u(\bar{Q}_m)_A$ in Sec. E1.1. The standard uncertainties for repeated observations at levels of T_m from 280 K to 360 K are summarized in Table 29.

Table 29. Standard uncertainties for repeated observations of $\bar{L}$.

T_m (K)	$L(T_m)$ (mm)	$u(\bar{L})_A$ (mm)	$u(\bar{L})_A$ (%)
280	24.861 9	0.000 11	0.000 44
300	25.211 2	0.000 06	0.000 23
320	24.931 3	0.000 12	0.000 48
340	25.028 2	0.000 08	0.000 30
360	25.072 1	0.000 13	0.000 51

E1.3.3 Contributory Thickness Uncertainties

The contributory uncertainties for $u(L)$ due to in-situ measurements include: a) calibration of the 25.4 mm diameter precision spheres (Fig. 63a); b) uncertainty in the measurement instruments; c) plate deflection; d) variation in the datum setting (Fig. 63a); and, e) plate flatness. Specific details for items a), b), and c) are discussed in this section. Separate experiments for items d) and e) are discussed in Secs. E1.3.4 and E1.3.5, respectively.

- *Sphere calibration*: The Bal-tec™, Grade 25, 25.4 mm diameter tungsten carbide balls were manufactured by Micro Surface Engineering, Inc. in 2004 and most recently calibrated on July 10, 2018 by the NIST Dimensional Metrology Group at 20 °C. Table 30 summarizes the NIST calibration data for the six balls.

Table 30. Calibration data for 25.4 mm diameter balls.

	Avg. Measured Diameter		U (k =2)	
Ball ID	**(in.)**	**(mm)**	**(µ in.)**	**(nm)**
1	1.000 129	25.403 267	6.9	174
2	1.000 180	25.404 570	4.9	125
3	1.000 102	25.402 583	25.4	644
4	1.000 064	25.401 624	6.5	165
5	1.000 125	25.403 180	4.1	105
6	1.000 162	25.404 103	4.5	115

The grand average of the ball diameters was 25.403 2 mm which was multiplied by a factor of two (L_{datum} = 50.806 4 mm) for application in the guarded-hot-plate apparatus (Fig. 63a). A conservative estimate of ±644 nm (i.e., expanded uncertainty for ball #3) was selected for the calibration uncertainty in Eq. (E-24).

$$u_1(L)_B = \frac{644\ \text{nm}}{2} = 322\ \text{nm} = 0.000\,322\ \text{mm} \tag{E-24}$$

- *Instrument uncertainty*: The thickness measurement was conducted with two Heidenhain-Metro MT12 Series length gages connected to the Heidenhain ND231B in sum display mode (X_1+X_2). The manufacturer specification for the system accuracy was equal to ±1 µm (0.001 mm) at a reference temperature of 20 °C. A uniform rectangular distribution was assumed for the accuracy specification and the standard uncertainty was computed from Eq. (E-25).

$$u_2(L)_B = \frac{0.001\ \text{mm}}{\sqrt{3}} = 0.000\,58\ \text{mm} \tag{E-25}$$

- *Plate deflection*: Because the plates were supported vertically from an overhead carriage rail system (not shown in Fig. 63) and were free to translate in the axial direction, no correction for the plate deflection during operation was necessary.

E1.3.4 Datum Setting Variability

As described in Sec. E1.3 (Fig. 63a), a datum setting of 50.8064 mm was established before each test using the calibrated 25.4 mm diameter Bal-tec™ precision spheres. For calibration, the outboard stanchion with the Metro MT12 length gage was removed and installed on a kinematic support platform. The gage plunger was retracted for removal of the gage.

The short-term repeatability of the linear position transducers was determined from replicate measurements taken over a four-day interval from September 24, 2019 to September 27, 2019. For each day, a datum setting of 50.8064 mm for the Heidenhain ND231 was established using the 25.4 mm diameter Bal-tec™ precision spheres. After setting the datum, the outboard Metro MT12 was removed from the kinematic-mount platform and the spheres were re-installed to verify the original datum setting. The process was repeated 5 times each day.

Table 31 summarizes the replication data for Days 1 through 4. Each datum in Table 31 was set with a pre-load of about 35.6 N (8 lb_f) and an ultimate loading of 151 N (34 lb_f). The laboratory ambient conditions during measurements was 24.4 °C and 40 % to 44 % relative humidity.

Table 31. Short-term replication data for the in-situ thickness measurement.

Datum setting (mm)	**50.8064**	**50.8064**	**50.8064**	**50.8064**
Observation	**Day 1 (mm)**	**Day 2 (mm)**	**Day 3 (mm)**	**Day 4 (mm)**
1	50.7711	50.7301	50.7755	50.8263
2	50.8688	50.7886	50.7438	50.8791
3	50.8005	50.7642	50.7879	50.7944
4	50.7717	50.7294	50.7607	50.8522
5	50.6916	50.6602	50.7367	50.8046
$\bar{L}_{\text{datum}}$	50.7807	50.7345	50.7609	50.8313
s	0.0638	0.0484	0.0213	0.0347

The standard uncertainty for $u_3(L)$ was determined using Eq. (E-29)

$$u_3(L) = \sqrt{s_a^2 + \left(\frac{r-1}{r}\right) s_d^2} \tag{E-29}$$

where s_a is the standard deviation of the daily averages (between-day variation), s_d is the (pooled) within-day standard deviation, and r is number of replicates per day ($r = 5$). Using the last two rows of data in Table 31, s_a and s_d were computed to be 0.040 94 mm and 0.044 92 mm, respectively. Substituting into Eq. (E-29), yields

$$u_3(L) = \sqrt{0.040\,94^2 + (0.8) \times 0.044\,92^2} = 0.057\,36 \text{ mm} \tag{E-30}$$

E1.3.5 Plate Surface Flatness

Prior to assembly in the apparatus, the plate surface variation was investigated in 2004 by placing the cold thermometer plates on a granite surface plate in a conditioned laboratory. Dimensional measurements were manually taken with a Mitutoyo Series 513 dial indicator having 0.0127 mm (0.0005 in.) graduations. A uniform rectangular distribution was assumed, and the standard uncertainty was computed from Eq. (E-31).

$$u\left(L_{\text{gage}}\right) = \frac{0.012\,7 \text{ mm}}{\sqrt{3}} = 0.007\,33 \text{ mm} \tag{E-31}$$

Figure 64 shows the measurement locations, 1 through 40, over the entire plate surface. The indicator was set to zero at the center location of the plate and all subsequent measurements were acquired relative to the center datum setting of zero. Table 32 summarizes the 40 measurements for cold plates #1 (inboard) and #2 (outboard). The original measurements were recorded in inches but are also presented here in SI, consistent with NIST policy on the use of the SI. The standard deviations of the data for cold plates #1 and #2 were 0.006 22 mm and 0.005 92 mm, respectively (Table 32). The conservative estimate for cold plate #1 was used in subsequent calculations.

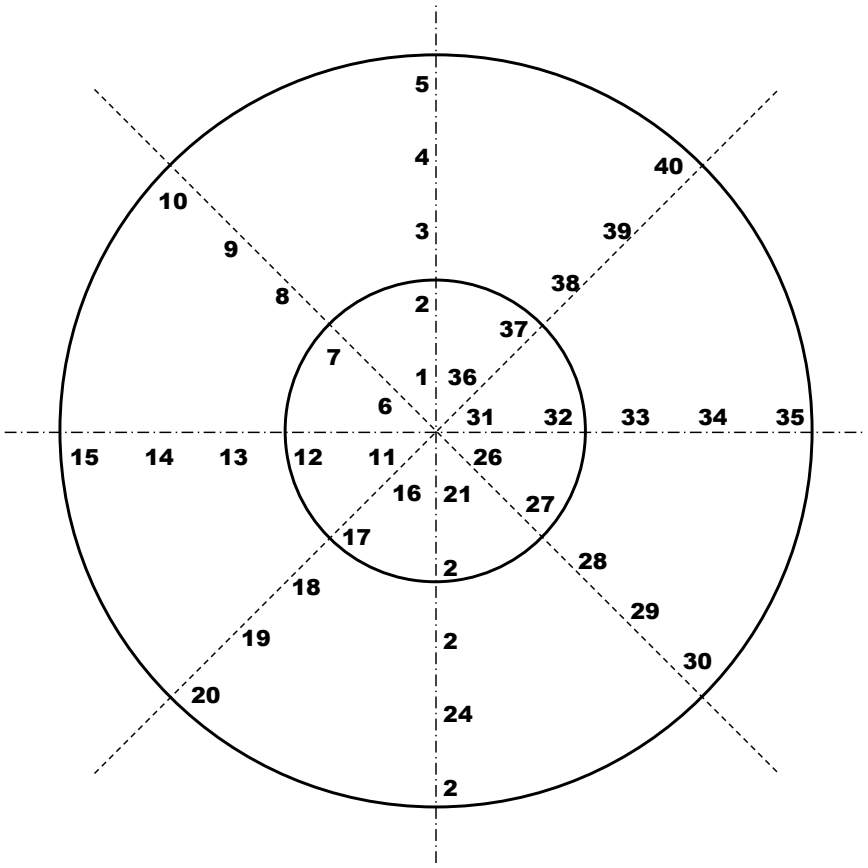

Fig. 64. Locations for surface flatness measurements for NIST 500 mm diameter plates.

The standard uncertainty was estimated from the variance of the mean given by Eq. (E-32).

$$u_{\text{plate}} = \frac{0.03936\ \text{mm}}{\sqrt{40}} = 0.00622\,\text{mm} \qquad \text{(E-32)}$$

The standard uncertainty for the surface plate flatness was computed from Eq. (E-33).

$$u_4(L) = \sqrt{(0.00733\ \text{mm})^2 + (0.00622\ \text{mm})^2} = 0.00962\ \text{mm} \qquad \text{(E-33)}$$

Appendix E

Table 32. Flatness variation of cold plates #1 and #2.

	Cold plate #1		Cold plate #2	
Location	**(mm)**	**(inch)**	**(mm)**	**(inch)**
1	-0.013	-0.0005	0	0
2	-0.025	-0.0010	0.013	0.0005
3	-0.038	-0.0015	0.025	0.0010
4	-0.091	-0.0036	0.038	0.0015
5	-0.135	-0.0053	0.056	0.0022
6	-0.013	-0.0005	0	0
7	0	0	0	0
8	-0.018	-0.0007	0.018	0.0007
9	-0.051	-0.0020	0.025	0.0010
10	-0.066	-0.0026	0.051	0.0020
11	0	0	-0.013	-0.0005
12	0.018	0.0007	0	0
13	0.005	0.0002	0.010	0.0004
14	-0.018	-0.0007	0.028	0.0011
15	-0.025	-0.0010	0.064	0.0025
16	0	0	-0.013	-0.0005
17	0.005	0.0002	0	0
18	-0.013	-0.0005	0.013	0.0005
19	-0.038	-0.0015	0.038	0.0015
20	-0.064	-0.0025	0.069	0.0027
21	0	0	0.008	0.0003
22	0	0	0.025	0.0010
23	-0.025	-0.0010	0.038	0.0015
24	-0.056	-0.0022	0.064	0.0025
25	-0.094	-0.0037	0.089	0.0035
26	0.005	0.0002	0.013	0.0005
27	0	0	0.043	0.0017
28	-0.010	-0.0004	0.064	0.0025
29	-0.025	-0.0010	0.102	0.0040
30	-0.043	-0.0017	0.165	0.0065
31	0	0	0.013	0.0005
32	0	0	0.033	0.0013
33	-0.010	-0.0004	0.051	0.0020
34	-0.023	-0.0009	0.076	0.0030
35	-0.023	-0.0009	0.114	0.0045
36	-0.013	-0.0005	0	0
37	-0.023	-0.0009	0.013	0.0005
38	-0.061	-0.0024	0.018	0.0007
39	-0.119	-0.0047	0.043	0.0017
40	-0.145	-0.0057	0.069	0.0027
Mean	-0.031	-0.0012	0.037	0.0014
s	0.03936	0.0015	0.03743	0.0015

E1.3.6 Combined Standard Uncertainty for *L*

Equation (E-34) computes the combined standard uncertainty ($k = 1$) for L.

$$u_c(L) = \sqrt{u^2(\bar{L}) + u_1^2(L) + u_2^2(L) + u_3^2(L) + u_4^2(L)}$$
$$u_c(L) = \sqrt{0.00013^2 + 0.000322^2 + 0.001^2 + 0.05736^2 + 2 \times 0.00962^2} = 0.0582 \text{ mm} \quad \text{(E-34)}$$

As evident in Eq. (E-34), the dominant contributory uncertainty was due to the set-up of the measurement datum. A factor of 2 was included for $u_4(L)$ to account for the flatness of the hot plate (which was assumed to be the same as the cold plate). The combined standard uncertainties are summarized in Table 33 as a function of T_m. The final column in Table 33 was reproduced in Table 15 (Sec. 7.4).

Table 33. Combined standard uncertainties ($k = 1$) for L.

T_m (K)	$L(T_m)$ (mm)	$u(L_{corr.})$ (mm)	$u(\bar{L})_A$ (mm)	$u_1(L)$ (mm)	$u_2(L)$ (mm)	$u_3(L)$ (mm)	$u_4(L)$ (mm)	$u_c(L)$ (mm)	$u_{c,r}(L)$ (%)
280	24.8619	0.000 13	0.000 11	0.000 32	0.000 58	0.0574	0.009 62	0.0590	0.24
300	25.2112	0.000 20	0.000 06	0.000 32	0.000 58	0.0574	0.009 62	0.0590	0.23
320	24.9313	0.000 18	0.000 12	0.000 32	0.000 58	0.0574	0.009 62	0.0590	0.24
340	25.0282	0.000 39	0.000 08	0.000 32	0.000 58	0.0574	0.009 62	0.0590	0.24
360	25.0721	0.000 45	0.000 13	0.000 32	0.000 58	0.0574	0.009 62	0.0590	0.24

E1.4 Meter Area (*A*)

The circular meter area was calculated from Eq. (E-35),

$$A = \frac{\pi}{2}\left(r_o^2 + r_i^2\right)\left(1 + \bar{\alpha}_{Ni}\,\Delta T_{mp}\right)^2 \quad \text{(E-35)}$$

where r_o is the outer radius of meter plate (m); r_i is the inner radius of guard plate (m); $\bar{\alpha}_{Ni}$ is the coefficient of thermal expansion of nickel (K^{-1}); and, ΔT_{mp} is the temperature difference (K) of the meter plate (T_h) from an ambient temperature of 20 °C.

Replacing the radius in Eq. (E-35) with the diameter (divided by 2) yields

$$A = \frac{\pi}{8}\left(d_o^2 + d_i^2\right)\left(1 + \bar{\alpha}_{Ni}\,\Delta T_{mp}\right)^2 \quad \text{(E-36)}$$

The contributory uncertainties for $u(A)$ include the following: a) calibration uncertainties for d_o and d_i; b) uncertainty in $\bar{\alpha}_{Ni}$ as a function of temperature; and, c) uncertainty in ΔT_{mp}. In addition, the uncertainty analysis includes a small correction due to a portion of the meter plate that was damaged during re-installation of one of the guard gap thermopiles.

- d_o and d_i: The outer diameter (d_o) of the meter plate and the inner diameter (d_i) of the guard plate were determined by the NIST Engineering Metrology Group in July 2006 (NIST Test Report 274749-07) using an error-mapped coordinate measuring machine. The expanded uncertainties ($k = 2$) for the diameter measurements from the NIST Report of Calibration are given by Eq. (E-37)

$$U = \left(\pm 10.20 + 0.2d\right)\ \mu\text{m} \quad \text{(E-37)}$$

where d is in meters. For d equal to a nominal meter plate diameter of 0.2 m, the standard uncertainty ($k = 1$) is computed from Eq. (E-38).

$$u(d) = \left(\frac{\pm 10.20 + 0.2 \times 0.2}{2} \right) \text{ µm} = \frac{10.24}{2} \text{ µm} = 5.12 \text{ µm}. \quad \text{(E-38)}$$

- $\bar{\alpha}_{Ni}$: The average values for the thermal expansion of nickel were obtained by application of the trapezoidal rule to thermal expansion coefficient data measured by Kollie [30] using a fused-quartz dilatometer. Based on the uncertainty estimate of ±1.6 % for the coefficient data [30], an upper limit of 2 % was assumed. Table 34 summarizes interpolated estimates of $\bar{\alpha}_{Ni}$ and corresponding values of $u(\bar{\alpha}_{Ni})$ for five levels of meter plate temperature (T_h).

Table 34. Standard uncertainties for $\bar{\alpha}_{Ni}$.

T_h (K)	$\bar{\alpha}_{Ni}$ (K^{-1})	$u(\bar{\alpha}_{Ni})$ (K^{-1})
292.5	1.28×10^{-5}	2.56×10^{-7}
312.5	1.29×10^{-5}	2.59×10^{-7}
332.5	1.31×10^{-5}	2.62×10^{-7}
352.5	1.32×10^{-5}	2.64×10^{-7}
372.5	1.33×10^{-5}	2.66×10^{-7}

- ΔT_{mp}: The temperature difference for meter plate was determined from Eq. (E-39). The uncertainty was estimated to be 0.010 K based on the measurement uncertainty of the SPRT in the meter plate.

$$\Delta T_{mp} = T_h - 293.15 \quad \text{(E-39)}$$

E1.4.1 Combined Standard Uncertainty for the Metering Area (A)

Propagating the contributory uncertainties in Eq. (E-36) based on a Taylor series approximation yields Eq. (E-40)

$$u_c(A) = \sqrt{c_{d_0}^2 u^2(d_o) + c_{d_i}^2 u^2(d_i) + c_{\bar{\alpha}}^2 u^2(\bar{\alpha}) + c_{\Delta T_{mp}}^2 u^2(\Delta T_{mp})} \quad \text{(E-40)}$$

with

$$c_{d_o} = \frac{\partial A}{\partial d_o} = \frac{\pi}{4} d_o \left(1 + \bar{\alpha}_{Ni} \Delta T_{mp}\right)^2$$

$$c_{d_i} = \frac{\partial A}{\partial d_i} = \frac{\pi}{4} d_i \left(1 + \bar{\alpha}_{Ni} \Delta T_{mp}\right)^2$$

$$c_{\bar{\alpha}_{Ni}} = \frac{\partial A}{\partial \bar{\alpha}} = \frac{\pi}{4} \Delta T_{mp} \left(d_o^2 + d_i^2\right)\left(1 + \bar{\alpha}_{Ni} \Delta T_{mp}\right)$$

$$c_{\Delta T_{mp}} = \frac{\partial A}{\partial \left(\Delta T_{mp}\right)} = \frac{\pi}{4} \bar{\alpha}_{Ni} \left(d_o^2 + d_i^2\right)\left(1 + \bar{\alpha}_{Ni} \Delta T_{mp}\right)$$

Table 35 summarizes the calculations for the combined standard uncertainty of A. The values of d_o and d_i were determined to be 200.070 mm and 201.920 mm, respectively, based on the

calibration data from NIST Report of Test 274749-07. Values of $\bar{\alpha}_{Ni}$ were taken from Table 34. The estimates for $u_c(A)$ are quite small.

Table 35. Combined standard uncertainties for A.

T_h (K)	c_{d_o} (m)	c_{d_i} (m)	$c_{\bar{\alpha}_{Ni}}$ (K·m²)	$c_{\Delta T}$ (K⁻¹·m²)	A (m²)	$u_c(A)$ (m²)	$u_{c,r}(A)$ (%)
292.5	0.1571	0.1585	-1.2689	8.120×10^{-7}	0.031714	1.19×10^{-6}	0.004
312.5	0.1572	0.1587	1.2283	8.217×10^{-7}	0.031746	1.19×10^{-6}	0.004
332.5	0.1573	0.1588	2.4984	8.304×10^{-7}	0.031763	1.32×10^{-6}	0.004
352.5	0.1574	0.1588	3.7693	8.386×10^{-7}	0.031780	1.52×10^{-6}	0.005
372.5	0.1575	0.1589	5.0409	8.464×10^{-7}	0.031797	1.77×10^{-6}	0.006

E1.4.2 Meter Area Correction

On August 26, 2005, a machinist's miscalculation resulted in a ⅛ inch dowel pin being punched through the inboard surface of the meter plate during fabrication. As a result, a small semi-circular section of the meter plate near the guard gap was removed from the meter plate as illustrated in Fig. 65.

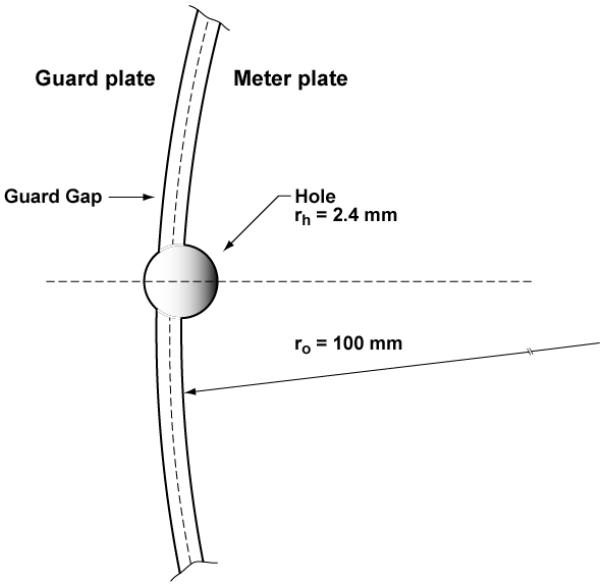

Fig. 65. Schematic illustration of the puncture hole located in the guard gap.

As shown in Fig. 65, the damaged portion of the meter plate is approximately equal to one-half of a circular area having a radius of 2.4 mm. The ratio of the damaged area to the meter plate area is computed from Eq. (E-41) as 0.00029. The uncertainty is about 5 to 7 times larger than the combined standard uncertainties in Table 35 and thus was used in Table 15 (Sec. 7.4).

$$\frac{A_h}{A_{mp}} = \frac{\pi r_h^2/2}{\pi r_o^2} = \frac{(2.4\,\text{mm})^2/2}{(100\,\text{mm})^2} = 0.00029 \qquad \text{(E-41)}$$